MARTIN MARIETTA ENERGY SYSTEMS LIBRARIES

3 4456 0354830 1

ORNL/CON-319

ornl

OAK RIDGE
NATIONAL
LABORATORY

MARTIN MARIETTA

Analysis of Annual Thermal and Moisture Performance of Radiant Barrier Systems

Kenneth E. Wilkes

OAK RIDGE NATIONAL LABORATORY
CENTRAL RESEARCH LIBRARY
CIRCULATION SECTION
4500N ROOM 175
LIBRARY LOAN COPY
DO NOT TRANSFER TO ANOTHER PERSON
If you wish someone else to see this report, send in name with report and the library will arrange a loan.

MANAGED BY
MARTIN MARIETTA ENERGY SYSTEMS, INC.
FOR THE UNITED STATES
DEPARTMENT OF ENERGY

This report has been reproduced directly from the best available copy.

Available to DOE and DOE contractors from the Office of Scientific and Technical Information, P.O. Box 62, Oak Ridge, TN 37831; prices available from (615) 576-8401, FTS 626-8401.

Available to the public from the National Technical Information Service, U.S. Department of Commerce, 5285 Port Royal Rd., Springfield, VA 22161.

This report was prepared as an account of work sponsored by an agency of the United States Government. Neither the United States Government nor any agency thereof, nor any of their employees, makes any warranty, express or implied, or assumes any legal liability or responsibility for the accuracy, completeness, or usefulness of any information, apparatus, product, or process disclosed, or represents that its use would not infringe privately owned rights. Reference herein to any specific commercial product, process, or service by trade name, trademark, manufacturer, or otherwise, does not necessarily constitute or imply its endorsement, recommendation, or favoring by the United States Government or any agency thereof. The views and opinions of authors expressed herein do not necessarily state or reflect those of the United States Government or any agency thereof.

ORNL/CON-319

Energy Division

ANALYSIS OF ANNUAL THERMAL AND MOISTURE PERFORMANCE OF RADIANT BARRIER SYSTEMS

K. E. Wilkes

Date Published - April 1991

Existing Buildings Research Program

Prepared for the
Consumer Systems Division
Electric Power Research Institute
RP2034-30
and the
U.S. Department of Energy
Office of Buildings Energy Research

Prepared by the
OAK RIDGE NATIONAL LABORATORY
Oak Ridge, Tennessee 37831
managed by
MARTIN MARIETTA ENERGY SYSTEMS, INC.
for the
U.S. DEPARTMENT OF ENERGY
Under Contract No. DE-AC05-84OR21400

MARTIN MARIETTA ENERGY SYSTEMS LIBRARIES

3 4456 0354830 1

CONTENTS

LIST OF FIGURES v

LIST OF TABLES vii

ACKNOWLEDGEMENTS ix

ABSTRACT xi

EXECUTIVE SUMMARY xiii

1. INTRODUCTION 1

2. MATHEMATICAL MODEL OF THERMAL AND MOISTURE PERFORMANCE . . . 5
   2.1 OVERVIEW OF THERMAL MODEL 5
   2.2 MODEL FOR MOISTURE EFFECTS 8

3. PERMEANCE OF RADIANT BARRIERS 13

4. COMPARISON OF MODEL WITH EXPERIMENT 19
   4.1 KARNS RESEARCH HOUSES 19
   4.2 MODEL PARAMETERS 20
   4.3 HEAT FLUX RESULTS 23
   4.4 MOISTURE ACCUMULATION 28

5. ANNUAL ENERGY SAVINGS DUE TO RADIANT BARRIERS 33
   5.1 PROTOTYPICAL HOUSE 33
   5.2 ANNUAL LOAD REDUCTIONS AND ENERGY SAVINGS 36
      5.2.1 Clean Horizontal Radiant Barrier 38
      5.2.2 Effect of Dust Accumulation on Horizontal Radiant Barrier 43
      5.2.3 Truss Radiant Barriers 48
      5.2.4 Increased Insulation Levels 53
      5.2.5 Effect of Ducts in Attics 53

6. ANALYSIS OF ANNUAL CYCLE MOISTURE ACCUMULATION 59
   6.1 IDENTIFICATION OF SIGNIFICANT VARIABLES 60
   6.2 PARAMETRIC STUDY FOR VARIOUS CLIMATES 67
   6.3 EFFECT OF CONVECTIVE MOISTURE TRANSPORT 83

7. SUMMARY AND CONCLUSIONS 85

8. REFERENCES 91

APPENDIX A, LISTING OF COMPUTER PROGRAM FOR ATTIC/RADIANT BARRIER MODEL 97

LIST OF FIGURES

2.1 Schematic of residential attic showing heat transfer phenomena . 6

3.1 Water vapor partial pressures measured at Karns House 1 17

3.2 Water vapor partial pressures measured at Karns House 2 17

4.1 Comparison of predicted and measured heat fluxes for House 1 between December 4 and December 11, 1987 24

4.2 Comparison of predicted and measured heat fluxes for House 1 between January 6 and January 14, 1988 24

4.3 Predicted moisture accumulation on horizontal radiant barrier in House 1 from December 4, 1987 to January 14, 1988 29

5.1 Prototypical ranch-style house used for model simulations . . . 34

5.2 Locations for energy savings estimates 37

5.3 Annual heating load reductions due to clean horizontal radiant barrier on top of R-11 insulation 41

5.4 Annual cooling load reductions due to clean horizontal radiant barrier on top of R-11 insulation 41

5.5 Locations where clean horizontal radiant barriers are cost-justified for cost of $0.15 per square foot 44

5.6 Estimated share of basement, crawl space, and slab foundations by state 58

6.1 Moisture condensation for Minneapolis with 50 percent indoor relative humidity 68

6.2 Moisture condensation for Minneapolis with 35 percent indoor relative humidity 68

6.3 Moisture condensation for Knoxville with 50 percent indoor relative humidity 69

6.4 Moisture condensation for Knoxville with 35 percent indoor relative humidity 69

6.5 Peak moisture condensation for Minneapolis 71

6.6 Peak moisture condensation for 50 percent indoor relative humidity 81

6.7 Peak moisture condensation for 35 percent indoor relative humidity 81

6.8 Regions for high, medium, and low potential for moisture condensation problems with horizontal RB with perm of 0.05 and with 35 percent indoor relative humidity 82

LIST OF TABLES

4.1 Thermal properties used in model for Karns house tests 21

4.2 Permeances used in model for Karns house tests 22

4.3 Regression analysis of ceiling heat flow data vs temperature difference across insulation, House 1, Dec. 4, 1987 - Jan. 14, 1988 26

4.4 Average ceiling heat flows for House 1 26

4.5 Comparison of observed and predicted moisture accumulation on radiant barrier, House 1 31

4.6 Comparison of blotter paper weight changes with predicted moisture accumulation, House 1 31

5.1 Annual heating load reductions due to clean horizontal radiant barrier 39

5.2 Annual cooling load reductions due to clean horizontal radiant barrier 40

5.3 Present value savings for clean horizontal radiant barrier . . 42

5.4 Effect of emissivity on load reductions due to horizontal radiant barriers with R-11 insulation 46

5.5 Present value savings for dusty horizontal radiant barrier . . 47

5.6 Load reductions for truss radiant barriers with reflective ($\epsilon = 0.05$) gables 49

5.7 Load reductions for truss radiant barriers with nonreflective ($\epsilon = 0.9$) gables 49

5.8 Present value savings for truss radiant barrier with reflective gables and effective roof emissivity of 0.05 51

5.9 Present value savings for truss radiant barrier with reflective gables and effective roof emissivity of 0.9 52

5.10 Annual heating load reduction due to increasing attic insulation level 54

5.11 Annual cooling load reduction due to increasing attic insulation level 55

5.12 Present value savings for increasing attic insulation level . . 56

6.1 Conditions for initial moisture model runs for Minneapolis . . 62

6.2 Results of initial moisture model runs for Minneapolis 63

6.3 Effect of variables on moisture accumulation for Minneapolis . 65

6.4 Moisture accumulation for Minneapolis 72

6.5 Moisture accumulation for Chicago 73

6.6 Moisture accumulation for St. Louis 74

6.7 Moisture accumulation for Washington, DC 75

6.8 Moisture accumulation for Knoxville 76

6.9 Moisture accumulation for Atlanta 77

6.10 Moisture accumulation for Portland, OR 77

6.11 Moisture accumulation for Waco, TX 78

6.12 Moisture accumulation for Phoenix 78

6.13 Moisture accumulation for Los Angeles 79

6.14 Moisture accumulation for Miami 79

ACKNOWLEDGEMENTS

The author would like to acknowledge the contributions of H. McLain and M. Gettings in coupling the attic model with the DOE-2.1C model and in performing the DOE-2 runs.

ABSTRACT

This report summarizes a project to model the annual thermal and moisture performance of radiant barrier systems installed in residential attics. A previously developed model for the thermal performance of attics with radiant barriers was modified to allow estimates of moisture condensation on the underside of radiant barriers that are laid directly on top of existing attic insulation. The model was partially validated by comparing its predictions of ceiling heat flows and moisture condensation with data and visual observations made during a field experiment with full-size houses near Knoxville, Tennessee. Since the model predictions were found to be in reasonable agreement with the experimental data, the models were used to estimate annual energy savings and moisture accumulation rates for a wide variety of climatic conditions. The model results have been used to identify locations where radiant barriers are cost effective and also where radiant barriers have potential for causing moisture problems.

EXECUTIVE SUMMARY

The use of radiant barriers (RBs) in residential attics is receiving increasing attention. These materials consist of a paper or polymer substrate with a highly reflective coating (usually aluminum) on one or both sides. Their function is to reduce radiative heat transfer between the roof and the attic floor. Radiant barriers are installed in attics in two basic configurations: 1) laid directly on top of existing attic insulation (sometimes called the horizontal configuration), or 2) attached beneath the roof deck (sometimes called the truss configuration).

A number of laboratory and field experiments have shown that radiant barriers can be effective in reducing heat flows through ceilings, and hence in reducing house heating and cooling loads. The experiments have also shown that radiant barriers are generally more effective in reducing summer cooling loads than in reducing winter heating loads. The field experiments have usually been conducted over periods of a few weeks and have been performed in the warmer regions of the country, such as in Florida or Tennessee.

Most of the field experiments indicate that the horizontal configuration produces the greatest reductions in ceiling heat flows. However, at the recent Radiant Barrier Workshop sponsored by the Electric Power Research Institute (EPRI) and the Tennessee Valley Authority (TVA), two issues were highlighted as ones that might hinder the use of horizontal radiant barriers: dust accumulation and moisture accumulation.

While dust accumulation can lead to a deterioration in the energy savings obtained with a horizontal radiant barrier, moisture accumulation can lead to structural damage. Since a horizontal radiant barrier can act as a vapor retarder, there is a potential for moisture to condense on its underside during periods of cold weather. If enough

water accumulates on the radiant barrier, the insulation beneath it may become wet, thus reducing its insulation value, or the wood structural members might absorb the moisture, which may lead to mold, mildew, or wood decay.

The only field data on moisture accumulation with horizontal RBs was obtained from a project sponsored jointly by EPRI, TVA, the Reflective Insulation Manufacturers Association, and the Department of Energy. This project was carried out at the Karns research houses near Knoxville, Tennessee during the winter of 1987-1988. A perforated horizontal radiant barrier was used, and the houses were operated at high indoor relative humidities. Although some condensation was observed on the bottom side of the radiant barrier, condensation that occurred during the night usually disappeared the next day as the attic warmed up. However, under sustained cold weather conditions, all the moisture did not disappear during the day.

These results gave some assurance that moisture problems will not be created with perforated horizontal radiant barriers in climates with winters that are no more severe than those in Knoxville. However, moisture problems might occur in more severe winter climates. Although a full assessment of moisture problems in cold climates can only be obtained from field data, much can be learned through modeling.

This report gives results of a modeling project that was undertaken to estimate the annual energy savings due to radiant barriers in various climates, and also to assess the potential for moisture problems with radiant barriers in various climates.

A previously developed model for the thermal performance of attics containing radiant barriers has been modified to allow predictions of moisture accumulation under horizontal radiant barriers. Flow of water vapor both by vapor diffusion and by convective flow of moist air has been included in the model. However, the convective flow portion has not yet been exercised.

Ceiling heat flows predicted by the model have been compared with those measured during the experiment at the Karns houses during the winter of 1987-1988. Heat fluxes measured by three transducers showed considerable variations that are thought to be due to local variations in the insulation R-value. Considering the variations among the transducers, the model predictions are felt to be in very reasonable agreement with the measured values.

The moisture accumulation model has been partially validated by comparing its predictions with observations of moisture accumulation during the same experiments with the Karns houses. The model predictions agree with the qualitative observations that the radiant barrier often had visible condensation in the morning that usually evaporated when the attic warmed up during the day. The model also predicts the continuing buildup of moisture that was observed during a very cold period of time. Quantitative predictions of amounts of condensed moisture are in rough agreement with weight changes measured for blotter paper that was placed between the insulation and the radiant barriers. Uncertainties in the permeances of the various layers in the ceiling result in corresponding uncertainties in the quantitative predictions of the amount of condensed moisture.

Because of the uncertainties in permeances, it is considered that the model can be used for parametric studies and for development of guidelines, but at this stage, it can't be used to predict actual moisture condensation rates for a particular application with a high degree of certainty. Additional research is needed to measure and document the permeances of various types of radiant barriers.

The thermal model has been used to estimate energy savings potentials for various types of radiant barriers in various climates. Using a prototypical ranch-style house, the attic/radiant barrier model was used to predict hour-by-hour heat fluxes through the ceiling. These heat fluxes were then brought into the DOE-2.1C model to estimate whole house heating and cooling loads. The difference between similar

runs with and without a radiant barrier gave the load reductions due to the radiant barrier. Using medium HVAC equipment efficiencies, national average fuel prices, a 7 percent real discount rate, and estimates of future fuel price increases, present value savings for radiant barriers were calculated.

Present value savings were calculated for: 1) clean horizontal radiant barriers, 2) horizontal radiant barriers that gradually become dusty over their life cycle, and 3) truss radiant barriers. These estimates were made for 27 locations and for four levels of existing attic insulation. As a byproduct of the calculations for radiant barriers, calculations of present value savings for increasing insulation levels (without radiant barriers) were also made.

Determination of cost-effectiveness of radiant barriers is complicated because of the wide range of installed costs. Using a low value of $0.15 per square foot of material, the model predicts that a horizontal radiant barrier that remains clean is cost justified for nearly all locations in the lower 48 states when applied over R-11 insulation. When applied over R-19 insulation, it is cost justified only for the southern locations. When applied over R-30 or R-38 insulation, it is not cost justified in any of the locations studied.

Using data from the literature, which are admittedly sketchy, for the rate of change of the emissivity of a horizontal radiant barrier due to dusting, the model predicts that such a radiant barrier is cost-justified only for Phoenix when applied over R-11 insulation. It should be noted that the performance of dusty horizontal radiant barriers is a subject of considerable controversy, and additional research is needed to define better the rates of emissivity changes in the field, and to define better the thermal performance as a function of emissivity.

In agreement with most experiments, the model predicts that the energy savings due to a truss radiant barrier are not as large as those

for a clean horizontal radiant barrier. This appears to be largely due to the truss radiant barrier configuration having a larger overall radiation heat transfer coefficient because of the combined areas of the roof and gables being larger than the area of the attic floor. In addition, since the gables are also covered with radiant barrier material in these applications, the total area of the gables and the roof result in a requirement for a larger amount of radiant barrier material than with the horizontal application. When these factors are included, the ranges of locations where truss radiant barriers are cost justified are somewhat smaller than those identified for the clean horizontal radiant barrier. It is not expected that the emissivity of the underside of a truss radiant barrier will degrade due to dust accumulation.

All of the load reduction and economic calculations presented in this report are based only on the impact of radiant barriers or ceiling insulation on house loads caused by heat gains or losses through the ceiling. Recent analytical work suggests that additional savings should be attributed to radiant barriers that are installed in houses where the HVAC ducts are run through the attic space. These additional savings are due to changes in the attic air temperature caused by the radiant barrier that result in changes in heat gains and losses by the ducts. The amount of extra savings should be sensitive to the overall characteristics of the house and the HVAC equipment. Because of the many factors involved, further work is needed to analyze the impacts of duct heat gains and losses. Also, experimental confirmation of the analyses are needed.

The model with moisture effects included has been used to estimate the hour-by-hour moisture accumulation on the underside of a clean horizontal radiant barrier due to diffusion of water vapor through the ceiling. The same prototypical ranch-style house that was used for the energy savings analyses was also used for the moisture analyses. Several measures of moisture accumulation have been examined. First is the total amount of moisture that condenses on the radiant barrier over

the year. This quantity would be of interest if it is assumed that all the moisture that condenses gets absorbed into the ceiling and is not released again. Other measures are the peak of the hourly values of condensed moisture (accounting for evaporation), the dates for start, peaking, and ending of condensation, and the duration of wetting. The model only estimates the amounts of water that have condensed or evaporated. It does not attempt to account for movement of liquid water after it has condensed.

A two-level factorial design was run for Minneapolis to estimate the relative influence of the following variables on moisture accumulation: indoor relative humidity, indoor temperature, radiant barrier permeance, vent area, and insulation level. The most important variable was found to be the indoor relative humidity. The total condensed water was 7 to 17 times higher with a relative humidity of 50 percent than with a relative humidity of 20 percent. The second most important variable was the radiant barrier permeance, and the least important variable was the vent area.

From the factorial runs, a worst case was identified as corresponding to a 50 percent relative humidity (the high value), 75°F indoor temperature (the high value), vent area to ceiling area ratio of 1/150 (the high value), R-11 insulation (the low value), and a radiant barrier permeance of 0.05 perms (the low value). Additional runs showed that the presence of a continuous polyethylene vapor retarder between the gypsum board and the insulation essentially eliminated moisture condensation, even for this worst case.

Following this, a parametric study was performed to investigate the influence of the two most important variables, the indoor relative humidity and the radiant barrier permeance, on moisture accumulation in 11 climatic locations. These studies held the other parameters constant: 75°F indoor temperature, vent area to ceiling area ratio of 1/150, R-11 insulation, and no vapor retarder.

Based on moisture content changes that could occur in the ceiling joists due to sorption of water that condenses on the radiant barrier, a high potential for moisture problems was defined as one where the peak condensed moisture exceeds 0.15 pounds per square foot, and a low potential for moisture problems is one where this quantity is less than 0.03 pounds per square foot.

With these criteria, the results of the parametric runs showed that with a 50 percent indoor relative humidity, a radiant barrier with a permeance of 0.05, which may be representative of unperforated foil-type radiant barriers, has a high potential for moisture problems in all locations studied, except Los Angeles and Miami. For the more normal case of a 35 percent relative humidity, a 0.05 perm radiant barrier has a high potential for moisture problems for locations having greater than about 4500 heating degree days, and a low potential for locations with less than about 3000 heating degree days.

The potential for moisture problems is much reduced with a radiant barrier having a permeance of 20, which may be representative of some perforated foil-type radiant barriers. With an indoor relative humidity of 50 percent, there is a high potential for moisture problems for heating degree days above about 4500, and a low potential for heating degree days below about 3000. With a 35 percent indoor relative humidity, the corresponding heating degree day figures are 6500 and 5000.

With a radiant barrier having a permeance of 100, which may be representative of metallized spunbonded polyolefin radiant barriers, the potential for moisture problems is virtually eliminated, except for the coldest climates and the highest indoor relative humidities.

While these modeling results may be used as a guide, there is a need for further experimental verification. Both experiments under controlled laboratory conditions and field experiments in very cold

climates would provide useful tests of the validity of the model predictions.

1. INTRODUCTION

The use of radiant barriers (RBs) in residential attics is receiving increasing attention. These materials consist of a paper or polymer substrate with a highly reflective coating (usually aluminum) on one or both sides. Their function is to reduce radiative heat transfer between the roof and the attic floor. Radiant barriers are installed in attics in two basic configurations: 1) laid directly on top of existing attic insulation (sometimes called the horizontal configuration), or 2) attached beneath the roof deck (sometimes called the truss configuration). The second basic configuration includes several variations, among which are: attachment to the bottoms of the rafters, attachment between the rafters, draping over the top of the rafters, and attachment directly to the underside of the roof deck.

A number of laboratory and field experiments have been performed to measure the thermal performance of attic radiant barrier systems.[1-18] These experiments have generally shown that radiant barriers can be effective in reducing heat flows through ceilings, and hence in reducing house heating and cooling loads. The experiments have also shown that radiant barriers are generally more effective in reducing summer cooling loads than in reducing winter heating loads. The field experiments have usually been conducted over periods of a few weeks and have been performed in the warmer regions of the country, such as in Florida or Tennessee.

A model for the thermal performance of attics containing radiant barriers has been developed at ORNL.[19] Predictions of the model have been compared with several sets of laboratory and field data.[19-22] In general, it was found that the model compared favorably with measured ceiling heat flow data, and was considered useful for extrapolating the results of the short term field tests to seasonal or annual performances, and for extrapolating to climatic conditions other than those under which the experiments were performed.

Most of the field experiments, and also the model, indicate that the horizontal configuration produces the greatest reductions in ceiling heat flows. However, at the recent Radiant Barrier Workshop sponsored by the Electric Power Research Institute (EPRI) and the Tennessee Valley Authority (TVA), two issues were highlighted as ones that might hinder the use of horizontal radiant barriers: dust accumulation and moisture accumulation.[23] These two issues had also been identified by the Radiant Barrier Systems Technical Panel.[24]

While dust accumulation can lead to a deterioration in the energy savings obtained with a horizontal radiant barrier, moisture accumulation can lead to structural damage. Since a horizontal radiant barrier can act as a partial vapor retarder, there is a potential for moisture to condense on its underside during periods of cold weather. If enough water accumulates on the radiant barrier, the insulation beneath it may become wet, thus reducing its insulation value, or the wood structural members might absorb the moisture, which may lead to mold, mildew, or wood decay.

The only field data on moisture accumulation with horizontal RBs were obtained from an experiment sponsored jointly by EPRI, TVA, the Reflective Insulation Manufacturers Association, and the Department of Energy. This experiment was carried out at the Karns research houses near Knoxville, Tennessee during the winter of 1987-1988.[25] A perforated horizontal radiant barrier was used, and the houses were operated at high indoor relative humidities. Although some condensation was observed on the bottom side of the radiant barrier, condensation that occurred during the night usually disappeared the next day as the attic warmed up. However, under sustained cold weather conditions, all the moisture did not disappear during the day.

These results gave some assurance that moisture problems will not be created with perforated horizontal radiant barriers in climates with winters that are no more severe than those in Knoxville. However, moisture problems might occur in more severe winter climates. Although

a full assessment of moisture problems in cold climates can only be obtained from experimental field data, much can be learned through modeling.

This report describes modifications that were made to the attic/radiant barrier thermal model to estimate moisture accumulation on horizontal RBs. The model was partially validated by comparing its predictions with the observations made in the Karns house experiments. The model was then used to perform parametric studies of moisture accumulation in a range of climatic conditions.

In addition to the moisture studies, this report includes the results of estimates of the energy savings that would be expected from radiant barriers in a wide range of climates. These estimates were obtained by coupling ceiling heat flows predicted by the attic/radiant barrier model with the DOE-2.1C whole-building simulation model.[26] These estimates were used to identify regions where radiant barriers are cost effective.

2. MATHEMATICAL MODEL OF THERMAL AND MOISTURE PERFORMANCE

The thermal performance model for attics with radiant barriers is described in detail in Reference 19. This section gives a brief overview of the thermal model, and gives a detailed description of the parts of the model related to moisture accumulation. A listing of the computer program for the model is given in Appendix A.

2.1 OVERVIEW OF THERMAL MODEL

The heat transfer mechanisms included in the thermal model are shown in the sketch in Figure 2.1. The model consists of a set of simultaneous heat balance equations that are written at the exterior and interior surfaces of the ceiling, roof sections, and gables, and also on the air mass within the attic space. Short vertical walls at the eaves are added in order to handle the case of raised trusses. Each of these surfaces is assumed to be isothermal. The set of heat balance equations is solved simultaneously to obtain surface temperatures, and then heat flows are calculated. This procedure is followed on an hour-by-hour basis throughout the time period being simulated.

Conduction through each of the surfaces is calculated using thermal response factors.[27,28] These factors account for both the thermal resistance and the heat capacity of the materials that comprise the section of the attic. Effects of framing are included by adding response factors using a parallel path approach. The model also includes an approximation to account for the temperature dependence of the thermal resistance.

Convective heat transfer is calculated using coefficients from the literature that are based on correlations for isolated isothermal flat plates.[29] These correlations account for the following factors: surface-to-air temperature difference, mean (film) temperature, heat flow direction (up vs. down), surface size and orientation, laminar vs.

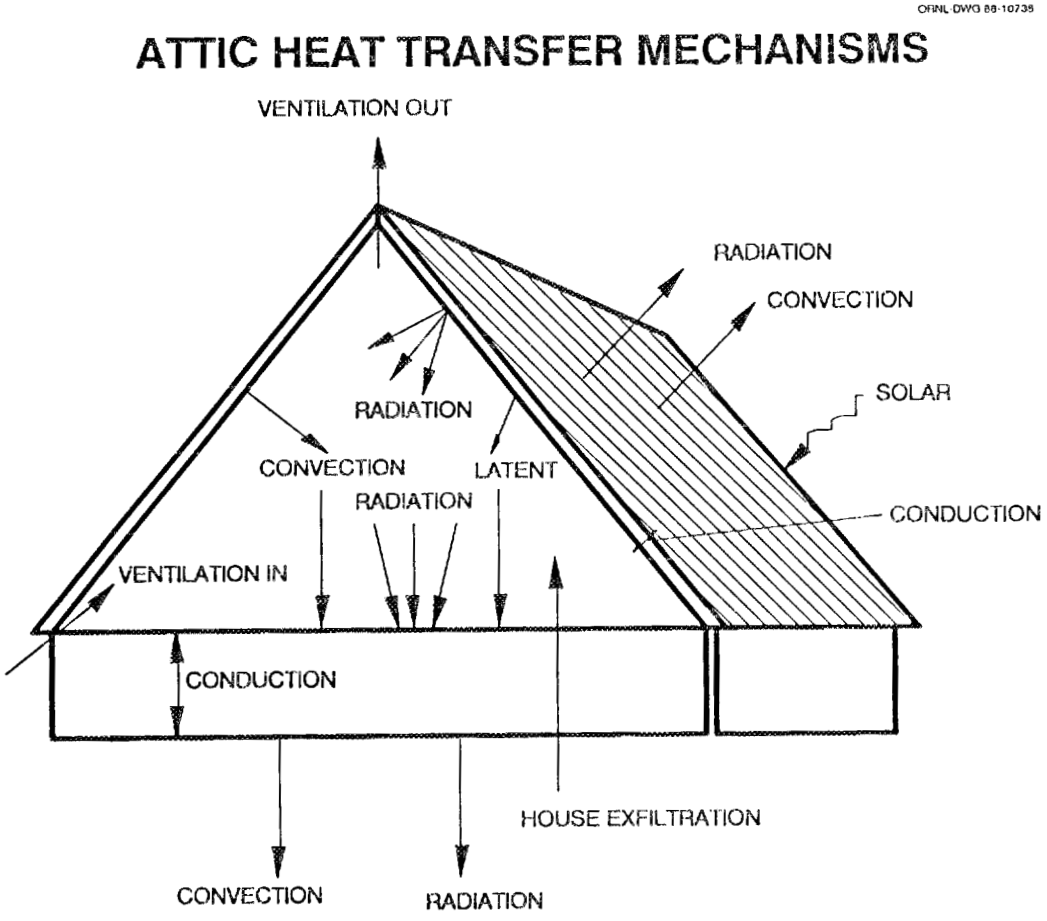

Fig. 2.1. Schematic of residential attic showing heat transfer phenomena

turbulent flow, and natural vs. forced flow. Separate coefficients are calculated for natural and forced flow, and a mixed coefficient is obtained by taking the third root of the sum of the cubes of the separate coefficients.[30]

Radiation heat transfer among the surfaces facing the attic space is calculated using an interchange analysis for enclosures.[31] This analysis assumes that the surfaces are plane, gray, isothermal, diffusely emitting and reflecting, and have a uniform radiant flux. Each of the surfaces may have a different emissivity. View factors are calculated among all the surfaces, and all interreflections are taken into account. The Stefan-Boltzmann (T^4) law is explicitly built into the model.

Heat transfer to the ventilation air stream is treated by the method used by Peavy.[32] Air at the outdoor air temperature enters the attic space and is heated by convection as it flows through the attic. Assuming each of the surfaces to be uniformly distributed along the flow path results in a first order differential equation from which an average air temperature and a different exit temperature may be calculated.

The rate of flow of ventilation air through the attic is calculated from a combination of stack and wind pressure effects.[33] Airflow rates are calculated as the product of the vent area, a discharge coefficient, and the square root of a pressure differential. The pressure differential for the stack effect is computed from the differences in density between the air inside the attic space and the outdoor air. The pressure differential due to wind is taken to vary with the square of the wind speed, so that the wind driven flow is proportional to the wind speed. Exfiltration of air from the house is added to the flow that comes from outdoors.

Heat balances at exterior surfaces consist of absorbed solar radiation, convection to the outdoor air, and radiation exchanges with

the surroundings. Solar radiation incident on surfaces with any orientation are calculated from solar algorithms taken from the DOE-2 program. Radiation to the surroundings is calculated using an effective sky temperature based on the work of Martin and Berdahl.[34]

2.2 MODEL FOR MOISTURE EFFECTS

The thermal model incorporates approximations to account for the latent heat effects due to sorption and desorption of moisture at the wood surfaces that face the attic space. These generally follow the suggestions given by Burch, et. al.[35] and Cleary.[36] In this model, the wood surface is assumed to be in moisture equilibrium with a thin layer of air adjacent to the surface. The humidity ratio of this layer of air is given by[36]

$$W_s = (b + c\,u + d\,u^2 + e\,u^3)\ \exp(T/a) \tag{1}$$

where

W_s = humidity ratio of air near wood surface

T = temperature of wood surface

u = moisture content of wood (dimensionless fraction)

a, b, c, d = constants from fit to equilibrium moisture content data.

The rate of transfer of moisture from the air in the attic space to the surface is given by

$$\dot{m}_w = h_w\,(W_a - W_s) \tag{2}$$

where

$\dot{m}_w$ = mass flow rate of moisture per unit area of exposed wood surface

W_a = humidity ratio of air in attic space

h_w = mass transfer coefficient

The mass transfer coefficient is obtained from the analogy between heat and mass transfer as

$$h_c/(h_w\ C_p) = (\alpha/D)^{2/3} \approx 1 \tag{3}$$

where

h_c = convection heat transfer coefficient

C_p = specific heat of air

α = thermal diffusivity of air

D = coefficient for diffusion of water vapor through air

The humidity ratio of the attic air is obtained by performing a moisture balance on the attic space, including diffusion of moisture through the boundary surfaces, convection of moisture into the attic space from the outside air and from exfiltration from the house, convection of moisture out of the attic space by the ventilation air, and moisture transfer to or from the wood surfaces. The attic moisture balance is given by

$$\sum_{j=1}^{M} A(j)\ P(j)\ (p(j) - p_a) + \dot{m}_v\ (W_o - W_a) + \dot{m}_E\ (W_i - W_a)$$

$$+ \sum_{j=1}^{M} h_w(j)\ A'(j)\ (W_s(j) - W_a) = 0 \tag{4}$$

where

M = number of surfaces facing the attic space

$P(j)$ = water vapor permeance of surface j

$\dot{m}_v$ = mass flow rate of ventilation air

$\dot{m}_E$ = mass flow rate of exfiltration air

$W_s(j)$ = humidity ratio at surface j

W_a = humidity ratio of air in attic space

W_o = humidity ratio of outside air

W_i = humidity ratio of indoor air

$p(j)$ = partial pressure of water vapor in air on outside of surface j

p_a = partial pressure of water vapor in attic air

$h_w(j)$ = water vapor mass transfer coefficient at surface j

$A(j)$ = area of surface j

$A'(j)$ = exposed wood area at surface j

When a horizontal radiant barrier is placed over the insulation, the model must be modified to account for condensation and evaporation of moisture on the radiant barrier surface. An approximate model has been constructed assuming one-dimensional diffusion and convection of moisture through the ceiling. It is assumed that the ceiling materials are nonhygroscopic and that the only place that moisture can condense is on the bottom side of the radiant barrier.

Under steady conditions, with no condensation, the flow of water vapor by diffusion across a layer of material is given by

$$\dot{m}_d = P * \Delta p_v \tag{5}$$

where P is the permeance of the layer and Δp_v is the drop in water vapor partial pressure across the layer. The water vapor partial pressure at the underside of the radiant barrier is then given by

$$PRB = p_a + (p_i - p_a) * P_c/P_{RB} \tag{6}$$

where p_a = water vapor partial pressure in attic space
p_i = water vapor partial pressure inside house
P_{RB} = permeance of the radiant barrier
P_c = overall permeance of the ceiling (includes the gypsum board, vapor retarder, insulation, and radiant barrier)

If the partial pressure at the radiant barrier that is predicted by Eqn. 6 exceeds the saturation vapor pressure for the temperature of the radiant barrier, then moisture will condense on the radiant barrier. When this occurs, the water vapor partial pressure profile through the ceiling will adjust itself so that it is equal to the saturation value at the RB. Also, whenever, condensed water is already on the RB, saturation conditions will exist. The rate of condensation (or evaporation) of water on the radiant barrier will be given by

$$\dot{m}_w = 1/(1/P_c - 1/P_{RB}) * (p_i - p_{RB}) + P_{RB} * (p_a - p_{RB}) \quad (7)$$

where the first term represents water vapor diffusion from the house toward the RB, and the second term represents vapor diffusion from the attic to the RB. If the water vapor partial pressure at the RB is given by Eqn. 6, then Eqn. 7 will give no condensation or evaporation.

If air exfiltrates from the house through the ceiling into the attic space, it also can carry moisture to the radiant barrier. If the humidity ratio of the air inside the house is greater than the saturation humidity ratio at the radiant barrier, then additional moisture condensation will be given by

$$\dot{m}_w = \dot{m}_E/A_c * (W_i - W_{sat}) \quad (8)$$

where W_i = humidity ratio inside the house
W_{sat} = saturation humidity ratio at the radiant barrier
A_c = area of ceiling
$\dot{m}_E$ = mass flow rate of exfiltration air

When moisture is condensing or evaporating from the radiant barrier, the terms in Eqn. 4 that relate to diffusion through the ceiling and to exfiltration from the house to the attic are modified to be consistent with Eqns. 7 and 8.

After mass transfer rates have been calculated, the latent heat transferred to the surface is calculated by

$$Q_{lat} = \dot{m}_w * h_v \quad (9)$$

where h_v is the latent heat of vaporization of water, which has been taken to have a constant value of 1060 Btu/lb. The latent heats are then coupled into the heat balance equations.

The algorithms for calculating moisture effects are embodied in several subprograms. The humidity ratio at the wood surface is calculated by function WDHUM. Subroutines PSY and PSY1 are used to calculate humidity ratios and partial pressures of water vapor from known values of air temperature and relative humidity. The mass transfer coefficients are calculated in subroutine HMASS, and the moisture balance is performed in subroutine MOISTM.

3. PERMEANCE OF RADIANT BARRIERS

The permeance of the radiant barrier is a dominant parameter in determining whether appreciable moisture will condense on the underside of a radiant barrier that is laid directly on top of the attic insulation. A search of the literature was performed in an effort to find published data on the permeance of perforated sheets or films. No data were found.

Two simple theories were used to obtain first order estimates of permeances. In addition, two sources of unpublished data became available. Finally, an estimate of the permeance of one perforated radiant barrier was obtained from analysis of data obtained from the Karns house experiment.[25]

The kinetic theory of gases was used to obtain a first estimate of the permeance of perforated films. From kinetic theory, the mass flux of water vapor across a unit area of a plane that separates two regions with different concentrations of water vapor is[37]

$$\dot{m}_w = p_1 \, [M/2\Pi kT_1]^{1/2} - p_2 \, [M/2\Pi kT_2]^{1/2} \tag{10}$$

where p_1, p_2 = water vapor partial pressures
T_1, T_2 = absolute temperatures
M = mass of water molecule
k = Boltzmann's constant

Since the mass flux through a perforated foil is equal to the mass flux from Equation 10 multiplied by the area fraction covered by holes, and the effective permeance is the mass flux divided by the water vapor partial pressure difference, the effective permeance of a perforated foil under isothermal conditions is

$$P = \dot{m}_w * (A_h/A)/(p_1 - p_2) \tag{11}$$

where A_h/A is the area fraction covered by holes.

Evaluating this equation at a $T_1 = T_2 = 75^oF$ gives

$$P = (A_h/A)\ [M/2\Pi kT]^{1/2} = 1.88 \times 10^7\ (A_h/A) \tag{12}$$

where P has the customary engineering units of grains per hour per square foot per inch of mercury vapor pressure differential (this unit is also called "perms").

Another approximation was obtained by considering diffusion of water vapor across a layer of air equal in thickness to a typical foil. Ignoring counterdiffusion of air, the mass flux of water vapor per unit area is[38]

$$\dot{m}_w = DM/R_oT * \Delta p/\Delta x \tag{13}$$

where D = coefficient for diffusion of water vapor through air, about 1 ft^2/hr at 75^oF

M = molecular weight of water, 18.016

R_o = universal gas constant

T = absolute temperature

Δp = water vapor pressure differential

Δx = thickness of foil

Using this equation, the permeance for a 0.003 inch thick perforated foil is

$$P = DM/R_oT\Delta x *(A_h/A) = 43100\ (A_h/A) \tag{14}$$

This value is a factor of about 400 lower than the simple kinetic theory estimate given in Equation 12, showing the importance of the resistance to vapor flow caused by diffusion through a small thickness of air.

D. Yarbrough of the Tennessee Technological University has performed a number of experiments on the permeance of perforated sheets

of aluminum foil.[39] His setup consisted of a 2 inch deep dish containing about 1/4 inch of water over which the specimen was placed. This dish was placed inside a chamber that was controlled at a temperature of 100°F and either 12 percent or 25 percent relative humidity. Perforated specimens of aluminum foil were prepared with holes of various sizes and spacings such that the percentage of the surface covered by holes ranged from 0.01 percent to 0.38 percent. Water vapor transmission data were converted to perms and the following equation was fitted through the data points:

$$P = 56200 * A_h/A \tag{15}$$

This result is in remarkably good agreement with the simple estimate obtained from the diffusion calculation.

D. Jones of DuPont has measured the permeance of several radiant barrier materials using ASTM E-96, Method B.[40] These data were obtained at 73.4°F with a 100 percent relative humidity on one side of the sample and a RH of 50 percent on the other side. Permeance values for metallized spunbonded polyolefin film were on the order of 100 perms, and permeance values for perforated foils having roughly one percent of the surface covered with holes were on the order of 20 to 30 perms.

Data obtained from the experiment at the Karns houses during the winter of 1987-88 were also used to estimate the permeance of the radiant barrier that was used in this experiment, which had a hole area that covered about 0.46 percent of the surface area, and which was laid directly on top of the attic insulation.[25] In this experiment, relative humidity sensors were placed inside the house, between the ceiling drywall and the insulation, between the insulation and the radiant barrier, and in the attic space. Temperatures were also measured at each of these locations.

These relative humidities and temperatures were used to calculate water vapor partial pressures on an hour-by-hour basis. Figures 3.1 and 3.2 show plots of partial pressures for Houses 1 and 2 during the first week of the test. (Note, during this period, the average indoor relative humidities in Houses 1 and 2 were 53 and 46 percent, respectively.) From Figure 3.1, it appears that there is little partial pressure difference across the ceiling drywall, while the pressure difference across the insulation is of the same magnitude as that across the radiant barrier. Figure 3.2 shows that for House 2, there is a substantial pressure difference across the drywall, but that the pressure differences across the insulation and the radiant barrier are of the same magnitude.

Under steady-state conditions, with no condensation or evaporation of moisture, the diffusion of water vapor should be a constant through the ceiling. Thus the partial pressure difference across a layer should be inversely proportional to the permeance of the layer. Since R-19 batts have a permeance of about 18.6,[41] these data suggest that the radiant barrier also has a permeance of about this magnitude. This permeance value for the radiant barrier is roughly in agreement with that measured by Jones, but is considerably lower than that measured by Yarbrough.

Although the various estimates of the permeance of perforated radiant barriers show considerable variation, they may be used to establish a rough range of values for use in the models.

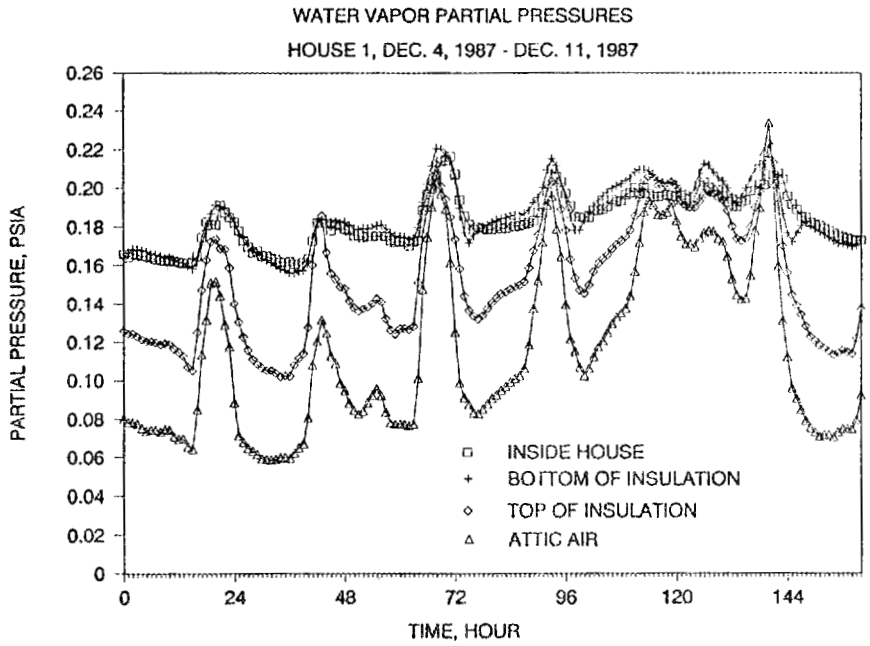

Fig. 3.1. Water vapor partial pressures measured at Karns House 1. A radiant barrier is located between the attic and the top of the insulation.

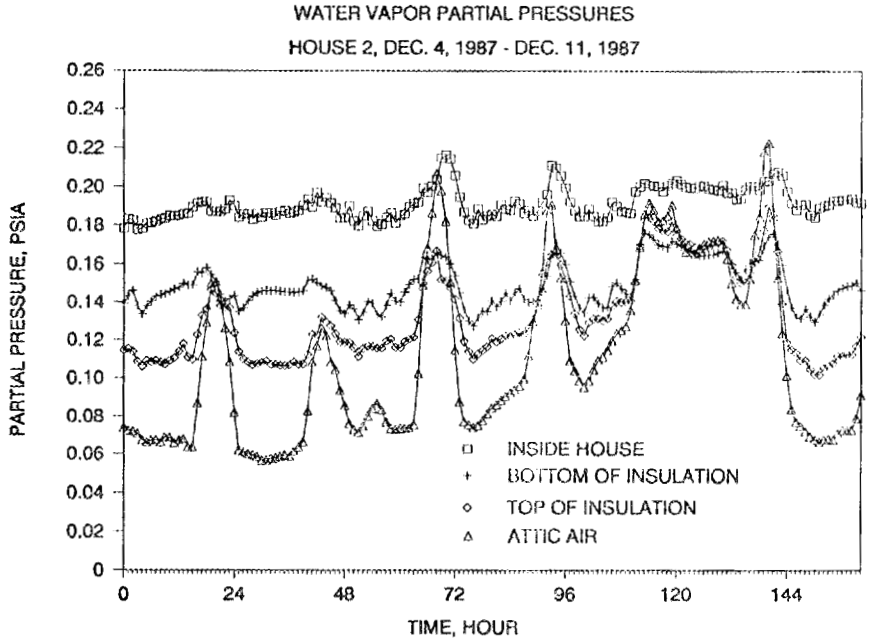

Fig. 3.2. Water vapor partial pressures measured at Karns House 2. A radiant barrier is located between the attic and the top of the insulation.

4. COMPARISON OF MODEL WITH EXPERIMENT

The model for heat transfer in attics has previously been compared with data from a number of laboratory and field experiments. It was generally concluded that the model is capable of predicting ceiling heat flows integrated over time to within about 10 percent of measured values.[19-22]

In this study, an additional comparison of the model with experiment has been performed, both for heat transfer aspects and for moisture accumulation aspects. These comparisons were done using data obtained at the Karns research houses.

4.1 KARNS RESEARCH HOUSES

The Karns research houses are described in detail in a number of reports by W. Levins and M. Karnitz.[6-11,25] The research facility consists of three very similar ranch-style houses located in the community of Karns, which is about midway between Oak Ridge and Knoxville, Tennessee. The houses are about 40 feet long and 30 feet wide, and have a roof pitch of 5 in 12. The roofs are covered with brown shingles. Ventilation of the attic is provided by soffit vents with a net free area of about 3.15 square feet and gable vents with a net free area of about 5.01 square feet.

The test data used here were obtained during the winter of 1987-88, and are described in Reference 25. During this time period, the attics were insulated with fiberglass batt insulation at a nominal level of R-19. Radiant barriers were placed directly over the insulation in all three houses. The radiant barrier was reflective on both sides and was perforated with holes that covered about 0.46 percent of the surface area.

Several variables were measured in this study, as described in detail in Reference 25. Data that have been used in this report consist of the following:

- Ceiling heat fluxes, measured with small (2 inch square) heat flux transducers that were placed between the insulation and the drywall midway between the ceiling trusses.

- Visual observations of the presence of moisture condensed on the underside of the radiant barrier.

- Changes in the weight of blotter paper placed between the radiant barrier and the insulation.

- Weather parameters: solar radiation, outdoor temperature, outdoor relative humidity, wind speed.

- Indoor conditions: indoor temperature, indoor relative humidity.

4.2 MODEL PARAMETERS

Thermal properties of materials that were used in the model are given in Table 4.1. Most of these values were obtained from the ASHRAE Handbook of Fundamentals.[41] The solar absorptance of all materials was taken to be 0.9. Thermal emissivities were also taken to be 0.9, except for the radiant barrier which was taken to have an emissivity of 0.05. (Radiant barrier emissivities measured in the houses averaged about 0.04, using an instrument that has an accuracy of ± 0.02; because of this uncertainty, the handbook value of 0.05 was used.)

Water vapor permeance values used in the model are given in Table 4.2. Many of these values were estimated from data given in the ASHRAE Handbook of Fundamentals. For example, the ASHRAE Handbook lists a value of 50 perms for 3/8 inch drywall. Extrapolating this value to the 1/2 inch drywall used in the experiments gives a value of 37.5

Table 4.1. Thermal properties used in model for Karns house tests.

Material	Thickness, in.	Thermal Conductivity, Btu/(hr-ft-°F)	Specific Heat, Btu/(lb-°F)	Density, lb/ft^3
Ceiling				
Drywall	0.5	0.0926	0.26	50
R-19 Insulation	6.25	0.02741	0.19	0.6
Joists*	3.5	0.06833	0.39	28
Roof				
Shingles	0.25	0.04734	0.30	70
Felt	0.085	0.04734	0.36	70
Plywood	0.5	0.0667	0.29	34
Rafters*	3.5	0.06833	0.39	28
Gables				
Hardboard Siding	0.4375	0.1242	0.28	40
Studs	1.5	0.06833	0.39	28
Eave Walls				
Hardboard Siding	0.4375	0.1242	0.28	40

*Trusses are 24 inch on center.

Table 4.2. Permeances used in model for Karns house tests.

	Run 1	Run 2	Run 3	Run 4
Ceiling				
Drywall	37.5	--	37.5	37.5
Vapor Retarder	--	--	--	0.06
Insulation	18.6	18.6	18.6	18.6
Radiant Barrier	259	18.6	18.6	18.6
Total	11.83	9.3	7.45	0.0595
Roof				
Shingles	--			
Felt	3.30			
Plywood	0.357			
Rafters	--			
Total	0.322			
Gables				
Hardboard Siding	10			
Studs	--			
Total	10			
Eave Walls				
Hardboard Siding	10			
Total	10			

perms. The ASHRAE Handbook lists a value of about 116 perms for a one-inch thick layer of mineral wool insulation. For a 6-1/4 inch thick layer of R-19 insulation, this would translate to 18.6 perms.

Several model runs were performed with various assumptions about the permeances of the materials in the ceiling. In Run 1, the permeance of the radiant barrier was taken to be 259, based on Yarbrough's data. For Run 2, the permeance of the radiant barrier was taken to be 18.6. This value was inferred from the analysis of data from relative humidity sensors in this experiment. Also, for Run 2, the water vapor diffusion resistance of the drywall was ignored since the data for House 1 indicated little difference in water vapor pressure across the drywall. Run 3 is a repeat of Run 2, but with the resistance of the drywall included. Finally, Run 4 was performed to investigate the effect of adding a continuous 6-mil polyethylene vapor retarder.

4.3 HEAT FLUX RESULTS

The four runs of the model as described above were performed for House 1 for the period of December 4, 1987 to January 14, 1988. During this 41 day period, the house was maintained near 70°F with an indoor relative humidity near 53 percent. During this period, the outdoor temperature ranged from a high of about 72°F on December 25 to a low of 3°F on January 11. A snow accumulation of about 6 inches occurred on January 7, a trace of which was still on the ground on January 18.

Model predictions from Run 2 are compared with measured heat fluxes in Figures 4.1 and 4.2. The time axis is the number of hours after the start of the test, which was at 6:00 pm on December 4, 1987. Thus Figure 4.1 starts at 6:00 pm on December 4 and ends at 10:00 am on December 11, while Figure 4.2 starts at midnight between January 5 and 6, and ends at 8:00 am on January 14.

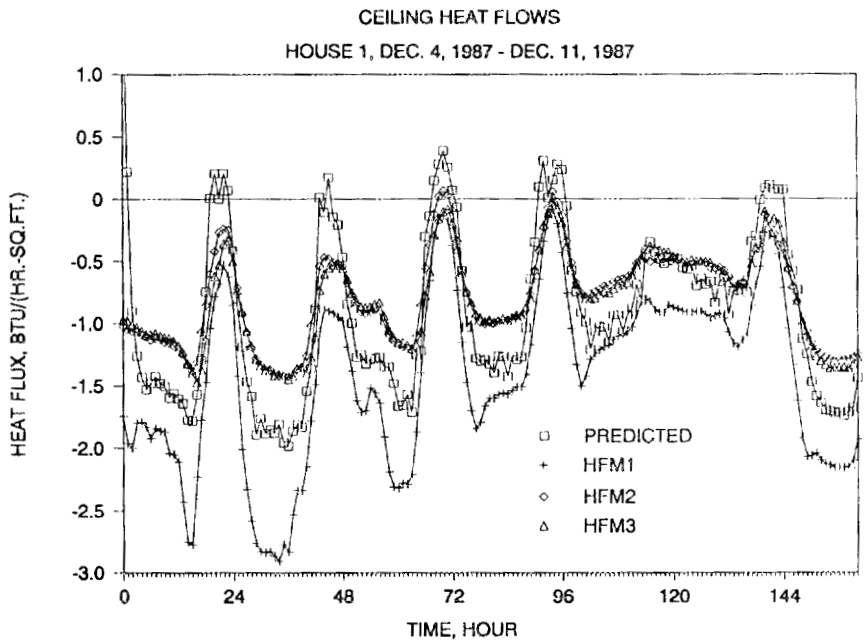

Fig. 4.1. Comparison of predicted and measured heat fluxes for House 1 between December 4 and December 11, 1987.

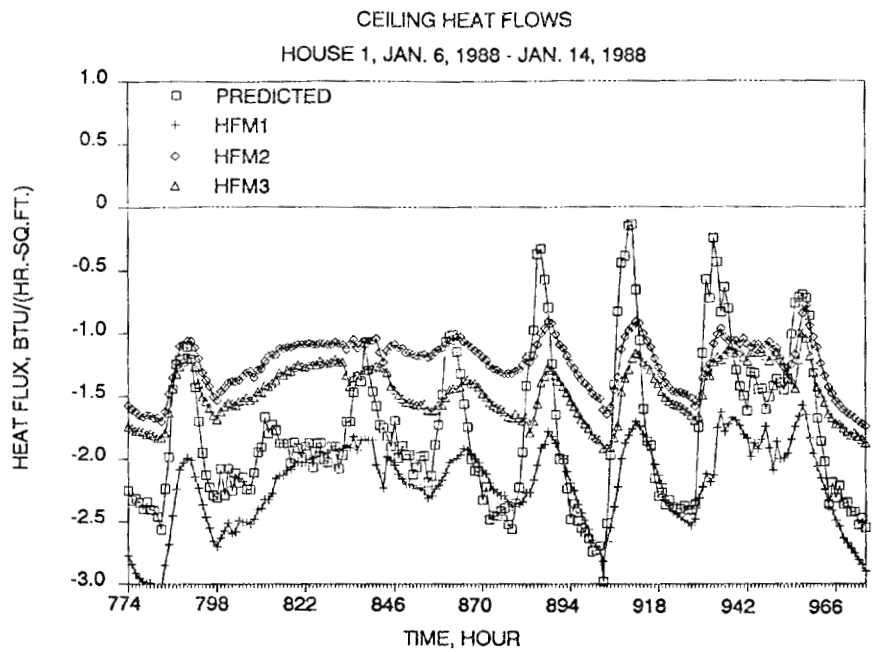

Fig. 4.2. Comparison of predicted and measured heat fluxes for House 1 between January 6 and January 14, 1988.

Both figures show a considerable variation among heat flows measured by the three heat flux transducers. At least part of this variation is thought to be due to differences in the insulation level at the spots where the transducers are located. Heat flux data along with temperatures measured at the top and bottom of the insulation were used in a linear regression analysis of the form

$$q = a + b\ \Delta T \tag{16}$$

with the results shown in Table 4.3. Identifying the slope of these regressions as the reciprocal of the insulation R-value yields the following local R-values at the three heat flux transducers: 14.5, 24.8, and 21.4.

Since the model assumed an insulation R-value of 19, it would be expected that the model predictions would fall between the values measured by heat flux transducer 1 and the values measured by the other two transducers. Figure 4.1 shows this expected behavior during most of the time. (Note: the predicted values during the first few hours in Figure 4.1 should be ignored since these are erroneous because of the startup of the transient calculations.)

The time variation of the predicted heat flux in Figure 4.1 follows the measured variations. However, this is not the case for all of the time period shown in Figure 4.2. For the first two days of this period (Hours 774-821), the model predictions vary about the same as the measured values. But, for the next five days (Hours 822-941), the model predicts wide swings in the heat flux that are not observed. Then, again during the last two days (Hours 942-974), the model variations are about the same as those measured. The qualitative differences between the predicted and measured heat fluxes during the middle five days appear to be due to snow cover on the roof. According to Knoxville airport weather records, snow started at 3:00 am on January 7 (Hour 791) and continued until about 9:00 pm (Hour 819). For the next five days, snow on the roof limited the roof temperature to a

Table 4.3. Regression analysis of ceiling heat flow data vs temperature difference across insulation, House 1, Dec. 4, 1987 - Jan. 14, 1988.

Transducer	Intercept	Slope	r^2	Inferred R-Value
1	0.00504	0.06886	0.960	14.5
2	-0.056149	0.04029	0.925	24.8
3	0.05700	0.04665	0.953	21.4

Table 4.4. Average ceiling heat flows for House 1.

	Insulation R-Value	Average Heat Flow, Btu/ft^2 Dec. 4 - Jan. 14	Jan. 6 - Jan. 14
Measured			
HFT 1	14.5*	1.63	2.20
HFT 2	24.8*	0.93	1.24
HFT 3	21.4*	1.02	1.46
Predicted			
Run 1	19**	1.16	1.80
Run 2	19**	1.19	1.79
Run 3	19**	1.19	1.80
Run 4	19**	1.19	1.80

*R-value inferred from regression analyses.

**R-value assumed in model.

high of about 32°F during the day, and provided some extra insulation during the night. Since the model does not account for snow, it overpredicted the roof temperatures during the daytime because of solar loading, and underpredicted the roof temperatures at night because of radiation to the sky. Apparently, the snow melted off the roof by around the beginning of January 13 (Hour 942), and the model once again tracked the measured values.

Average heat flows over the period from December 4 to January 14 are compared in Table 4.4. The predicted heat flows from the four model runs that made different assumptions about the ceiling and radiant barrier permeances are all within a few percent of each other, indicating that diffusion of water vapor through the ceiling has little effect on the heat flows. The measured average heat flows show considerable variation. However, they vary in a regular manner with the inferred insulation R-values. A linear regression of the measured heat flows versus the reciprocal of the inferred insulation R-values yields an r^2 of 0.995. This regression gives a heat flow of 1.21 Btu/ft^2 for an R-value of 19, which is within 2 to 4 percent of the model predictions. Using the same procedure, but eliminating the period from January 6 to January 14, during which snow was on the roof, gives an average heat flow that is within 6 to 10 percent of the model predictions.

Average heat flows for the period from January 6 to January 14 (during which a snow cover was on the roof) are also given in Table 4.4. A linear regression of the measured data gives a heat flow of 1.66 Btu/ft^2 for an insulation R-value of 19, which is within about 8 percent of the model predictions. Thus, even though the hourly heat flows predicted by the model do not show the right trends when snow is on the roof, the average heat flows predicted by the model are in reasonable agreement with the measured data.

Based on these comparisons of predicted and measured heat flows, it is concluded that the model yields reasonably good predictions if the installed local R-values of the insulation are taken into account.

4.4 MOISTURE ACCUMULATION

The model was used to calculate the amount of condensed moisture (pounds per square foot) that existed on the underside of the radiant barrier in House 1 on an hour-by-hour basis for the period from December 4 to January 14. It was assumed that the radiant barrier was dry at the beginning of this simulation.

Figure 4.3 shows the results of three model runs for House 1. The legends on the figure refer to the assumed values of permeances for the entire ceiling and for the radiant barrier, as given in Table 4.2. The fourth model run, which assumed a continuous polyethylene vapor retarder, is not shown since it predicted that no moisture would condense over the entire period. The first run, which assumes a radiant barrier permeance that corresponds to Yarbrough's data, shows very little condensation.

The other two runs assume the radiant barrier to have a permeance equal to that of the R-19 insulation. One run accounts for the permeance of the ceiling drywall and the other run ignores the drywall. Both of these runs show similar trends, differing only in the magnitude of predicted condensation. During the early parts of the time period, both runs predict that moisture will often condense on the radiant barrier at night, but then will disappear the next day. During the later parts of this period, however, both runs predict a continuous accumulation of condensed moisture. The maximum amounts of condensed water predicted by Runs 2 and 3 are 0.033 and 0.011 pounds per square foot. If these amounts of moisture were uniformly distributed over the radiant barrier, they would correspond to films only 0.006 and 0.002 inches thick, respectively.

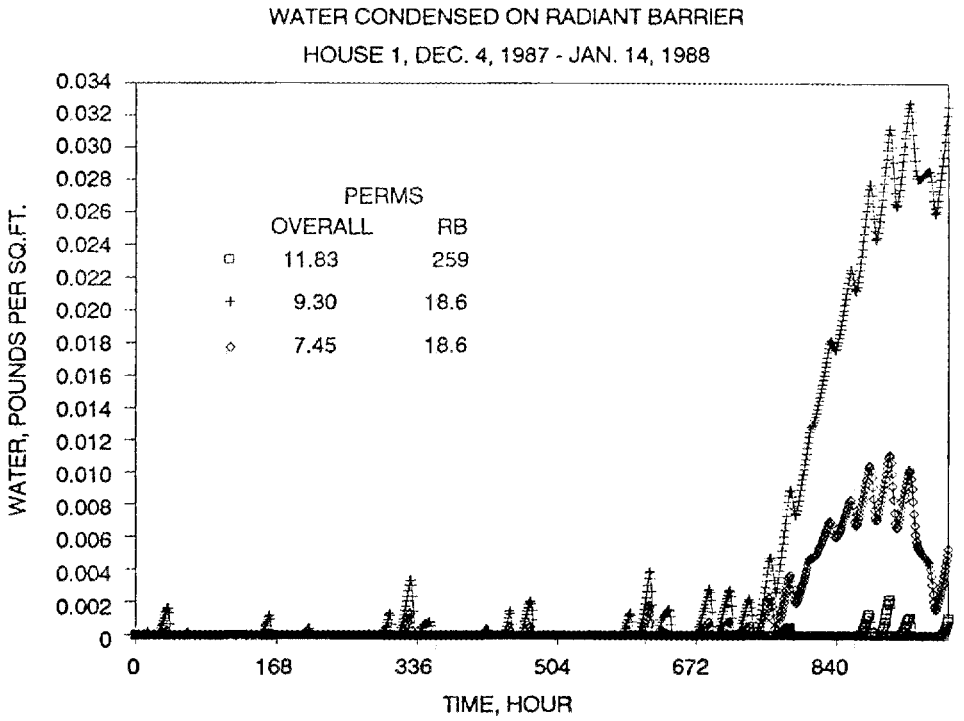

Fig. 4.3. Predicted moisture accumulation on horizontal radiant barrier in House 1 from December 4, 1987 to January 14, 1988. For each curve, the first perm value applies to the total ceiling, including gypsum board, vapor retarder, insulation, and radiant barrier, and the second value applies to the radiant barrier only. See Table 4.2.

During the experiments, visual observations of the underside of the radiant barrier were taken periodically. Table 4.5 lists the observations for House 1, along with predictions of the models for corresponding times. The results of Runs 2 and 3 are in good qualitative agreement with the observations. Each time the radiant barrier was observed to be dry, the models also predicted a dry condition, and when the radiant barrier was observed to be wet, the model also predicted a finite amount of condensation. The quantitative predictions of condensed moisture are also in reasonably good agreement with the observations of light, medium, or heavy moisture.

Quantitative data were obtained by noting weight changes of blotter papers that were placed between the insulation and the radiant barrier. It was thought that the blotter paper weight changes would be an indicator of moisture accumulation that might occur under the radiant barrier. The data for House 1 for December 4 to January 14 are compared with the model predictions in Table 4.6. The model results for Runs 2 and 3 are in reasonably good agreement with the blotter paper weight changes, with the measured values falling between the two runs during the period of heavy condensation.

These comparisons of predicted moisture accumulation and observations show that the model is in reasonably good qualitative agreement with the observations. However, uncertainties in the appropriate values for the permeances of the layers in the ceiling result in some uncertainty in the quantitative predictions. Because of this, it is considered that the model can be used for parametric studies and for development of guidelines, but at this stage, it can't be used to predict actual moisture condensation rates with a high degree of certainty.

Table 4.5. Comparison of observed and predicted moisture accumulation on radiant barrier, House 1.

Date	Time	Observed Moisture	Predicted Water, Pounds per Square Foot Run 1	Run 2	Run 3	Run 4
Dec. 11	0830	Light	0	0.0011	0.0001	0
Dec. 14	0920	Dry	0	0	0	0
Dec. 17	1115	Light	0	0.0006	0	0
Dec. 18	1345	Medium	0	0.0005	0	0
Dec. 21	1100	Dry	0	0	0	0
Dec. 22	0900	Light	0	0.0001	0	0
Dec. 23	1030	Light	0	0.0010	0.0001	0
Dec. 28	1200	Dry	0	0	0	0
Dec. 29	0745	Light	0	0.0012	0.0003	0
Dec. 31	0915	Medium	0	0.0016	0	0
Jan. 4	1030	Medium	0	0.0021	0.0003	0
Jan. 5	0845	Heavy	0	0.0045	0.0022	0
Jan. 8	0945	Heavy	0	0.0180	0.0070	0
Jan. 11	0900	Heavy	0.0021	0.0309	0.0109	0
Jan. 14	0900	Heavy	0.0011	0.0325	0.0053	0

Table 4.6. Comparison of blotter paper weight changes with predicted moisture accumulation, House 1.

Date	Weight Gain lb/ft^2	Predicted Moisture, Pounds per Square Foot Run 1	Run 2	Run 3	Run 4
Dec. 23	0.0057	0	0.0010	0.0001	0
Jan. 8	0.0111	0	0.0180	0.0070	0
Jan. 14	0.0105	0.0011	0.0325	0.0053	0

5. ANNUAL ENERGY SAVINGS DUE TO RADIANT BARRIERS

This section presents the results of analyses of the annual energy savings due to radiant barriers. A prototypical ranch style house was used as the basis for the calculations. Weather data from Typical Meteorological Year tapes were used with the attic/radiant barrier model to calculate hour-by-hour ceiling heat flows. The ceiling heat flows were then brought into the DOE-2.1C model, which combined them with the other heat flows in the house to obtain hour-by-hour, and annual, heating and cooling loads. The difference between similar runs with and without a radiant barrier was the measure of radiant barrier performance. The load reductions were converted to energy bill reductions using average equipment efficiencies and fuel prices. Present values of energy savings were obtained by discounting future savings and by accounting for projected increases in fuel prices.

It is expected that many of the assumptions about the prototypical house would be critical if the radiant barrier performance parameter were chosen to be the percentage reduction in the loads for the whole house. By concentrating on differences in heating and cooling loads due to the radiant barrier, these assumptions should not be critical, since they should nearly subtract out.

5.1 PROTOTYPICAL HOUSE

The prototypical house used for these studies is shown in Figure 5.1.[42,43] This basic house has been used for several other studies. The house is 55 feet long and 28 feet wide, with a floor area of 1540 square feet. The window area is 184.8 square feet, or 12 percent of the floor area. The window area is distributed as follows: 88.8 square feet on the north wall, 70.4 square feet on the south wall, and 25.6 square feet on the west wall. A door on the south wall occupies 19.5 square feet.

ORNL-DWG 89-15373

ONE-STORY HOUSE FOR THERMAL SIMULATIONS

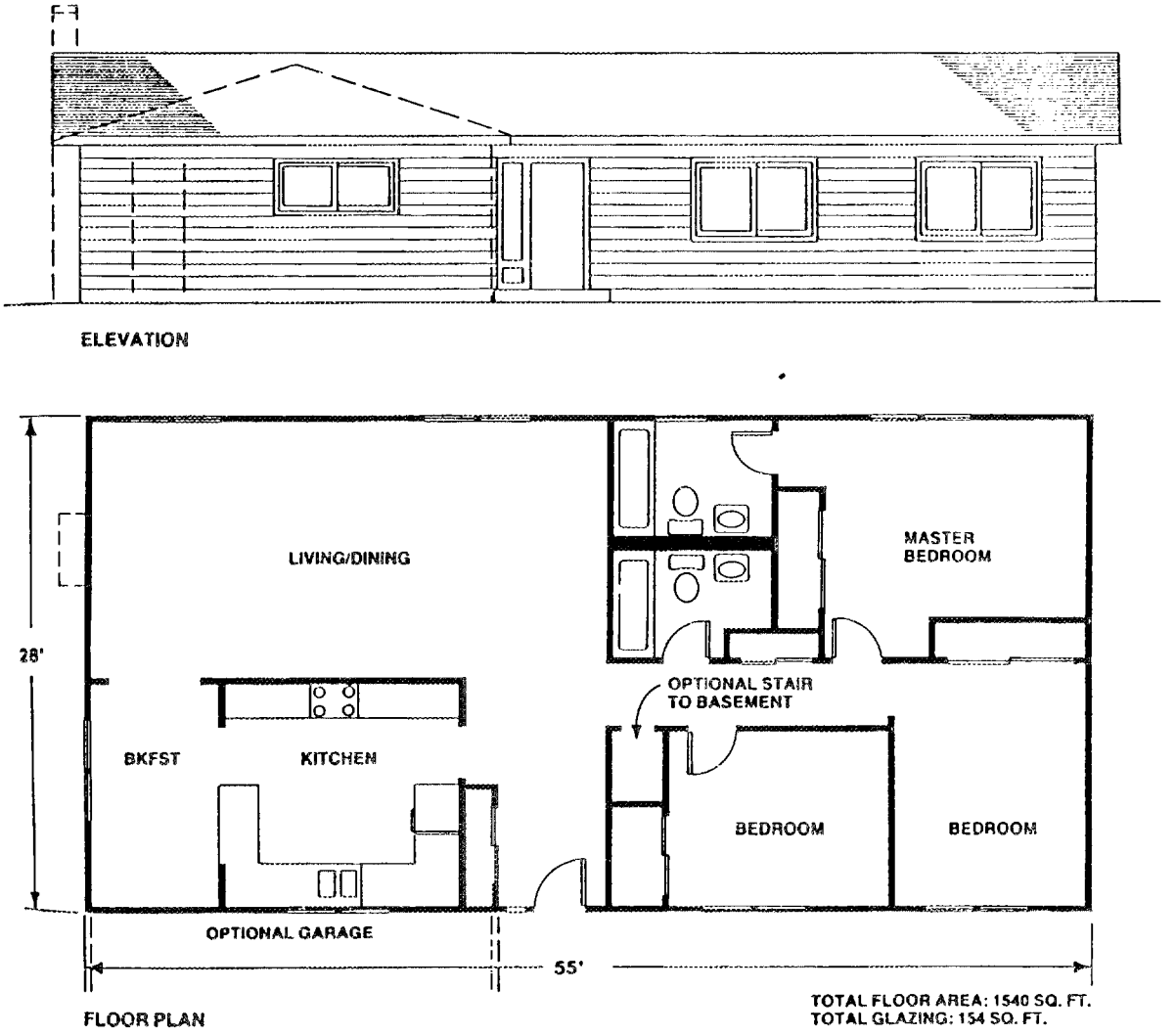

Fig. 5.1. Prototypical ranch-style house used for model simulations.

The walls are constructed with 2X4 wood studs 16 inches on center (24 percent framing), with 1/2 inch gypsum wallboard, R-11 insulation, 1/2 inch fiberboard sheathing, and aluminum siding. The walls have a solar absorptance of 0.7. Windows are double-glazed, with a shading coefficient of 0.52 in the summer and 0.70 in the winter. Also, there is a 2 foot overhang on the south side. The floor is insulated with R-19 insulation between 2X8 wood joists 16 inches on center, and is built over a 3 foot crawl space.

The ceiling is constructed with 2X4 wood joists 24 inches on center, with 1/2 inch gypsum board. The ceiling is insulated with either R-11, R-19, R-30, or R-38 fiberglass insulation, and the joists are assumed to be covered with insulation for levels greater than R-11. The roof has a pitch of 5 in 12, a solar absorptance of 0.9, and has the ridge oriented in the east-west direction. Venting of the attics is assumed through soffit and ridge vents, with a total net free area equal to 1/150 of the ceiling area. One-third of the vent area is assumed to be in the ridge vent, and the other two-thirds are assumed to be in the soffit vents. This corresponds to typical construction practice.[44] The solar absorptance of the gables was taken to be 0.7. Emissivities of all surfaces were taken to be 0.9, except as noted below.

The thermostat settings were taken to be 78°F in the summer and 70°F in the winter. During the summer, window venting was assumed when: 1) opening windows provides enough cooling to keep the zone temperature between 68 and 78°F, 2) the outside air enthalpy is lower than the inside air enthalpy, and 3) the air-conditioning load during the hour can be met totally through natural ventilation at 10 air changes per hour. Since occupants typically would not adjust windows after going to bed, a time of day schedule was added to keep windows closed between 11 p.m. and 7 a.m. During the winter, window venting was assumed when indoor temperatures would rise above 78°F.

Infiltration was calculated using the Sherman-Grimsrud model for average residential construction in a typical suburban area with low buildings and trees within 30 feet.[45] Internal loads were taken to be 55,100 Btu per day, corresponding to 3.2 people, 1 kWh per square foot lighting, and average appliance levels. Hourly internal load profiles were taken from a schedule developed by the California Energy Commission.[46]

5.2 ANNUAL LOAD REDUCTIONS AND ENERGY SAVINGS

The models were run for the 27 cities shown in Figure 5.2 (TMY weather tapes were used for all cities, except for Riverside, CA, for which a California climate zone tape was used). Annual heating and cooling loads were calculated for houses with or without a radiant barrier and with various levels of attic insulation. By using differences between similar runs with and without a radiant barrier, the load reduction due to a radiant barrier was obtained. As a byproduct of assuming various levels of attic insulation, estimates were also obtained for the load reductions that would result from increasing the level of attic insulation. The whole house load reductions were normalized by dividing them by the ceiling area, and were converted to energy bill savings by dividing by the efficiency of the heating or cooling equipment and by multiplying by the cost of fuel. The results presented in this report are based on medium efficiencies of 65 percent for a gas furnace and a coefficient of performance of 2.34 for a central air-conditioner.[47] Average fuel prices of $0.527 per therm for natural gas, and $0.0786 per kWh for electricity were used. These values correspond to those used in the development of ASHRAE Standard 90.2P.[48] The present value of life cycle savings was estimated using a 7 percent real discount rate, a 25 year life, and fuel price escalation rates from Reference 49.

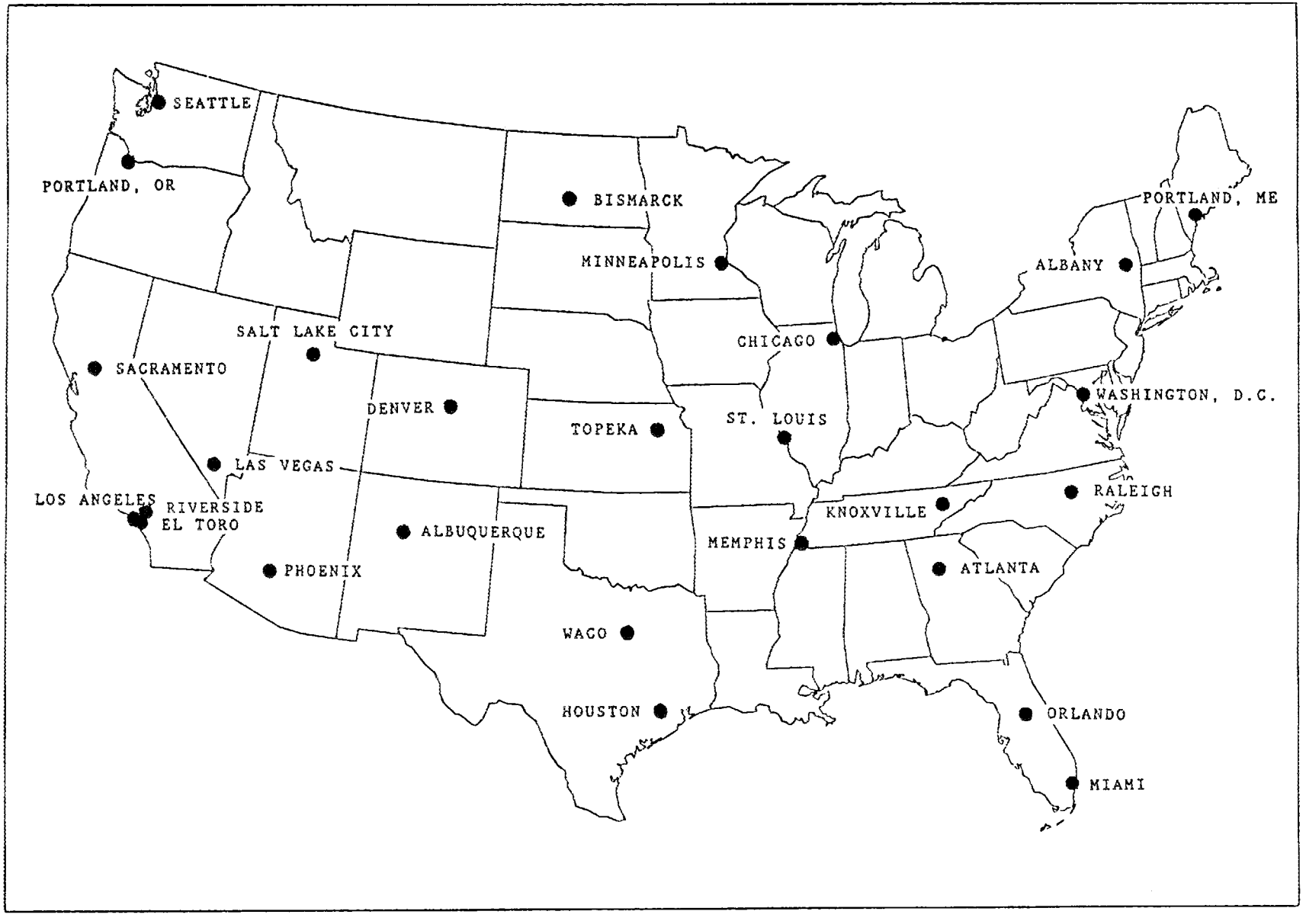

Fig. 5.2. Locations for energy savings estimates.

5.2.1 Clean Horizontal Radiant Barrier

Since experiments have shown that the greatest ceiling heat flow reductions are obtained with the radiant barrier laid directly over the insulation (sometimes called the horizontal configuration), the greatest effort was aimed at this configuration. An upper bound on radiant barrier performance was estimated by assuming the horizontal radiant barrier to stay clean for its lifetime, with a constant emissivity of 0.05.

Estimated heating and cooling load reductions due to a clean horizontal radiant barrier are listed in Tables 5.1 and 5.2. The tables give entries for the 27 cities and for four levels of existing attic insulation. As expected, these tables show that the load reductions vary widely with climate. Also, as expected, the load reductions are greatest when the radiant barrier is added to the lower levels of attic insulation.

Load reductions for the R-11 insulation level are plotted in Figures 5.3 and 5.4 as functions of heating degree days and cooling degree hours. These plots show a reasonable degree of correlation between the load reductions and simple climatic indicators, which may ultimately prove to be a useful method of simplification of the results.

Using the assumptions given above, the reductions in heating and cooling loads have been converted to present value savings and combined with the results shown in Table 5.3. These values can be used as a guide in making a decision about investing in a radiant barrier. A radiant barrier is cost-justified if the present value savings is greater than or equal to the cost of the radiant barrier. Clearly, the decision is complicated by the wide range in price of radiant barriers. However, a price of $0.15 per square foot appears to be near the low end for contractor installed horizontal radiant barriers.[50]

Table 5.1. Annual heating load reductions due to clean horizontal radiant barrier.

City	Load Reduction, Btu/square foot/year			
	R-11*	R-19	R-30	R-38
Albany, NY	929	400	193	140
Albuquerque, NM	931	476	299	238
Atlanta, GA	605	282	163	137
Bismarck, ND	1192	513	293	206
Chicago, IL	842	377	210	144
Denver, CO	989	473	277	236
El Toro, CA	792	378	242	197
Houston, TX	387	182	108	80
Knoxville, TN	725	337	206	164
Las Vegas, NV	774	438	277	227
Los Angeles, CA	738	390	227	188
Memphis, TN	630	304	180	164
Miami, FL	99	47	28	26
Minneapolis, MN	1062	447	223	154
Orlando, FL	275	130	77	62
Phoenix, AZ	606	321	191	162
Portland, ME	1112	490	253	194
Portland, OR	937	427	238	186
Raleigh, NC	741	342	219	162
Riverside, CA	892	422	248	189
Sacramento, CA	821	397	236	192
Salt Lake City, UT	906	415	223	187
St. Louis, MO	738	324	169	136
Seattle, WA	904	364	197	133
Topeka, KS	868	379	219	176
Waco, TX	477	225	138	119
Washington, DC	912	386	212	182

*Level of attic insulation.

Table 5.2. Annual cooling load reductions due to clean horizontal radiant barrier.

City	Load Reduction, Btu/square foot/year			
	R-11*	R-19	R-30	R-38
Albany, NY	876	409	259	211
Albuquerque, NM	1598	851	522	426
Atlanta, GA	1673	832	516	405
Bismarck, ND	706	388	245	191
Chicago, IL	960	475	284	229
Denver, CO	1020	550	357	294
El Toro, CA	1232	636	405	351
Houston, TX	2162	1120	672	521
Knoxville, TN	1597	823	517	411
Las Vegas, NV	2535	1210	703	539
Los Angeles, CA	429	256	168	148
Memphis, TN	1823	907	555	440
Miami, FL	3090	1631	938	727
Minneapolis, MN	769	418	257	204
Orlando, FL	2575	1299	832	662
Phoenix, AZ	3308	1595	942	738
Portland, ME	297	120	82	62
Portland, OR	551	299	178	147
Raleigh, NC	1440	738	460	359
Riverside, CA	1999	931	556	448
Sacramento, CA	1592	849	542	445
Salt Lake City, UT	1286	651	409	332
St. Louis, MO	1466	757	479	369
Seattle, WA	223	119	80	65
Topeka, KS	1523	790	512	397
Waco, TX	2371	1175	713	552
Washington, DC	1221	622	386	301

*Level of attic insulation.

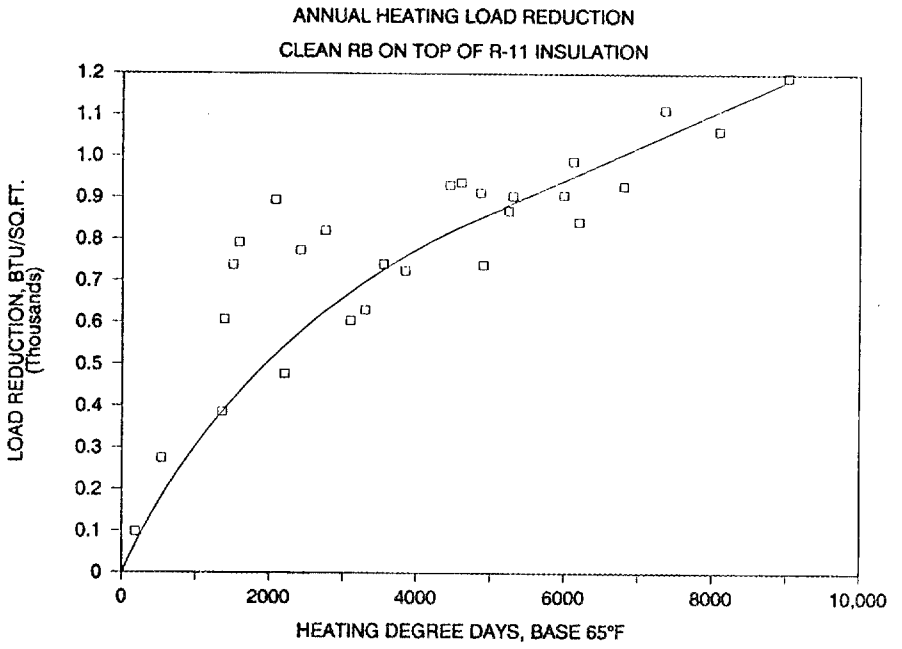

Fig. 5.3. Annual heating load reductions due to clean horizontal radiant barrier on top of R-11 insulation.

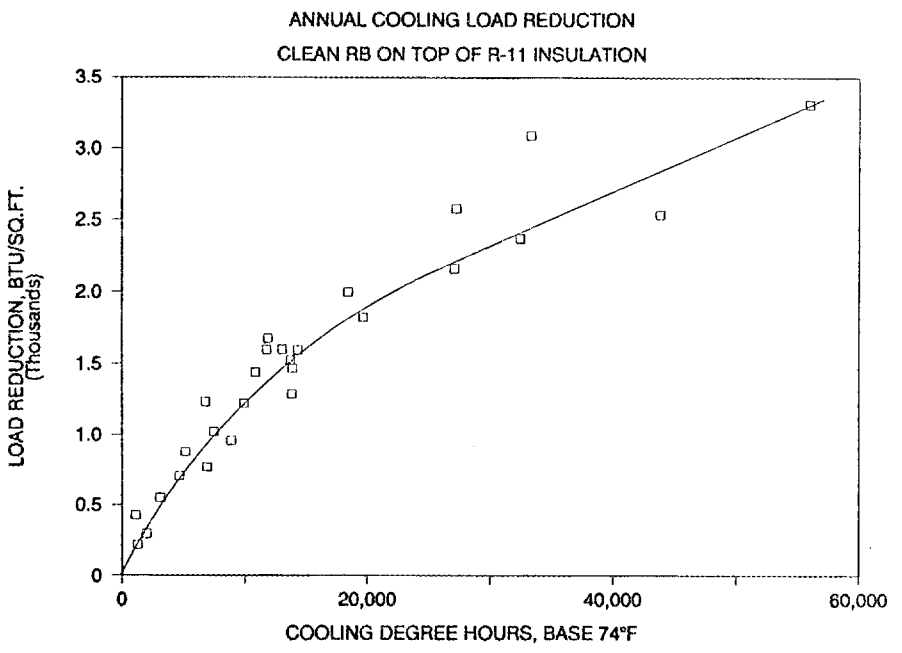

Fig. 5.4. Annual cooling load reductions due to clean horizontal radiant barrier on top of R-11 insulation.

Table 5.3. Present value savings for clean horizontal radiant barrier.

City	Present Value Savings, Dollars per Square Foot			
	R-11*	R-19	R-30	R-38
Albany, NY	0.21	0.09	0.05	0.04
Albuquerque, NM	0.29	0.15	0.09	0.08
Atlanta, GA	0.26	0.13	0.08	0.06
Bismarck, ND	0.22	0.10	0.06	0.04
Chicago, IL	0.21	0.10	0.06	0.04
Denver, CO	0.23	0.12	0.07	0.06
El Toro, CA	0.23	0.12	0.07	0.06
Houston, TX	0.29	0.15	0.09	0.07
Knoxville, TN	0.27	0.13	0.08	0.06
Las Vegas, NV	0.38	0.19	0.11	0.09
Los Angeles, CA	0.13	0.07	0.04	0.04
Memphis, TN	0.28	0.14	0.08	0.07
Miami, FL	0.36	0.19	0.11	0.09
Minneapolis, MN	0.21	0.10	0.06	0.04
Orlando, FL	0.32	0.16	0.10	0.08
Phoenix, AZ	0.45	0.22	0.13	0.10
Portland, ME	0.16	0.07	0.04	0.03
Portland, OR	0.17	0.08	0.05	0.04
Raleigh, NC	0.25	0.12	0.08	0.06
Riverside, CA	0.33	0.16	0.09	0.07
Sacramento, CA	0.28	0.14	0.09	0.07
Salt Lake City, UT	0.25	0.12	0.07	0.06
St. Louis, MO	0.25	0.12	0.07	0.06
Seattle, WA	0.13	0.06	0.03	0.02
Topeka, KS	0.27	0.13	0.08	0.05
Waco, TX	0.32	0.16	0.10	0.08
Washington, DC	0.24	0.12	0.07	0.06

*Level of attic insulation.

Comparing this figure with the values in Table 5.3 shows that, if the attic has R-11 insulation, a clean horizontal radiant barrier is cost-justified for all locations except Los Angeles and Seattle. Since the weather data for Los Angeles were taken at the Los Angeles International Airport, they are probably not representative of the climate where most of the population of greater Los Angeles reside. The values for El Toro, taken at the El Toro Marine Corps Air Station are probably more representative of this area, but still may have some moderating influence due to the ocean that is not felt by locations farther inland, such as Riverside. Thus, with R-11 attic insulation, a clean horizontal radiant barrier is cost-justified for essentially all of the lower 48 states of the U.S.

With R-19 attic insulation, a clean horizontal radiant barrier is cost-justified over the southern parts of the country, including Riverside, CA, as shown in Figure 5.5. With insulation levels of R-30 or R-38, a clean horizontal radiant barrier at a cost of $0.015 per square foot is not cost-justified in any of the locations studied.

5.2.2 Effect of Dust Accumulation on Horizontal Radiant Barrier

The horizontal configuration is susceptible to accumulation of dust, which should result in an increased emissivity, and hence a smaller load reduction. The impact on radiant barrier performance comes from two factors. The first is the rate at which dust accumulates, and hence the rate at which the emissivity increases, while the second is the effect of increased emissivity on the load reductions.

Cook, et. al., have studied the effects of dust on the emissivity of radiant barrier materials.[51] Laboratory testing with artificially dusted samples was used to establish the relationship between amount of dust and emissivity. High emissivities, on the order of 0.8, were measured when a sufficiently large amount of dust was applied. In addition, samples were retrieved from residential attics that had

Fig. 5.5. Locations where clean horizontal radiant barriers are cost-justified for cost of $0.15 per square foot. North of line, RB is justified when used with R-11 insulation. South of line, RB is justified when used with R-11 or R-19 insulation.

radiant barriers installed for around four years. While individual measurements showed a large amount of scatter, a grand average value of 0.24 was obtained for the samples which had been in the field for about four years. An approximation to the relationship between emissivity and time has been obtained by forcing an equation through Cook's four year field average value and his laboratory values for clean and very dusty samples, giving

$$\epsilon = 0.03 + 0.761\ [1 - \exp(-0.0807*t)] \tag{17}$$

where t is the time in years.

The models have been run with various assumed levels of emissivity. Load reductions obtained from these calculations were normalized with respect to the load reductions from a clean horizontal radiant barrier, with the results given in Table 5.4. The model predicts that the performance drops off significantly with increases in emissivity, with the cooling performance dropping off faster than the heating performance. The model also predicts that the normalized reductions do not vary significantly with climate. Empirical equations fit to these results are

$$NRH = 192.2\ [0.596 - 1/(1 + 0.61/\epsilon)] \tag{18}$$

$$NRC = 162.3\ [0.8318 - 1/(1 + 0.182/\epsilon)] \tag{19}$$

where NRH and NRC are the normalized heating and cooling load reductions and ϵ is the radiant barrier emissivity.

Using this rate of change of emissivity and the model predictions for the effect of emissivity on load reductions results in the present value savings given in Table 5.5. Using the $0.15 per square foot criterion, a dusty horizontal radiant barrier (as defined here) is cost-justified only for Phoenix when the attic contains R-11 insulation.

Table 5.4. Effect of emissivity on load reductions due to horizontal radiant barriers with R-11 insulation.

Emissivity	Percent of Clean Horizontal RB Load Reduction		
	Miami, Cooling	Minneapolis, Cooling	Minneapolis, Heating
0.05	100	100	100
0.10	73.4	74.8	87.8
0.20	48.0	50.8	66.7
0.30	33.5	35.7	51.6
0.40	23.4	24.9	38.5
0.50	16.0	17.4	28.0

It should be noted that the performance of dusty horizontal radiant barriers is a subject of considerable controversy. First, there is considerable scatter in measured values of emissivity versus time. The analysis presented here uses what is considered to be a representative relationship. However, other curves might be chosen which would alter the performance values either up or down. Second, there is a question of how well the model accounts for the effects of emissivity changes. Data taken by the Tennessee Valley Authority with test cells having horizontal radiant barriers that were artificially dusted with "Arizona test dust" do not show such a rapid decline in performance as predicted by the model.[52] There is a need for continued research on the rates of emissivity changes in the field, and also a need for thermal performance tests under well-controlled laboratory conditions.

Table 5.5. Present value savings for dusty horizontal radiant barrier.

City	Present Value Savings, Dollars per Square Foot			
	R-11*	R-19	R-30	R-38
Albany, NY	0.08	0.04	0.02	0.02
Albuquerque, NM	0.11	0.06	0.03	0.03
Atlanta, GA	0.09	0.05	0.03	0.02
Bismarck, ND	0.09	0.04	0.02	0.02
Chicago, IL	0.08	0.04	0.02	0.02
Denver, CO	0.08	0.04	0.03	0.02
El Toro, CA	0.09	0.04	0.03	0.02
Houston, TX	0.10	0.05	0.03	0.02
Knoxville, TN	0.10	0.05	0.03	0.02
Las Vegas, NV	0.13	0.07	0.04	0.03
Los Angeles, CA	0.05	0.03	0.02	0.02
Memphis, TN	0.10	0.05	0.03	0.02
Miami, FL	0.12	0.06	0.04	0.03
Minneapolis, MN	0.08	0.04	0.02	0.02
Orlando, FL	0.11	0.06	0.04	0.03
Phoenix, AZ	0.16	0.08	0.05	0.04
Portland, ME	0.07	0.03	0.02	0.01
Portland, OR	0.07	0.03	0.02	0.01
Raleigh, NC	0.09	0.04	0.03	0.02
Riverside, CA	0.12	0.06	0.03	0.03
Sacramento, CA	0.10	0.05	0.03	0.03
Salt Lake City, UT	0.09	0.04	0.03	0.02
St. Louis, MO	0.09	0.04	0.03	0.02
Seattle, WA	0.05	0.02	0.01	0.01
Topeka, KS	0.10	0.05	0.03	0.02
Waco, TX	0.11	0.06	0.03	0.03
Washington, DC	0.09	0.04	0.02	0.02

*Level of attic insulation.

5.2.3 Truss Radiant Barriers

Truss radiant barriers are installed in a number of configurations, which may be expected to have different performances. Among the methods for installing truss radiant barriers are: 1) attaching them directly to the bottoms of the rafters, covering the bottoms of the rafters, 2) attaching them between the rafters, thus leaving the bottom surfaces of the rafters exposed, 3) draping them over the tops of the rafters, which leaves more of the rafters exposed, and 4) attaching them directly to the underside of the roof decking. With any of these configurations, the interior of the gables may also be covered with radiant barrier, as recommended by the Reflective Insulation Manufacturers Association.[53]

Load reductions for truss radiant barriers were estimated by running the model with various levels of effective or average emissivities for the underside of the roof, and for either reflective or nonreflective gables. Predicted load reductions, normalized to the values for a clean horizontal radiant barrier, are given in Tables 5.6 and 5.7. In general, these tables show that the normalized values do not vary significantly with climate or insulation level, but do vary considerably with roof emissivity and also vary somewhat between the heating and cooling seasons. In addition, the model predicts that better performance is obtained with reflective gables, especially with low roof emissivities. Also, with a low roof emissivity and reflective gables, the performance of a truss radiant barrier is nearly equal to that of a clean horizontal radiant barrier.

These model results may be used to estimate the load reductions due to truss radiant barriers if appropriate values can be selected for the effective emissivity of the underside of the roof. While this is a complicated task, and subject to some controversy, it is interesting to look at two assumptions. First, it is assumed that the radiant barrier covers the bottoms of all rafters and the gables, and that a negligible amount of the roof deck is exposed to allow for passage of ventilation

Table 5.6. Load reductions for truss radiant barriers with reflective (ϵ = 0.05) gables.

City	Season	Insulation level	Percent of Clean HRB Load Reduction ϵ = 0.05*	ϵ = 0.10	ϵ = 0.15
Miami	Cooling	R-11	92.4	68.2	53.8
		R-19	94.1	70.7	56.8
		R-30	94.5	73.0	58.2
		R-38	94.6	71.8	57.9
Minneapolis	Cooling	R-11	93.2	70.0	56.2
		R-19	95.0	74.5	60.7
Miami	Heating	R-11	95.4	84.9	74.3
		R-19	95.9	83.6	69.9
		R-30	95.3	88.4	76.7
		R-38	97.5	82.5	72.5
Minneapolis	Heating	R-11	96.3	84.2	73.2
		R-19	95.6	80.4	71.2

*Effective emissivity of underside of roof.

Table 5.7. Load reductions for truss radiant barriers with nonreflective (ϵ = 0.9) gables.

City	Season	Insulation level	Percent of Clean HRB Load Reduction ϵ = 0.05*	ϵ = 0.10	ϵ = 0.15
Miami	Cooling	R-11	78.1	61.5	49.9
		R-19	81.5	64.8	52.9
Minneapolis	Cooling	R-11	80.5	63.7	52.7
		R-19	84.9	69.1	57.5
Miami	Heating	R-11	81.6	73.7	64.4
		R-19	80.8	69.9	60.3
Minneapolis	Heating	R-11	78.7	68.0	59.6
		R-19	77.6	66.0	58.7

*Effective emissivity of underside of roof.

air. In this case, the effective emissivity is 0.05 and from Table 5.6, the normalized load reduction is about 95 percent for either heating or cooling. For the second case, it is again assumed that the gables are reflective, but that 6.25 percent of the roof surface has an emissivity of 0.9 (this percentage corresponds to the assumed framing factor, 1.5 inch wide rafters every 24 inches). Area averaging the high and low emissivity surfaces gives an effective emissivity of 0.10, and from Table 5.6, the normalized load reductions are about 70 percent for cooling and 85 percent for heating.

Present value savings calculated with these assumptions are given in Tables 5.8 and 5.9. For judging cost-effectiveness, radiant barrier costs must take into account the fact that the roof and gable areas are larger than the ceiling. For the prototypical house described above the total area of the roof and gables is about 19 percent larger than the ceiling. With an installed cost of $0.15 per square foot of material, the cost per square foot of ceiling will be about $0.18.

Comparing the present value savings in Table 5.8 with $0.18 per square foot shows that, with R-11 insulation, a truss radiant barrier with an effective emissivity of 0.05 is cost justified for all locations except Los Angeles (at the airport), Portland, ME, Portland, OR, and Seattle. With R-19 insulation, this radiant barrier is cost justified only for climates typified by Las Vegas, Phoenix, and Miami. For higher insulation levels, this radiant barrier is not cost justified.

Comparing the present value savings in Table 5.9 with $0.18 per square foot indicates that, with R-11 insulation, a truss radiant barrier with an effective emissivity of 0.10 is cost justified for all locations except those typified by Albany, Bismarck, Chicago, Los Angeles (at the airport), Minneapolis, both Portlands, and Seattle. For higher insulation levels, this radiant barrier is not cost justified.

Table 5.8. Present value savings for truss radiant barrier with reflective gables and effective roof emissivity of 0.05.

City	Present Value Savings, Dollars per Square Foot			
	R-11*	R-19	R-30	R-38
Albany, NY	0.20	0.09	0.05	0.04
Albuquerque, NM	0.28	0.14	0.09	0.07
Atlanta, GA	0.25	0.12	0.07	0.06
Bismarck, ND	0.21	0.10	0.06	0.04
Chicago, IL	0.20	0.09	0.05	0.04
Denver, CO	0.22	0.11	0.07	0.06
El Toro, CA	0.22	0.11	0.07	0.06
Houston, TX	0.28	0.14	0.08	0.06
Knoxville, TN	0.25	0.13	0.08	0.06
Las Vegas, NV	0.36	0.18	0.11	0.08
Los Angeles, CA	0.13	0.07	0.04	0.04
Memphis, TN	0.27	0.13	0.08	0.07
Miami, FL	0.34	0.18	0.10	0.08
Minneapolis, MN	0.20	0.09	0.05	0.04
Orlando, FL	0.31	0.15	0.10	0.08
Phoenix, AZ	0.42	0.21	0.12	0.10
Portland, ME	0.15	0.07	0.04	0.03
Portland, OR	0.16	0.08	0.04	0.04
Raleigh, NC	0.24	0.12	0.07	0.06
Riverside, CA	0.31	0.15	0.09	0.07
Sacramento, CA	0.26	0.14	0.08	0.07
Salt Lake City, UT	0.24	0.12	0.07	0.06
St. Louis, MO	0.24	0.12	0.07	0.05
Seattle, WA	0.12	0.05	0.03	0.02
Topeka, KS	0.26	0.13	0.08	0.06
Waco, TX	0.31	0.15	0.09	0.07
Washington, DC	0.23	0.11	0.06	0.05

*Level of attic insulation.

Table 5.9. Present value savings for truss radiant barrier with reflective gables and effective roof emissivity of 0.10.

City	Present Value Savings, Dollars per Square Foot			
	R-11*	R-19	R-30	R-38
Albany, NY	0.16	0.07	0.04	0.03
Albuquerque, NM	0.22	0.11	0.07	0.06
Atlanta, GA	0.19	0.09	0.06	0.05
Bismarck, ND	0.17	0.08	0.05	0.04
Chicago, IL	0.16	0.08	0.04	0.03
Denver, CO	0.18	0.09	0.06	0.05
El Toro, CA	0.18	0.09	0.06	0.05
Houston, TX	0.21	0.11	0.06	0.05
Knoxville, TN	0.20	0.10	0.06	0.05
Las Vegas, NV	0.28	0.14	0.08	0.07
Los Angeles, CA	0.11	0.06	0.04	0.03
Memphis, TN	0.21	0.10	0.06	0.05
Miami, FL	0.26	0.13	0.08	0.06
Minneapolis, MN	0.17	0.08	0.04	0.03
Orlando, FL	0.23	0.12	0.07	0.06
Phoenix, AZ	0.32	0.16	0.09	0.07
Portland, ME	0.13	0.06	0.03	0.02
Portland, OR	0.14	0.07	0.04	0.03
Raleigh, NC	0.19	0.09	0.06	0.04
Riverside, CA	0.25	0.12	0.07	0.05
Sacramento, CA	0.21	0.11	0.07	0.05
Salt Lake City, UT	0.19	0.09	0.05	0.04
St. Louis, MO	0.19	0.09	0.05	0.04
Seattle, WA	0.11	0.04	0.03	0.02
Topeka, KS	0.21	0.10	0.06	0.05
Waco, TX	0.24	0.12	0.07	0.06
Washington, DC	0.19	0.09	0.05	0.04

*Level of attic insulation.

5.2.4 Increased Insulation Levels

As a byproduct of these calculations, load reductions due to increasing the level of attic insulation were also calculated. Heating and cooling load reductions are given in Tables 5.10 and 5.11. Table 5.12 contains present value savings for increases of the insulation from R-11 to R-19, from R-19 to R-30, or from R-11 to R-30.

A rough estimate for contractor installed insulation is $0.02 per square foot per R-value. For example, increasing the insulation level from R-11 to R-30 costs about $0.38 per square foot. Table 5.12 shows that increasing the insulation level from R-11 to R-30 is cost justified for all locations except Los Angeles (airport), Miami, and Orlando (borderline).

5.2.5 Effect of Ducts in Attics

All of the load reduction and economic calculations presented thus far are based only on the impact of radiant barriers or ceiling insulation on house loads caused by heat gains or losses through the ceiling. Recent analytical work suggests that another factor that may increase the cost effectiveness of radiant barriers is related to heat gains or losses from HVAC ducts that are run through attic spaces.[54] In addition to decreasing heat flows through the ceiling, truss radiant barriers alter the temperature in the attic space and may reduce heat gains to air-conditioning ducts or heat losses from heating ducts.

The amount of extra energy saved will depend upon the general characteristics of the house and the HVAC equipment. Hoeschele[55] gives simulated results for the effects of duct insulation level and ceiling insulation level for houses in Sacramento having attics with and without truss radiant barriers. Expressing his results in terms of a percentage increase in cooling energy savings due to a radiant barrier in an attic with ducts referenced to one in an attic without ducts

Table 5.10. Annual heating load reductions due to increasing attic insulation level.

City	Load Reduction, Btu/square foot/year		
	R-11 to R-19*	R-19 to R-30	R-30 to R-38
Albany, NY	5358	2751	1030
Albuquerque, NM	3460	1697	626
Atlanta, GA	2660	1332	497
Bismarck, ND	7072	3610	1369
Chicago, IL	4923	2569	952
Denver, CO	4765	2450	872
El Toro, CA	1977	923	336
Houston, TX	1358	632	242
Knoxville, TN	3145	1584	599
Las Vegas, NV	2114	1042	375
Los Angeles, CA	1706	814	295
Memphis, TN	2711	1359	489
Miami, FL	254	121	38
Minneapolis, MN	6399	3323	1239
Orlando, FL	712	390	125
Phoenix, AZ	1444	744	318
Portland, ME	5870	3096	1137
Portland, OR	3980	1992	738
Raleigh, NC	2977	1489	606
Riverside, CA	2302	1121	406
Sacramento, CA	2651	1294	467
Salt Lake City, UT	4623	2321	858
St. Louis, MO	4010	2038	759
Seattle, WA	4328	2295	831
Topeka, KS	4297	2199	802
Waco, TX	1966	968	353
Washington, DC	3999	2014	731

*Initial and final levels of attic insulation.

Table 5.11. Annual cooling load reductions due to increasing attic insulation level.

City	Load Reduction, Btu/square foot/year		
	R-11 to R-19*	R-19 to R-30	R-30 to R-38
Albany, NY	1171	258	87
Albuquerque, NM	1100	698	189
Atlanta, GA	1649	508	184
Bismarck, ND	695	226	84
Chicago, IL	1061	293	99
Denver, CO	715	344	117
El Toro, CA	854	384	123
Houston, TX	1310	945	247
Knoxville, TN	1476	527	193
Las Vegas, NV	1960	997	369
Los Angeles, CA	214	122	25
Memphis, TN	1797	584	219
Miami, FL	1694	883	315
Minneapolis, MN	471	259	90
Orlando, FL	1435	691	284
Phoenix, AZ	3175	1334	488
Portland, ME	392	66	27
Portland, OR	368	316	60
Raleigh, NC	1375	434	153
Riverside, CA	1983	713	241
Sacramento, CA	1145	582	194
Salt Lake City, UT	966	462	159
St. Louis, MO	1482	444	186
Seattle, WA	169	73	23
Topeka, KS	991	465	193
Waco, TX	1606	819	317
Washington, DC	1210	392	138

*Initial and final levels of attic insulation.

Table 5.12. Present value savings for increasing attic insulation level.

City	Present value savings, dollars per square foot		
	R-11 to R-19*	R-19 to R-30	R-11 to R-30
Albany, NY	0.76	0.35	1.10
Albuquerque, NM	0.53	0.28	0.80
Atlanta, GA	0.50	0.21	0.71
Bismarck, ND	0.90	0.45	1.35
Chicago, IL	0.69	0.33	1.02
Denver, CO	0.64	0.32	0.96
El Toro, CA	0.33	0.15	0.48
Houston, TX	0.31	0.18	0.49
Knoxville, TN	0.53	0.24	0.78
Las Vegas, NV	0.47	0.23	0.70
Los Angeles, CA	0.22	0.11	0.33
Memphis, TN	0.52	0.22	0.74
Miami, FL	0.22	0.11	0.34
Minneapolis, MN	0.80	0.42	1.21
Orlando, FL	0.25	0.12	0.37
Phoenix, AZ	0.53	0.24	0.77
Portland, ME	0.73	0.37	1.09
Portland, OR	0.50	0.27	0.77
Raleigh, NC	0.50	0.22	0.72
Riverside, CA	0.49	0.21	0.70
Sacramento, CA	0.44	0.22	0.65
Salt Lake City, UT	0.65	0.32	0.97
St. Louis, MO	0.63	0.29	0.92
Seattle, WA	0.52	0.28	0.80
Topeka, KS	0.61	0.31	0.92
Waco, TX	0.41	0.21	0.62
Washington, DC	0.60	0.28	0.88

*Initial and final levels of attic insulation.

gives the following percentage increases for a duct insulation level of R-2.1: 19 percent, 35 percent, and 54 percent for ceiling insulation levels of R-7, R-19, and R-38.

It is interesting to examine the map shown in Figure 5.6, which shows the prevalence of basement, crawl spaces, and slab foundations.[56] The significance of this map is that houses built on slabs will generally have the HVAC ducts in the attic space, while houses built on crawl spaces and basements are less likely to have ducts in attics. While houses built on slabs constitute a large proportion of the houses south of the solid line, slabs are much less prevalent north of the line.

The region south of the solid line is also the region where radiant barriers are cost justified when used with the lower levels of attic insulation. Factoring in the effects on duct heat gains and losses may also make them cost justified for higher levels of insulation. These factors may also increase the radiant barrier cost that can be justified. Because of the many factors involved, further work is needed to analyze the impacts of duct heat gains and losses on radiant barrier performance.

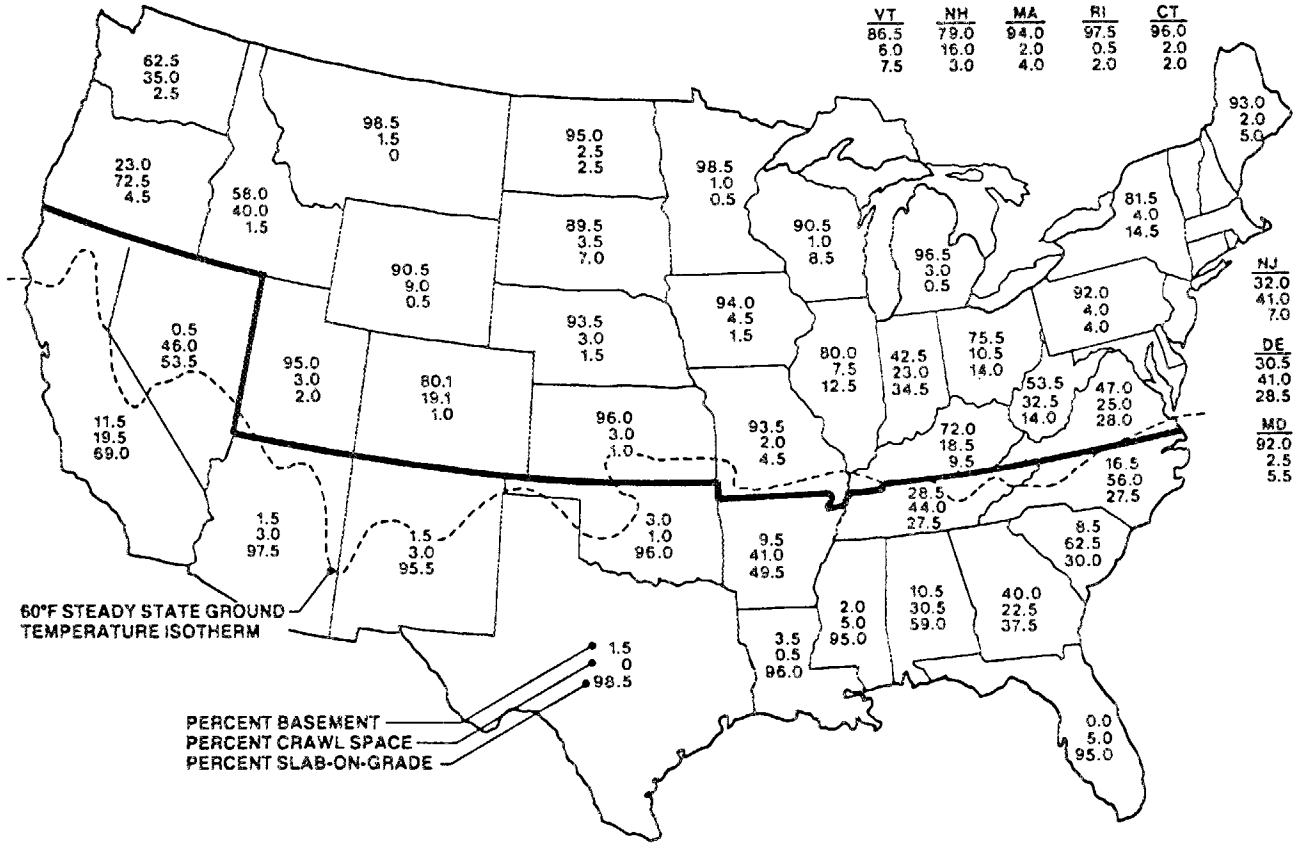

Fig. 5.6. Estimated share of basement, crawl space, and slab foundations by state.

6. ANALYSIS OF ANNUAL CYCLE MOISTURE ACCUMULATION

The model with moisture effects included has been used to estimate the hour-by-hour moisture accumulation on the underside of a clean horizontal radiant barrier due to diffusion of water vapor through the ceiling. Estimates have been made for a number of climatic conditions, and for a range of parameters, using basically the same prototypical house as was used for the annual energy analyses. One difference is that the areas of soffit and ridge vents are taken to be equal for the moisture modeling runs, with different vent areas being studied. For all runs, the drywall was taken to have a permeance of 37.5 and the insulation was taken to have a reciprocal permeance of 0.0086 per inch of thickness.

Several measures of moisture accumulation have been examined. First is the total amount of moisture that condenses on the radiant barrier over the year. This quantity would be of interest if it is assumed that all the moisture that condenses gets absorbed into the ceiling and is not released again. The second measure is the predicted peak of the hourly values. This number will be less than the total condensation due to evaporation that occurs during the year. Dates have been estimated for the occurrence of the peak, the first occurrence of significant accumulation, and the end of significant condensed moisture. From these dates is derived the duration of significant condensed moisture. "Significant condensation" has been defined with the somewhat arbitrary criterion of 0.005 pounds of water per square foot, or a continuous film only about 0.001 inches thick.

The model only estimates the amounts of water that have condensed and evaporated. It does not attempt to account for movement of liquid water after it has condensed. However, a yardstick has been used to develop somewhat arbitrary criteria for severity of potential moisture problems. The ceiling that is modeled has 2X4 wood joists 24 inches on center. With a density of 28 pounds per cubic foot, this corresponds to about 1 pound of wood per square foot. If all the condensed water

were absorbed by the wood, the fractional wood moisture content would increase by an amount equal to the amount of water per square foot. Assuming that the wood starts with a moisture content of about 10 percent, 0.1 pounds of water per square foot would increase the moisture content to 20 percent. The wood moisture content required to sustain decay is 24 to 31 percent. To provide a sufficient safety margin, ASHRAE recommends that the moisture content remain at 20 percent or less.[57] With this recommendation, we have arbitrarily defined a high potential for moisture problems as one in which the peak condensed water exceeds 0.15 pounds per square foot. Medium potentials are those between 0.03 and 0.15 pounds per square foot, and low potentials are those below 0.03 pounds per square foot. Since many attics will have more wood per unit area (e.g., 2X6 joists 16 inches on center), these ranges will be conservative. These ranges will also be conservative since a sustained high moisture content is needed for decay to occur.

6.1 IDENTIFICATION OF SIGNIFICANT VARIABLES

In addition to climate, the influence of the following parameters has been studied: indoor relative humidity, indoor temperature, radiant barrier permeance, ventilation area, insulation level, and vapor retarder permeance. The effect of some parameters is easy to envision, while other parameters will have competing effects. Increasing the indoor relative humidity would obviously be expected to increase moisture accumulation.

Increasing the indoor temperature may have two competing effects. First, for a fixed indoor relative humidity, an increase in indoor temperature will increase the indoor water vapor partial pressure and should increase condensation. But, an increased indoor temperature will also raise the temperature of the radiant barrier, reducing condensation.

An increase in radiant barrier permeance would allow water vapor to pass through more easily, thus reducing condensation. An increase in attic ventilation area should increase the ventilation rate. This should flush out water vapor that comes through the ceiling, reducing condensation, but it will also lower the radiant barrier temperature, increasing condensation.

Increasing the insulation level also has two competing effects. First, an increase in insulation level lowers the radiant barrier temperature, promoting condensation. But an increase in insulation level also lowers the permeance of the insulation, thus reducing condensation. Finally, increasing the permeance of a vapor retarder should increase condensation by allowing more water vapor to pass through the ceiling.

To determine the influence of these parameters, a number of model runs were made for a severe climate, Minneapolis. The conditions for the initial runs for this city are given in Table 6.1, with the results given in Table 6.2.

The first 32 runs constitute a two-level factorial design to investigate the relative influence of five parameters: relative humidity, indoor temperature, radiant barrier permeance, ventilation area, and insulation level.[58] For these 32 runs, the ceiling was assumed not to have a vapor retarder. Among these 32 runs, the worst case is Run 12, which corresponds to a 50 percent relative humidity, 75°F indoor temperature, a radiant barrier permeance of 0.05 (essentially a vapor retarder), an attic vent area to ceiling area ratio of 1/150, and R-11 insulation. For this case, the total accumulated water is 2.6 pounds per square foot. The best case is Run 29, which corresponds to a 20 percent relative humidity, a 70°F indoor temperature, a radiant barrier permeance of 20 (close to the value derived from field data at the Karns houses), a vent ratio of 1/150, and R-38 insulation. For this case, the total accumulated water is 0.03 pounds per square foot. Predicted durations of wetting varied

Table 6.1. Conditions for initial moisture model runs for Minneapolis.

Run	Relative Humidity, %	Indoor Temperature, °F	RB Perm	Vent/ Ceiling Area Ratio	Insulation Level	Vapor Retarder Perm
1	20	70	0.05	1/300	R-11	None
2	50	70	0.05	1/300	R-11	None
3	20	75	0.05	1/300	R-11	None
4	50	75	0.05	1/300	R-11	None
5	20	70	20	1/300	R-11	None
6	50	70	20	1/300	R-11	None
7	20	75	20	1/300	R-11	None
8	50	75	20	1/300	R-11	None
9	20	70	0.05	1/150	R-11	None
10	50	70	0.05	1/150	R-11	None
11	20	75	0.05	1/150	R-11	None
12	50	75	0.05	1/150	R-11	None
13	20	70	20	1/150	R-11	None
14	50	70	20	1/150	R-11	None
15	20	75	20	1/150	R-11	None
16	50	75	20	1/150	R-11	None
17	20	70	0.05	1/300	R-38	None
18	50	70	0.05	1/300	R-38	None
19	20	75	0.05	1/300	R-38	None
20	50	75	0.05	1/300	R-38	None
21	20	70	20	1/300	R-38	None
22	50	70	20	1/300	R-38	None
23	20	75	20	1/300	R-38	None
24	50	75	20	1/300	R-38	None
25	20	70	0.05	1/150	R-38	None
26	50	70	0.05	1/150	R-38	None
27	20	75	0.05	1/150	R-38	None
28	50	75	0.05	1/150	R-38	None
29	20	70	20	1/150	R-38	None
30	50	70	20	1/150	R-38	None
31	20	75	20	1/150	R-38	None
32	50	75	20	1/150	R-38	None
33	50	75	0.05	1/150	R-11	0.06
34	50	75	20	1/150	R-11	0.06
35	50	75	0.05	1/150	R-11	1
36	50	75	20	1/150	R-11	1

Table 6.2. Results of initial moisture model runs for Minneapolis.

Run	Total Water, lb/ft^2	Peak Water, lb/ft^2	Start Date	Peak Date	Dry Date	Duration of Wetting, days
1	0.178	0.107	12/06	02/11	03/17	102
2	1.848	1.696	10/02	04/01	07/22	294
3	0.272	0.184	12/06	02/11	04/02	118
4	2.520	2.252	10/01	04/24	Wet	>304
5	0.058	0.018	01/12	01/22	01/26	15
6	0.995	0.864	11/06	03/16	05/15	191
7	0.092	0.035	01/11	01/22	02/12	33
8	1.433	1.311	11/03	04/01	06/02	212
9	0.195	0.127	12/06	02/11	03/22	107
10	1.910	1.762	10/02	04/01	07/26	298
11	0.297	0.213	12/06	02/17	04/06	122
12	2.608	2.349	09/30	04/24	Wet	>305
13	0.064	0.023	01/11	01/22	02/04	25
14	1.061	0.942	11/04	03/16	05/20	197
15	0.104	0.042	12/24	02/09	02/16	55
16	1.528	1.420	11/03	04/01	06/07	217
17	0.127	0.090	12/14	02/17	04/07	115
18	0.939	0.838	10/02	04/01	07/22	294
19	0.188	0.149	12/06	03/06	04/21	137
20	1.267	1.119	09/30	04/24	Wet	>305
21	0.034	0.010	01/16	01/22	01/26	11
22	0.405	0.324	11/17	04/01	04/25	160
23	0.052	0.018	01/12	01/22	02/12	32
24	0.582	0.493	11/05	03/16	05/12	189
25	0.128	0.094	12/14	03/06	05/09	117
26	0.946	0.850	10/02	04/01	07/27	299
27	0.189	0.155	12/06	03/06	04/25	141
28	1.279	1.151	09/30	05/02	Wet	>305
29	0.032	0.010	01/16	01/22	01/27	12
30	0.413	0.337	11/17	03/06	04/27	162
31	0.051	0.020	01/12	02/09	02/15	35
32	0.597	0.513	11/05	03/16	05/15	191
33	0.006	0.006	03/05	04/01	04/12	41
34	0.000	0.000	-	-	-	0
35	0.137	0.123	11/13	04/14	Wet	>261
36	0.000	0.000	-	01/17	-	0

greatly, ranging from 12 days to more than 300 days. For some of the worst cases, the radiant barrier was not dry at the end of the annual cycle, indicating that a continuous buildup of moisture could occur.

The influence of each parameter can be determined by examining runs that are identical except for a change in one parameter. With the two-level factorial design, 16 sets of runs can be examined for each parameter. A summary of such an analysis of the factorial runs is given in Table 6.3. The quantities given are the ratio of either total or peak water for the first level of a variable to the value for the second level. The order of levels of the variables is given in parentheses. A range of ratios is given for the 16 sets of runs.

As expected, the most important variable was found to be the relative humidity. The total condensed water was 7 to 17 times higher with a relative humidity of 50 percent than with a relative humidity of 20 percent. The larger values of this ratio corresponded to an indoor temperature of 75°F (also as might be expected).

The second most important variable was found to be the radiant barrier permeance. Total water accumulated with an RB with a permeance of 0.05 was 1.7 to 4 times as high as that with an RB with a permeance of 20.

The next two most important variables are the indoor temperature and the insulation level. Changing the indoor temperature from 70°F to 75°F produced an increase in total water of 35 to 63 percent. It was found that higher insulation levels result in lower amounts of water, presumably because of their higher resistance to vapor flow. With R-11 insulation, the total water was 40 percent to 2.6 times as high as with R-38 insulation.

Table 6.3. Effect of variables on moisture accumulation for Minneapolis.

Variable	Ratios*	
	Total Water, lb/ft^2	Peak Water, lb/ft^2
Relative humidity (50%/20%)	6.7 - 17.2	7.4 - 49.1
Indoor temperature (75°F/70°F)	1.35 - 1.63	1.33 - 2.01
Radiant barrier perm (0.05/20)	1.71 - 4.05	1.65 - 9.13
Vent area (1/150 / 1/300)	0.94 - 1.13	1.00 - 1.31
Insulation level (R-11/R-38)	1.40 - 2.57	1.20 - 2.79

* Values in table are ratios for two levels of one parameter, with all other parameters equal.

The least important variable was found to be the vent area. For most of the runs, the larger vent area resulted in the higher amount of water, but only up to 13 percent more.

Because of the smaller sensitivity of condensed moisture to the vent area, it's value was held constant at 1/150 for all succeeding model runs. Also, for succeeding runs, the insulation level was taken to be R-11. This corresponds to the worst case, but is also the configuration where radiant barriers come closest to being economically justified. Also, the indoor temperature was chosen to be 75°F for other runs, to give a worst case. With these simplifications, the two remaining variables, the radiant barrier permeance and the indoor relative humidity, could be studied in greater detail for a wide range of climates.

Before looking at these two parameters in detail, it is important to determine the impact of an existing vapor retarder. Run 33 is a repeat of the worst case, Run 12, with the addition of a vapor retarder with a permeance of 0.06 on the bottom of the ceiling. This resulted in a total amount of water of only 0.006 pounds per square foot, which is practically insignificant. Run 34 is a repeat of Run 16 (radiant barrier perm of 20), with a 0.06 perm vapor retarder. In this case, it was predicted that no water would condense. The significance of these runs is that the potential for water condensation is essentially eliminated for all climates and radiant barrier permeances if a continuous vapor retarder with a permeance of 0.06 is present.

Runs 35 and 36 are repeats of runs 33 and 34, but with a vapor retarder having a permeance of 1, which is characteristic of vapor retarder paints. Clearly, this type of vapor retarder is a great improvement over no vapor retarder, but does not provide as much protection as one with a permeance of 0.06.

6.2 PARAMETRIC STUDY FOR VARIOUS CLIMATES

Parametric runs of the moisture model were performed for a subset of the locations that were used for the energy savings analyses in Section 5. These locations, arranged in order of expected decreasing severity of moisture accumulation problems, are: Minneapolis, Chicago, St. Louis, Washington, DC, Knoxville, Atlanta, Portland, OR, Waco, TX, Phoenix, Los Angeles, and Miami. For each location, runs were performed over a wide range of radiant barrier permeances, and for most locations, also over a wide range of indoor relative humidities. For all runs in this section, the following conservative conditions were used: 75°F indoor temperature, vent area to ceiling area ratio of 1/150, R-11 ceiling insulation, and no vapor retarder.

Representative plots of amount of condensed water versus time are given in Figures 6.1 through 6.4. These figures illustrate two locations, Minneapolis and Knoxville, two relative humidity levels, 50 percent and 35 percent, and three radiant barrier permeance levels, 0.05, 20, and 100. The worst case is Minneapolis with a 50 percent relative humidity and a 0.05 perm radiant barrier. For this case, condensed moisture becomes significant at the end of September, rises to a peak of 2.3 pounds per square foot on April 24, and at the end of July still has over 0.6 pounds per square foot of water left. When the radiant barrier permeance is raised to 20, significant condensation is delayed until November, a peak of 1.4 pounds per square foot occurs on April 1, and the moisture has disappeared by early June. With a radiant barrier permeance of 100, significant condensation does not occur until December, the peak of 0.15 pounds per square foot is reached on February 9 and the radiant barrier is dry after February 20.

Lowering the relative humidity to 35 percent, as shown in Figure 6.2, delays the occurrence of significant condensation, significantly lowers the peak condensation, and hastens the occurrence of drying.

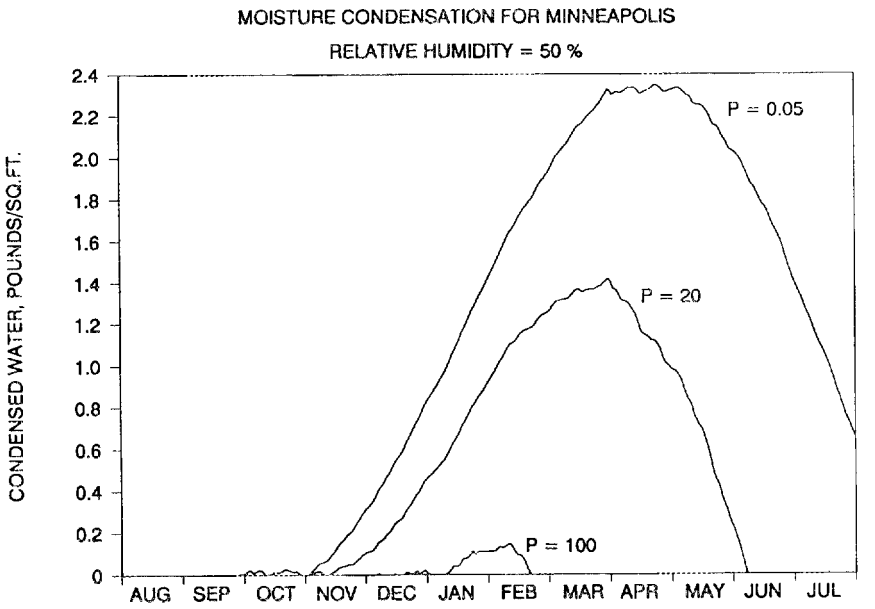

Fig. 6.1. Moisture condensation for Minneapolis with 50 percent indoor relative humidity. Labels on curves indicate the perm values of the radiant barrier.

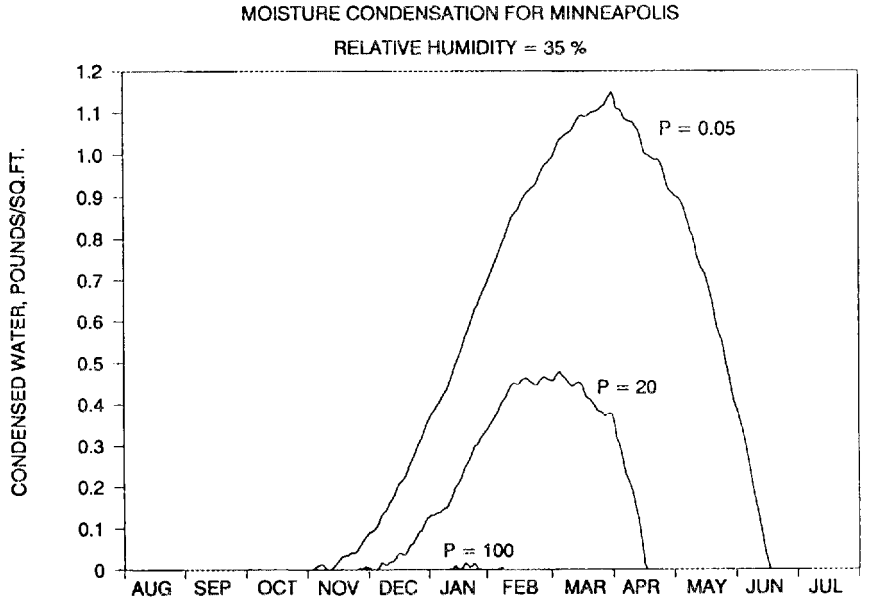

Fig. 6.2. Moisture condensation for Minneapolis with 35 percent indoor relative humidity. Labels on curves indicate the perm values of the radiant barrier.

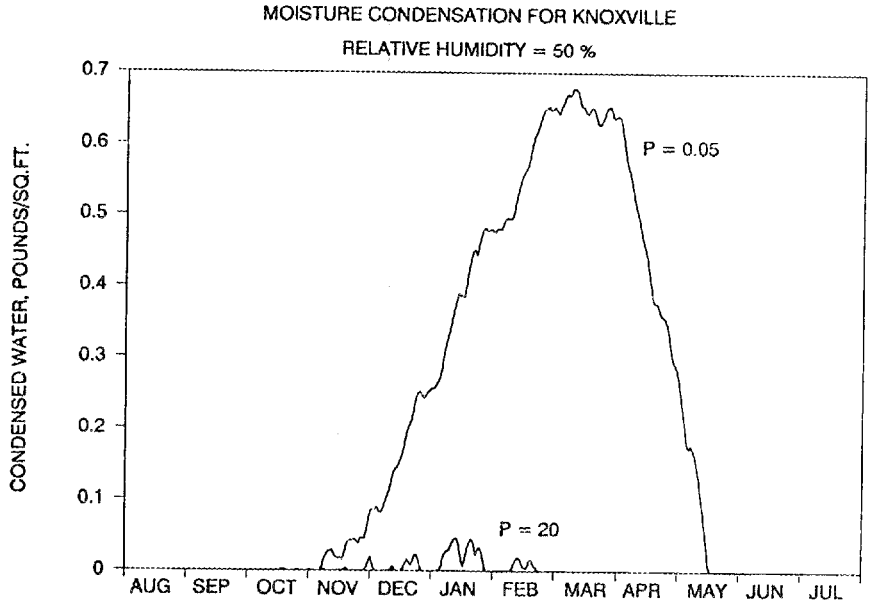

Fig. 6.3. Moisture condensation for Knoxville with 50 percent indoor relative humidity. Labels on curves indicate the perm values of the radiant barrier.

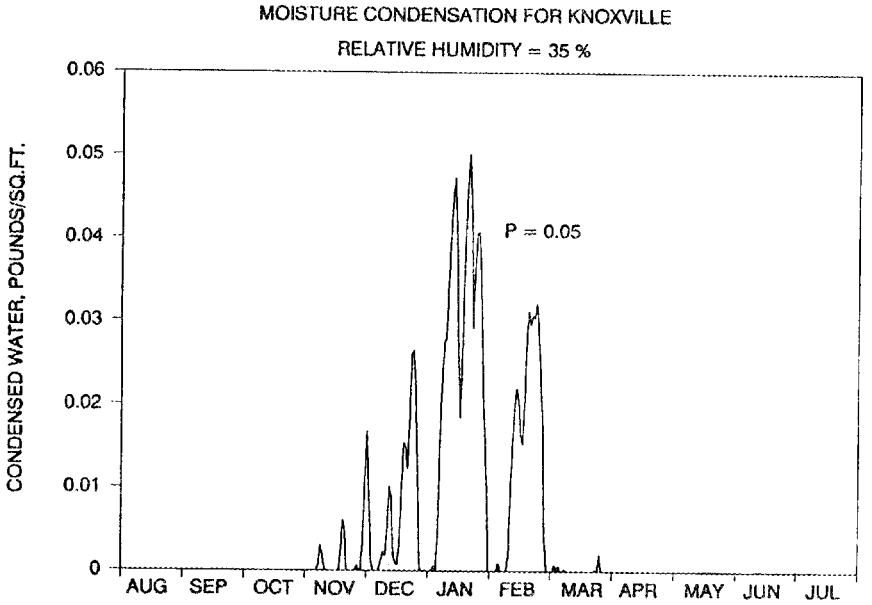

Fig. 6.4. Moisture condensation for Knoxville with 35 percent indoor relative humidity. Label on curve indicates the perm value of the radiant barrier.

An indication of the significant role of climate may be obtained by comparing corresponding plots for Minneapolis and Knoxville. Figure 6.3 shows that for Knoxville, with 50 percent relative humidity and a radiant barrier permeance of 0.05, condensation begins early in November, rises to a peak of 0.7 pounds per square foot on March 10, and is dried out by the middle of May. With a permeance of 20, the plot shows different qualitative features. Instead of having continuous condensed water, the radiant barrier shows several periods of wetting and drying, with a much reduced peak value. Figure 6.4 also shows the alternate periods of wetting and drying with a relative humidity of 35 percent and a radiant barrier permeance of 0.05.

Summaries of all the runs for each location are given in Tables 6.4 through 6.14. These tables show the total amount of water that condenses on the radiant barrier over the year, the peak amount of condensed water, the dates for start of significant condensation, the date on which the peak amount occurs, the date on which the moisture has disappeared, and the duration of the wetting period.

A full matrix of runs was performed for Minneapolis. The peak amount of water is plotted in Figure 6.5 as a function of radiant barrier permeance and relative humidity. This figure shows that the peak amount of water is a very strong function of both these variables. Considering a peak level of more than 0.15 pounds per square foot as a high potential for moisture problems, these results indicate that radiant barrier permeances less than 100, 50, and 5 will have high potential for problems if the indoor relative humidity is 50 percent, 35 percent, and 20 percent, respectively. To obtain peak water amounts below 0.03 pounds per square foot, for a low potential for moisture problems, requires radiant barrier permeances greater than about 190, 95, and 30 for the same relative humidities.

As the climate becomes milder, Tables 6.4 through 6.14 show that the amounts of condensed moisture also become less. For the milder climates, model runs concentrated on the higher indoor relative

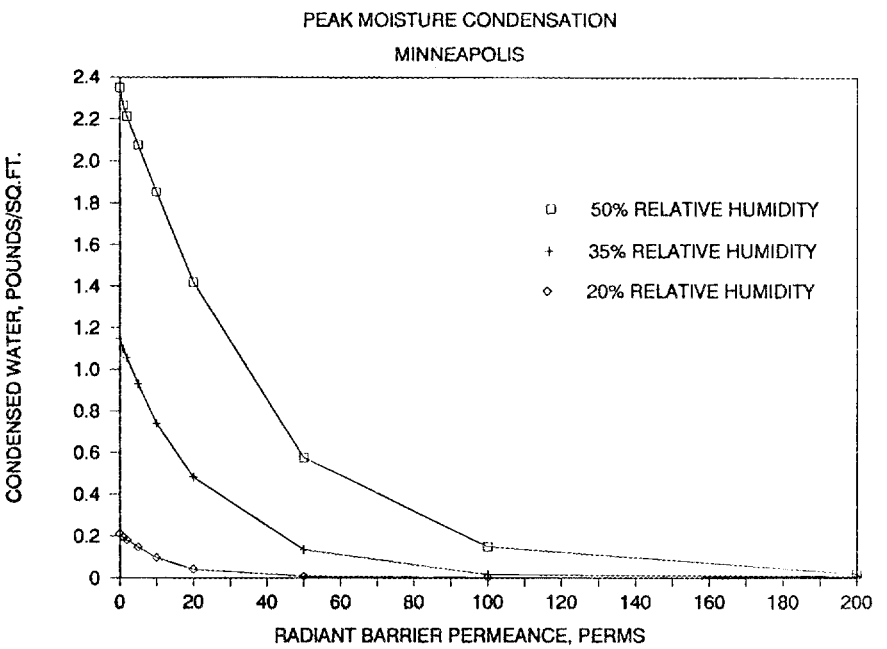

Fig. 6.5. Peak moisture condensation for Minneapolis.

Table 6.4. Moisture accumulation for Minneapolis.

Relative Humidity, %	RB Perm	Total Water, lb/ft^2	Peak Water, lb/ft^2	Start Date	Peak Date	Dry Date	Duration of Wetting, days
50	0.05	2.608	2.349	09/30	04/24	Wet	>305
50	1	2.513	2.265	10/01	04/24	Wet	>304
50	2	2.444	2.213	10/01	04/01	Wet	>304
50	5	2.253	2.077	10/01	04/01	07/29	302
50	10	1.976	1.855	10/01	04/02	07/08	280
50	20	1.528	1.420	11/03	04/01	06/07	217
50	50	0.736	0.577	11/28	02/17	04/13	137
50	100	0.283	0.150	12/06	02/09	02/20	77
50	200	0.077	0.020	01/12	01/17	02/04	24
35	0.05	1.232	1.149	11/04	04/01	06/17	226
35	1	1.176	1.098	11/04	04/01	06/13	222
35	2	1.133	1.056	11/04	04/01	06/09	218
35	5	1.013	0.931	11/04	04/01	05/29	207
35	10	0.842	0.741	11/14	03/16	05/14	182
35	20	0.593	0.481	11/28	03/06	04/17	141
35	50	0.240	0.138	12/06	02/09	02/26	83
35	100	0.074	0.018	01/12	01/22	02/04	24
35	200	0.017	0.007		01/17		1
20	0.05	0.297	0.213	12/06	02/17	04/06	122
20	1	0.279	0.195	12/06	02/11	04/04	120
20	2	0.264	0.182	12/06	02/11	04/02	118
20	5	0.223	0.148	12/06	02/11	03/22	107
20	10	0.170	0.099	12/20	02/11	03/07	78
20	20	0.104	0.042	12/24	02/09	02/16	55
20	50	0.030	0.008	01/17	01/17	01/21	6
20	100	0.007	0.003		01/17		1
20	200	0.001	0.001		01/17		

Note, fixed parameters: Indoor temperature = 75°F
Vent area/ceiling area = 1/150
Insulation level = R-11
No vapor retarder

Table 6.5. Moisture accumulation for Chicago.

Relative Humidity, %	RB Perm	Total Water, lb/ft^2	Peak Water, lb/ft^2	Start Date	Peak Date	Dry Date	Duration of Wetting, days
50	0.05	1.910	1.726	10/16	04/14	07/25	283
50	1	1.822	1.646	10/16	04/14	07/19	277
50	2	1.752	1.579	10/16	04/14	07/14	272
50	5	1.560	1.405	11/09	04/02	06/29	233
50	10	1.279	1.133	11/10	04/02	06/08	211
50	20	0.840	0.721	11/18	03/07	05/09	173
50	50	0.251	0.118	12/01	02/07	03/07	97
50	100	0.051	0.019	01/27	01/30	02/20	25
50	200	0.004	0.002	01/27	01/27	01/27	
35	0.05	0.725	0.608	11/17	03/16	05/21	186
35	1	0.676	0.565	11/18	03/16	05/15	179
35	2	0.635	0.527	11/18	03/16	05/12	176
35	5	0.526	0.418	11/19	03/07	04/29	162
35	10	0.387	0.252	11/28	03/06	04/07	131
35	20	0.221	0.102	12/01	02/21	03/10	100
35	50	0.051	0.019	01/27	01/30	02/20	25
35	100	0.007	0.002	01/27	01/27	01/27	
35	200	0.000	0.000				
20	0.05	0.106	0.048	12/02	02/07	03/06	95
20	1	0.097	0.044	12/02	02/06	03/06	95
20	2	0.089	0.040	12/02	02/06	02/22	83
20	5	0.069	0.029	12/02	02/06	02/21	82
20	10	0.045	0.017	01/27	01/31	02/21	26
20	20	0.019	0.008	01/28	01/30	01/31	4
20	50	0.002	0.001	01/27	01/27	01/27	
20	100	0.000	0.000				

Note, fixed parameters: Indoor temperature = 75°F
Vent area/ceiling area = 1/150
Insulation level = R-11
No vapor retarder

Table 6.6. Moisture accumulation for St. Louis.

Relative Humidity, %	RB Perm	Total Water, lb/ft^2	Peak Water, lb/ft^2	Start Date	Peak Date	Dry Date	Duration of Wetting, days
50	0.05	1.461	1.223	10/19	04/02	06/17	242
50	1	1.385	1.143	10/30	03/31	06/11	225
50	2	1.325	1.073	10/30	03/31	06/17	221
50	5	1.159	0.866	10/30	03/31	05/15	208
50	10	0.927	0.625	11/09	02/17	05/12	175
50	20	0.605	0.343	11/10	02/16	04/11	143
50	50	0.191	0.060	12/04	01/12	02/13	72
50	100	0.033	0.006	01/10	01/10	01/11	2
50	200	0.001	0.001		01/10		
35	0.05	0.499	0.280	11/10	02/16	04/09	151
35	1	0.464	0.250	11/10	02/16	04/05	147
35	2	0.435	0.221	11/10	02/16	04/02	144
35	5	0.359	0.136	11/30	02/15	03/31	122
35	10	0.266	0.072	12/11	01/13	02/18	80
35	20	0.151	0.048	12/05	01/12	02/14	72
35	50	0.031	0.007	01/10	01/12	02/09	31
35	100	0.002	0.001		01/10		
35	200	0.000	0.000				
20	0.05	0.061	0.020	12/18	01/12	02/11	56
20	20	0.009	0.002		02/09		

Note, fixed parameters: Indoor temperature = 75°F
Vent area/ceiling area = 1/150
Insulation level = R-11
No vapor retarder

Table 6.7. Moisture accumulation for Washington, DC.

Relative Humidity, %	RB Perm	Total Water, lb/ft^2	Peak Water, lb/ft^2	Start Date	Peak Date	Dry Date	Duration of Wetting, days
50	0.05	1.377	1.091	10/03	04/01	06/20	261
50	1	1.295	1.005	10/04	04/01	06/13	253
50	2	1.226	0.927	10/04	04/01	06/07	247
50	5	1.038	0.725	10/31	03/24	05/21	203
50	10	0.779	0.514	10/31	03/02	04/29	181
50	20	0.431	0.177	11/11	02/22	04/01	142
50	50	0.092	0.026	01/01	01/19	02/15	46
50	100	0.016	0.005		01/31		
50	200	0.003	0.002		01/31		
35	0.05	0.425	0.235	11/08	03/01	04/06	150
35	1	0.387	0.195	11/08	03/01	04/02	146
35	2	0.354	0.157	11/11	02/27	04/01	142
35	5	0.272	0.088	12/16	02/22	03/09	84
35	10	0.178	0.044	12/30	01/20	02/27	60
35	20	0.085	0.023	01/15	01/19	02/05	22
35	50	0.014	0.004		01/31		
35	100	0.003	0.002		01/31		
35	200	0.000	0.000		01/31		

Note, fixed parameters: Indoor temperature = 75°F
Vent area/ceiling area = 1/150
Insulation level = R-11
No vapor retarder

Table 6.8. Moisture accumulation for Knoxville.

Relative Humidity, %	RB Perm	Total Water, lb/ft^2	Peak Water, lb/ft^2	Start Date	Peak Date	Dry Date	Duration of Wetting, days
50	0.05	1.003	0.682	11/07	03/10	05/17	192
50	1	0.935	0.607	11/07	03/10	05/12	187
50	2	0.878	0.536	11/07	03/10	05/08	183
50	5	0.728	0.373	11/07	02/24	04/12	157
50	10	0.533	0.161	11/07	01/24	03/26	140
50	20	0.289	0.051	11/18	01/12	02/21	96
50	50	0.054	0.018	01/05	01/18	01/20	16
50	100	0.006	0.002		01/16		
50	200	0.000	0.000				
35	0.05	0.288	0.051	11/08	01/20	02/26	111
35	1	0.262	0.045	11/18	01/12	02/26	101
35	2	0.239	0.042	11/19	01/12	02/25	99
35	5	0.183	0.032	11/29	01/12	02/19	83
35	10	0.119	0.022	11/30	01/19	02/18	81
35	20	0.051	0.014	01/05	01/18	01/20	16
35	50	0.007	0.002		01/16		
35	100	0.000	0.000				
35	200	0.000	0.000				

Note, fixed parameters: Indoor temperature = 75°F
Vent area/ceiling area = 1/150
Insulation level = R-11
No vapor retarder

Table 6.9. Moisture accumulation for Atlanta.

Relative Humidity, %	RB Perm	Total Water, lb/ft^2	Peak Water, lb/ft^2	Start Date	Peak Date	Dry Date	Duration of Wetting, days
50	0.05	0.765	0.467	11/07	03/02	04/26	171
50	1	0.708	0.412	11/07	03/02	04/23	168
50	2	0.660	0.359	11/07	03/02	04/17	162
50	5	0.535	0.211	11/07	02/28	04/01	146
50	10	0.378	0.081	11/18	01/15	03/31	134
50	20	0.187	0.052	11/29	01/14	02/20	84
50	50	0.015	0.003		01/13		
50	100	0.000	0.000				
50	200	0.000	0.000				
35	0.05	0.175	0.040	11/29	01/14	02/20	84
35	2	0.140	0.035	11/29	01/14	02/20	84
35	20	0.014	0.003		01/13		

Note, fixed parameters: Indoor temperature = 75°F
Vent area/ceiling area = 1/150
Insulation level = R-11
No vapor retarder

Table 6.10. Moisture accumulation for Portland, OR.

Relative Humidity, %	RB Perm	Total Water, lb/ft^2	Peak Water, lb/ft^2	Start Date	Peak Date	Dry Date	Duration of Wetting, days
50	0.05	0.960	0.745	10/13	04/01	06/21	252
50	2	0.817	0.618	10/14	03/19	06/06	236
50	10	0.425	0.260	11/22	02/19	04/13	143
50	20	0.175	0.040	11/26	12/22	02/12	79
50	50	0.007	0.002		12/13		
50	100	0.000	0.000		12/20		
35	0.05	0.133	0.037	12/13	12/22	02/12	62
35	2	0.100	0.029	12/13	12/21	02/06	56
35	20	0.005	0.001		12/13		

Note, fixed parameters: Indoor temperature = 75°F
Vent area/ceiling area = 1/150
Insulation level = R-11
No vapor retarder

Table 6.11. Moisture accumulation for Waco, TX.

Relative Humidity, %	RB Perm	Total Water, lb/ft^2	Peak Water, lb/ft^2	Start Date	Peak Date	Dry Date	Duration of Wetting, days
50	0.05	0.520	0.144	11/08	02/24	03/23	136
50	2	0.442	0.100	11/09	02/17	03/17	129
50	10	0.239	0.030	12/01	01/31	03/15	105
50	20	0.111	0.019	12/29	01/31	02/13	57
50	50	0.006	0.001		01/16		
50	100	0.000	0.000				
35	0.05	0.106	0.013	12/18	01/06	02/14	59
35	2	0.083	0.011	12/19	01/06	02/14	58
35	20	0.006	0.002		01/05		

Note, fixed parameters: Indoor temperature = 75°F
Vent area/ceiling area = 1/150
Insulation level = R-11
No vapor retarder

Table 6.12. Moisture accumulation for Phoenix.

Relative Humidity, %	RB Perm	Total Water, lb/ft^2	Peak Water, lb/ft^2	Start Date	Peak Date	Dry Date	Duration of Wetting, days
50	0.05	0.300	0.060	12/10	01/07	02/23	76
50	1	0.262	0.050	12/27	01/07	02/23	59
50	2	0.229	0.043	12/27	01/06	01/13	18
50	5	0.153	0.026	12/27	01/01	01/08	13
50	10	0.078	0.011	12/28	12/31	01/02	6
50	20	0.022	0.003		12/31		
50	50	0.000	0.000		12/31		
50	100	0.000	0.000				
50	200	0.000	0.000				
35	0.05	0.034	0.003		12/31		
35	2	0.022	0.002		12/31		
35	20	0.000	0.000		12/31		

Note, fixed parameters: Indoor temperature = 75°F
Vent area/ceiling area = 1/150
Insulation level = R-11
No vapor retarder

Table 6.13. Moisture accumulation for Los Angeles.

Relative Humidity, %	RB Perm	Total Water, lb/ft^2	Peak Water, lb/ft^2	Start Date	Peak Date	Dry Date	Duration of Wetting, days
50	0.05	0.075	0.007	12/29	12/30	12/30	2
50	1	0.057	0.005		12/29		
50	2	0.044	0.004		12/29		
50	5	0.019	0.003		12/29		
50	10	0.004	0.001		12/29		
50	20	0.000	0.000		12/29		

Note, fixed parameters: Indoor temperature = 75°F
Vent area/ceiling area = 1/150
Insulation level = R-11
No vapor retarder

Table 6.14. Moisture accumulation for Miami.

Relative Humidity, %	RB Perm	Total Water, lb/ft^2	Peak Water, lb/ft^2	Start Date	Peak Date	Dry Date	Duration of Wetting, days
50	0.05	0.022	0.004		12/16		
50	1	0.018	0.004		12/16		
50	2	0.015	0.004		12/16		
50	5	0.009	0.003		12/16		
50	10	0.003	0.002		12/16		
50	20	0.000	0.000				

Note, fixed parameters: Indoor temperature = 75°F
Vent area/ceiling area = 1/150
Insulation level = R-11
No vapor retarder

humidities and lower radiant barrier permeances. The runs for St. Louis show that there is a low potential for moisture problems with any radiant barrier permeance if the relative humidity is 20 percent. Because of this, the 20 percent level was not used for milder climates. An abbreviated set of runs was performed for the 35 percent level for climates milder than Knoxville, and no runs for this level were performed for Los Angeles or Miami.

Figure 6.6 shows the peak amount of water plotted against heating degree days for a relative humidity of 50 percent and for three radiant barrier permeances. Figure 6.7 is a similar plot, except with a humidity of 35 percent. Visually fitted curves have been drawn through the points. Both figures show a good correlation between peak condensed water and heating degree days. The points at 4600 degree days that appear to be below the curves are for Portland, OR. These may be below the curves for the other locations because of the particular climatic conditions that occur in the Pacific Northwest.

Figure 6.6 shows that with a 50 percent relative humidity, a radiant barrier with a permeance of 0.05, which may be representative of unperforated foil-type radiant barriers, has a high potential for moisture problems in almost all locations. Exceptions are Los Angeles and Miami. For the more normal case of a 35 percent relative humidity, this radiant barrier permeance would have a high potential for moisture problems (greater than 0.15 pounds per square foot of condensed water) for locations having greater than about 4500 heating degree days, and a low potential (less than 0.03 pounds per square foot) for locations with less than about 3000 heating degree days. Zones for high, medium, and low potential for moisture problems with a 35 percent relative humidity and a 0.05 perm radiant barrier are shown in Figure 6.8.

Increasing the radiant barrier permeance to 20, which may be typical of the perforated type used in the Karns house experiments, leads to much reduced potential for moisture problems. With a 50 percent relative humidity, there is a high potential for heating degree

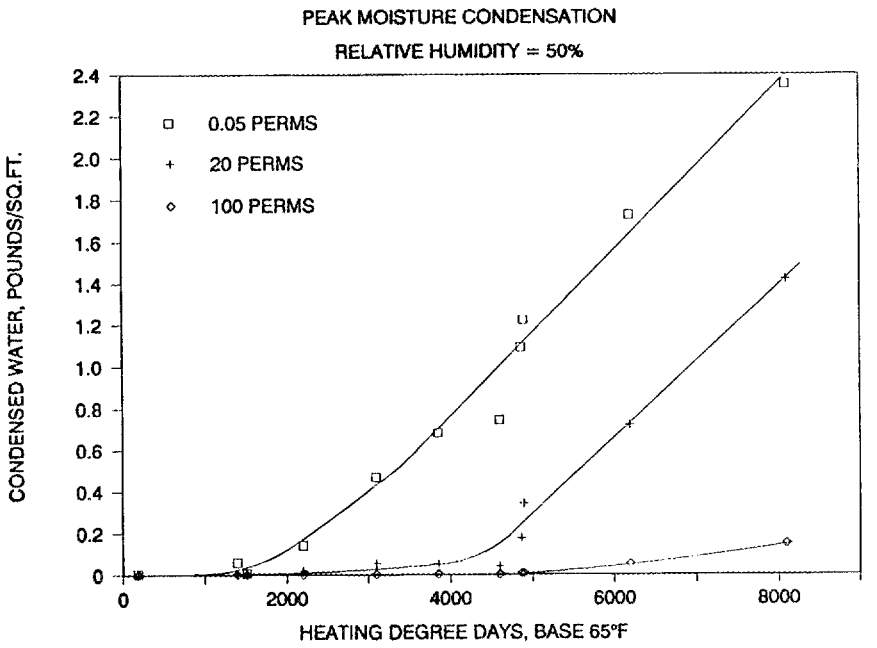

Fig. 6.6. Peak moisture condensation for 50 percent indoor relative humidity. Legends indicate perm values for the radiant barrier.

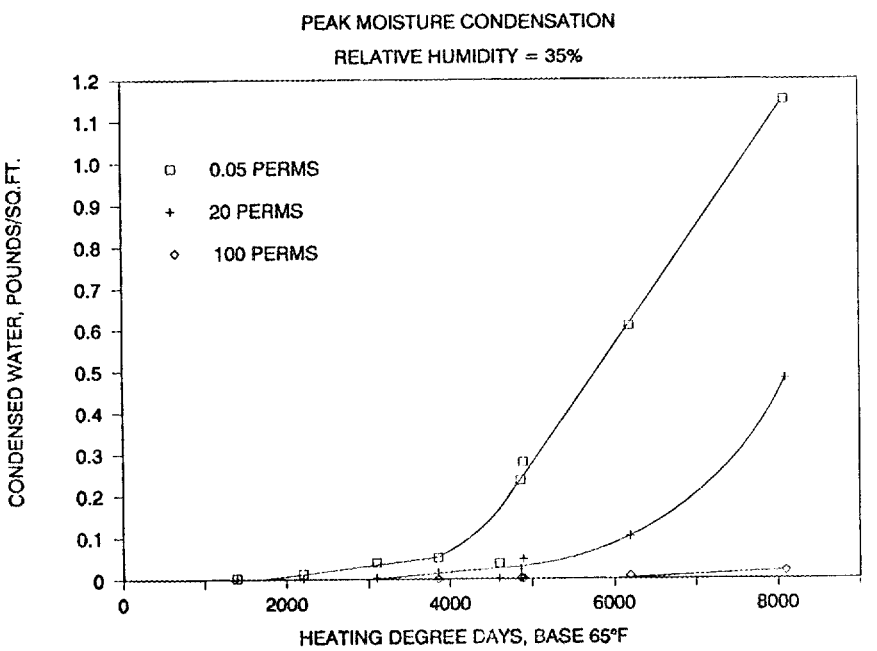

Fig. 6.7. Peak moisture condensation for 35 percent indoor relative humidity. Legends indicate perm values for the radiant barrier.

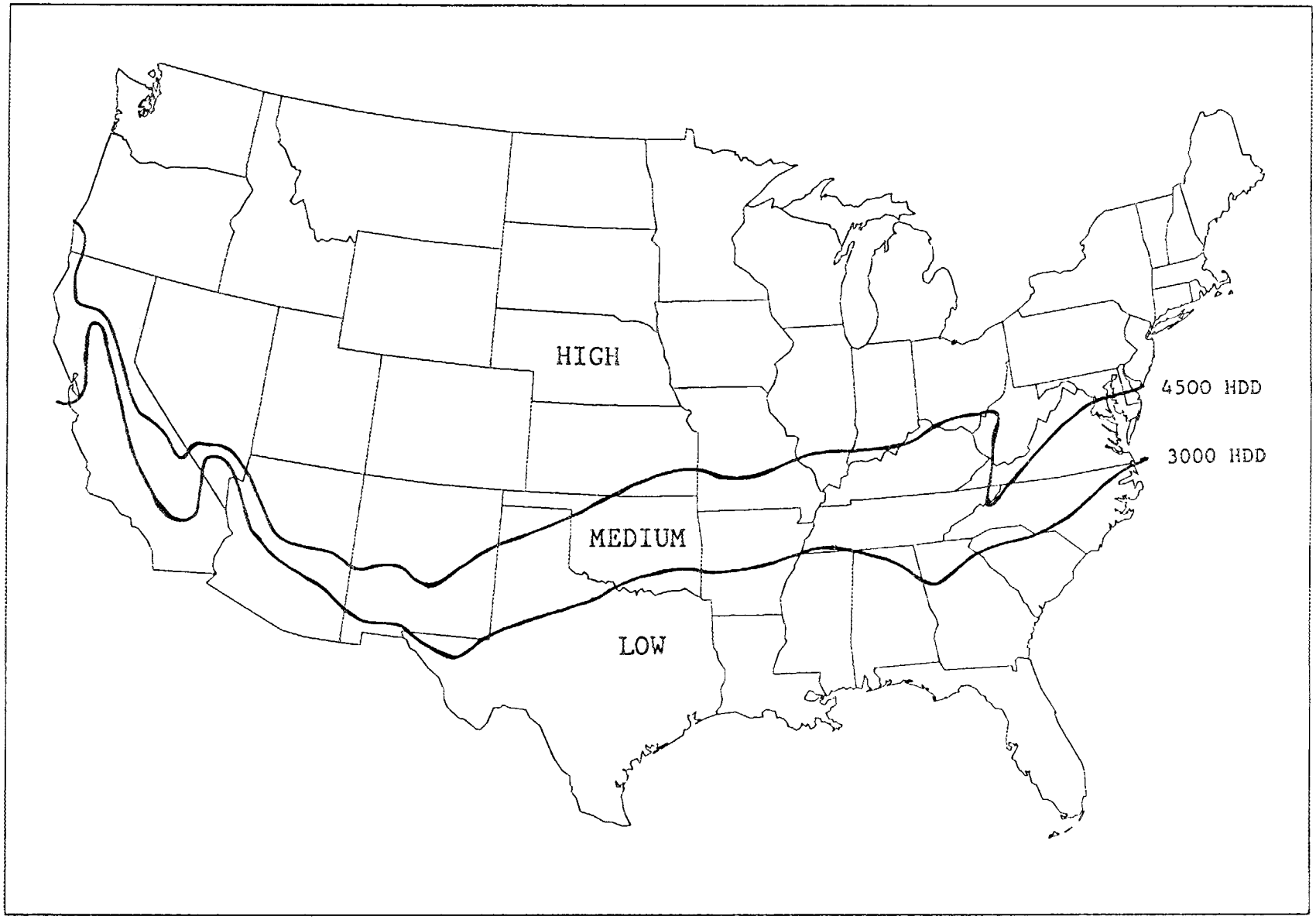

Fig. 6.8. Regions for high, medium, and low potential for moisture condensation problems with horizontal RB with perm of 0.05 and with 35 percent indoor relative humidity.

days above about 4500, and a low potential for degree days below about 3000. With a 35 percent relative humidity and a perm of 20, these heating degree day figures are about 6500 and 5000.

Increasing the radiant barrier permeance to 100, which may be typical of metallized spunbonded polyolefins, essentially eliminates the potential for moisture problems, except in the coldest climates and for the highest humidities.

6.3 EFFECT OF CONVECTIVE MOISTURE TRANSPORT

All of the calculations given above are based on diffusion of water vapor through the ceiling. A bulk flow of moist air has the potential to carry much larger quantities of water vapor. Although the model has convective flow built into it, this feature has not been exercised. This is largely because of a lack of data on air flow rates through ceilings. In addition, while diffusive flow would exist over the entire ceiling area, convective air flows would be expected to be localized around areas where the ceiling is penetrated, for example, by vents and light fixtures. The best policy would appear to be to locate these penetrations and avoid placing radiant barriers over them.

7.0 SUMMARY AND CONCLUSIONS

The model for the thermal performance of attics containing radiant barriers has been modified to allow predictions of moisture accumulation under horizontal radiant barriers. Flow of water vapor both by vapor diffusion and by convective flow of moist air has been included in the model. However, the convective flow portion has not yet been exercised.

Ceiling heat flows predicted by the model have been compared with those measured during the experiment at the Karns houses during the winter of 1987-1988. Heat fluxes measured by three transducers showed considerable variations that are thought to be due to local variations in the insulation R-value. Considering the variations among the transducers, the model predictions are felt to be in very reasonable agreement with the measured values.

The moisture accumulation model has been partially validated by comparing its predictions with observations of moisture accumulation during the same experiments with the Karns houses. The model predictions agree with the qualitative observations that the radiant barrier often had visible condensation in the morning that usually evaporated when the attic warmed up during the day. The model also predicts the continuing buildup of moisture that was observed during a very cold period of time. Quantitative predictions of amounts of condensed moisture are within the right magnitude of weight changes measured for blotter paper that was placed between the insulation and the radiant barriers. Uncertainties in the permeances of the various layers in the ceiling result in corresponding uncertainties in the quantitative predictions.

Because of the uncertainties in permeances, it is considered that the model can be used for parametric studies and for development of guidelines, but at this stage, it can't be used to predict actual moisture condensation rates for a particular application with a high

degree of certainty. Additional research is needed to measure and document the permeances of various types of radiant barriers.

The thermal model has been used to estimate energy savings potentials for various types of radiant barriers in various climates. Using a prototypical ranch-style house, the attic/radiant barrier model was used to predict hour-by-hour heat fluxes through the ceiling. These heat fluxes were then brought into the DOE-2.1C model to estimate whole house heating and cooling loads. The difference between similar runs with and without a radiant barrier gave the load reductions due to the radiant barrier. Using medium HVAC equipment efficiencies, national average fuel prices, a 7 percent real discount rate, and estimates of future fuel price increases, present value savings for radiant barriers were estimated.

Present value savings estimates were made for: 1) clean horizontal radiant barriers, 2) horizontal radiant barriers that gradually become dusty over their life cycle, and 3) truss radiant barriers. These estimates were made for 27 locations and for four levels of existing attic insulation. As a byproduct of the calculations for radiant barriers, estimates of present value savings for increasing insulation levels (without radiant barriers) were also obtained.

Determination of cost-effectiveness of radiant barriers is complicated because of the wide range of installed costs. Using a low value of $0.15 per square foot of material, the model predicts that a horizontal radiant barrier that remains clean is cost justified for nearly all locations in the lower 48 states when applied over R-11 insulation. When applied over R-19 insulation, it is cost justified only for the southern locations. When applied over R-30 or R-38 insulation, it is not cost justified in any of the locations studied.

Using data from the literature, which are admittedly sketchy, for the rate of change of the emissivity of a horizontal radiant barrier due to dusting, the model predicts that such a radiant barrier is cost-

justified only for Phoenix when applied over R-11 insulation. It should be noted that the performance of dusty horizontal radiant barriers is a subject of considerable controversy, and additional research is needed to define better the rates of emissivity change in the field, and to define better the thermal performance as a function of emissivity.

In agreement with most experiments, the model predicts that the energy savings due to a truss radiant barrier are not as large as those for a clean horizontal radiant barrier. In addition, since the gables are also covered with radiant barrier material in these applications, the total area of the gables and the roof result in a requirement for a larger amount of radiant barrier material than with the horizontal application. When these factors are included, the ranges of locations where truss radiant barriers are cost justified are somewhat smaller than those identified for the clean horizontal radiant barrier.

All of the load reduction and economic calculations presented in this report are based only on the impact of radiant barriers or ceiling insulation on house loads caused by heat gains or losses through the ceiling. Recent analytical work suggests that additional savings should be attributed to radiant barriers that are installed in houses where the HVAC ducts are run through the attic space. These additional savings are due to changes in the attic air temperature caused by the radiant barrier that result in changes in heat gains and losses by the ducts. The amount of extra savings should be sensitive to the overall characteristics of the house and the HVAC equipment. Because of the many factors involved, further work is needed to analyze the impacts of duct heat gains and losses. Also, experimental confirmation of the analyses is needed.

The model with moisture effects included has been used to estimate the hour-by-hour moisture accumulation on the underside of a clean horizontal radiant barrier due to diffusion of water vapor through the ceiling. The same prototypical ranch-style house that was used for the

energy savings analyses was also used for the moisture analyses. Key model predictions are the total amount of moisture that condenses on the radiant barrier over the year, the peak of the hourly values, the dates for start, peaking, and ending of condensation, and the duration of wetting. The model only estimates the amounts of water that have condensed or evaporated. It does not attempt to account for movement of liquid water after it has condensed.

A two-level factorial design was run for Minneapolis to estimate the relative influence on moisture accumulation due to the following variables: indoor relative humidity, indoor temperature, radiant barrier permeance, vent area, and insulation level. The most important variable was found to be the relative humidity. The total condensed water was 7 to 17 times higher with a relative humidity of 50 percent than with a relative humidity of 20 percent. The second most important variable was the radiant barrier permeance, and the least important variable was the vent area.

From the factorial runs, a worst case was identified that corresponded to a 50 percent relative humidity, 75°F indoor temperature, vent area to ceiling area ratio of 1/150, R-11 insulation, and a radiant barrier permeance of 0.05. Additional runs showed that the presence of a continuous polyethylene vapor retarder essentially eliminated moisture condensation, even for this worst case.

Following this, a parametric study was performed to investigate the influence of the two most important variables, the indoor relative humidity and the radiant barrier permeance, on moisture accumulation in 11 climatic locations. These studies held the other parameters constant: 75°F indoor temperature, vent area to ceiling area ratio of 1/150, R-11 insulation, and no vapor retarder.

Based on moisture content changes that could occur in the ceiling joists due to sorption of water that condenses on the radiant barrier, a high potential for moisture problems was defined as one where the

peak condensed moisture exceeds 0.15 pounds per square foot, and a low potential for moisture problems is one where this quantity is less than 0.03 pounds per square foot.

With these criteria, the results of the parametric runs showed that with a 50 percent indoor relative humidity, a radiant barrier with a permeance of 0.05, which may be representative of unperforated foil-type radiant barriers, has a high potential for moisture problems in all locations studied, except Los Angeles and Miami. For the more normal case of a 35 percent relative humidity, a 0.05 perm radiant barrier has a high potential for moisture problems for locations having greater than about 4500 heating degree days, and a low potential for locations with less than about 3000 heating degree days.

The potential for moisture problems is much reduced with a radiant barrier having a permeance of 20, which may be representative of some perforated foil-type radiant barriers. With an indoor relative humidity of 50 percent, there is a high potential for moisture problems for heating degree days above about 4500, and a low potential for heating degree days below about 3000. With a 35 percent indoor relative humidity, the corresponding heating degree day figures are 6500 and 5000.

With a radiant barrier having a permeance of 100, which may be representative of metallized spunbonded polyolefin radiant barriers, the potential for moisture problems is virtually eliminated, except for the coldest climates and the highest indoor relative humidities.

While these modeling results may be used as a guide, there is a need for further experimental verification. Both experiments under controlled laboratory conditions and field experiments in very cold climates would provide useful tests of the validity of the model predictions.

8. REFERENCES

1. F. A. Joy, "Improving Attic Space Insulating Values," ASHAE Trans., Vol. 64, pp. 251-266 (1958).

2. F. C. McQuiston, S. L. Der, and S. B. Sandoval, "Thermal Simulation of Attic and Ceiling Spaces," ASHRAE Trans., Vol. 90, Part 1, pp. 139-163 (1984).

3. P. W. Fairey III, "Effect of Infrared Radiation Barriers on the Effective Thermal Resistance of Building Envelopes," Proceedings, ASHRAE/DOE Conference on Thermal Performance of the Exterior Envelopes of Buildings II, ASHRAE SP 38 (1983).

4. P. W. Fairey III, "The Measured Side-by-Side Performance of Attic Radiant Barrier Systems in Hot-Humid Climates," 19th International Thermal Conductivity Conference, in Thermal Conductivity 19, Plenum Press (1988).

5. J. A. Hall, "Performance Testing of Radiant Barriers," Third Annual Symposium on Improving Building Energy Efficiency in Hot and Humid Climates, pp. 57-67 (1986).

6. W. P. Levins and M. A. Karnitz, Cooling Energy Measurements of Unoccupied Single-Family Houses with Attics Containing Radiant Barriers, Oak Ridge National Laboratory, ORNL/CON-200 (July, 1986).

7. W. P. Levins and M. A. Karnitz, Heating Energy Measurements of Unoccupied Single-Family Houses with Attics Containing Radiant Barriers, Oak Ridge National Laboratory, ORNL/CON-213 (January 1987).

8. W. P. Levins and M. A. Karnitz, Cooling Energy Measurements of Single-Family Houses with Attics Containing Radiant Barriers in Combination with R-11 and R-30 Ceiling Insulation, Oak Ridge National Laboratory, ORNL/CON-226 (May 1987).

9. W. P. Levins, M. A. Karnitz, and D. K. Knight, "Cooling Energy Measurements of Houses with Attics Containing Radiant Barriers," Third Annual Symposium on Improving Building Energy Efficiency in Hot and Humid Climates, pp. 78-87 (1986).

10. W. P. Levins and M. A. Karnitz, "Energy Measurements of Single-Family Houses with Attics Containing Radiant Barriers", presented at the ASHRAE Summer Meeting, Nashville, TN (June 1987).

11. W. P. Levins and M. A. Karnitz, Heating Energy Measurements of Single-Family Houses with Attics Containing Radiant Barriers in Combination with R-11 and R-30 Ceiling Insulation, Oak Ridge National Laboratory, ORNL/CON-239 (August 1988).

12. W. E. Lear, T. E. Barrup, and K. E. Davis, "Preliminary Study of a Vented Attic Radiant Barrier System in Hot, Humid Climates Using Side-by-Side, Full-Scale Test Houses", Fourth Annual Symposium on Improving Building Energy Efficiency in Hot and Humid Climates, pp. 195-198 (1987).

13. S. Katipamula and D. L. O'Neal, "An Evaluation of the Placement of Radiant Barriers on their Effectiveness in Reducing Heat Transfer in Attics", Third Annual Symposium on Improving Building Energy Efficiency in Hot and Humid Climates, pp. 68-77 (1986).

14. S. Katipamula, D. O'Neal, W. D. Turner, and W. E. Murphy, "Experimental Study of Heat Transfer in Attics with a Small-Scale Simulator", ASHRAE Trans., Vol. 93, Part 1, pp. 122-134 (1987).

15. J. A. Hall, "Performance Testing of Radiant Barriers (RB) with R11, R19, and R30 Cellulose and Rock Wool Insulation," Fifth Annual Symposium on Improving Building Energy Efficiency in Hot and Humid Climates, pp. 174-185 (1988).

16. D. G. Ober and T. W. Volckhausen, "Radiant Barrier Insulation Performance in Full-Scale Attics with Soffit and Ridge Venting," Fifth Annual Symposium on Improving Building Energy Efficiency in Hot and Humid Climates, pp. 169-173 (1988).

17. H. Wu, "The Effect of Various Attic Venting Devices on the Performance of Radiant Barrier Systems in Hot Arid Climates," Thermal Performance of the Exterior Envelopes of Buidlings IV, ASHRAE, pp. 261-270 (1989).

18. D. G. Ober, "Full-Scale Radiant Barrier Tests in Ocala, Florida: Summer 1988," Thermal Performance of the Exterior Envelopes of Buidlings IV, ASHRAE, pp. 286-293 (1989).

19. K. E. Wilkes, Thermal Model of Attic Systems with Radiant Barriers, Oak Ridge National Laboratory, ORNL/CON-262 (to be published in 1991).

20. K. E. Wilkes, Analysis of Reductions in House Heating and Cooling Loads with Radiant Barriers, Oak Ridge National Laboratory, ORNL/CON-281 (to be published in 1991).

21. K. E. Wilkes, "Modeling of Residential Attics with Radiant Barriers," Fifth Annual Symposium on Improving Building Energy Efficiency in Hot and Humid Climates, pp. 169-173 (1988).

22. K. E. Wilkes, "Thermal Modeling of Residential Attics with Radiant Barriers: Comparison with Laboratory and Field Data," Thermal Performance of the Exterior Envelopes of Buidlings IV, ASHRAE, pp. 294-311 (1989).

23. L. Isaksen, Radiant Barrier Applications: Symposium and Workshop Proceedings, EPRI CU-6255 (February 1989).

24. K. E. Wilkes and D. W. Yarbrough, Radiant Barrier Research Plan, Oak Ridge National Laboratory, ORNL/CON-256 (1988).

25. W. P. Levins, M. A. Karnitz, and J. A. Hall, Moisture Measurements in Single-Family Houses Containing Radiant Barriers, Oak Ridge National Laboratory, ORNL/CON-255 (February 1989).

26. DOE-2 Reference Manual, Version 2.1A, Lawrence Berkeley Laboratory Report LBL-8706, Rev 2 (May 1981), DOE-2 Supplement, Version 2.1C, Lawrence Berkeley Laboratory Report LBL-8706, Rev 4 Supplement (May 1984).

27. G. P. Mitalas and J. G. Arseneault, "Fortran IV Program to Calculate Heat Flux Response Factors for Multi-Layer Slabs," DBR Computer Program No. 23, Division of Building Research, National Research Council of Canada, 1967.

28. T. Kusuda, "Thermal Response Factors for Multi-Layer Structures of Various Heat Conduction Systems," ASHRAE Trans., Vol. 75, Part 1, pp. 246-271 (1969).

29. J. P. Holman, Heat Transfer, 5th ed., pp. 191, 202, 272-286 (1981).

30. T. S. Chen, B. F. Armaly, and N. Ramachandran, "Correlations for Laminar Mixed Convection Flows on Vertical, Inclined, and Horizontal Flat Plates," ASME Journal of Heat Transfer, Vol. 108, pp. 835-840 (1986).

31. E. M. Sparrow and R. D. Cess, Radiation Heat Transfer, pp. 86-90, Brooks/Cole Publishing Company, Belmont, CA (1966).

32. B. A. Peavy, "A Model for Predicting the Thermal Performance of Ventilated Attics," in Summer Attic and Whole-House Ventilation, NBS Special Publication 548, pp. 119-149 (1979).

33. Chapter 22, ASHRAE Handbook of Fundamentals, American Society of Heating, Refrigerating, and Air Conditioning Engineers, Atlanta, GA (1985).

34. M. Martin and P. Berdahl, "Characteristics of Infrared Sky Radiation in the United States," Solar Energy, Vol. 33, pp. 321-336 (1984).

35. D. M. Burch, M. R. Lemay, B. J. Rian, and E. J. Parker, "Experimental Validation of an Attic Condensation Model", ASHRAE Trans., Vol. 20, Part 2A, pp. 59-77, 1984.

36. P. G. Cleary, "Moisture Control by Attic Ventilation - An In-Situ Study", ASHRAE Trans., Vol. 91, Part 1, pp. 227-239 (1985).

37. C. V. Heer, Statistical Mechanics, Kinetic Theory, and Stochastic Processes, Academic Press (1972).

38. J. P. Holman, Heat Transfer, 5th ed., pg. 488 (1981).

39. D. W. Yarbrough, private communication (1989).

40. D. C. Jones, private communication (1989).

41. Chapter 22, ASHRAE Handbook of Fundamentals, American Society of Heating, Refrigerating, and Air Conditioning Engineers, Atlanta, GA (1989).

42. K. Labs, J. Carmody, R. Sterling, L. Shen, Y. J. Huang, and D. Parker, Building Foundation Design Handbook, ORNL/Sub/86-72143/1, pp. 94-97 (May 1988).

43. J Huang, R. L. Ritschard, J. C. Bull, and L. Chang, "Climatic Indicators for Estimating Residential Heating and Cooling Loads," ASHRAE Trans., Vol. 93, Pt. 1, (1987).

44. B. Howard, private communication (1989).

45. M. H. Sherman and D. T. Grimsrud, Infiltration-Pressurization Correlations: Simplified Physical Modeling, Lawrence Berkeley Laboratory Report LBL-10163, Berkeley, California (1980).

46. California Energy Commission, "Application Package for Interim Certification of Space Conditioning Energy Performance Calculation Methods for Residential Buildings," California Energy Commission, Sacramento, California (1984).

47. S. R. Petersen, ZIP - The ZIP-Code Insulation Program (Version 1.0) Economic Insulation Levels for New and Existing Houses by Three-Digit ZIP Code: Users Guide and Reference Manual, ORNL/TM-11009, NISTIR 88-3801, Oak Ridge National Laboratory (January 1989).

48. D. Ober, private communication (1989).

49. B. C. Lippiatt and R. T. Ruegg, Energy Prices and Discount Factors for Life-Cycle Cost Analysis 1988, Annual Supplement to NBS Handbook 135 and NBS Publication 709, NISTIR 85-3273-3 (Rev. 11/88), National Institute of Standards and Technology, U.S. Department of Commerce (November 1988).

50. R. Akers, private communication (1989).

51. J. C. Cook, D. W. Yarbrough, and K. E. Wilkes, "Contamination of Reflective Foils in Horizontal Applications and the Effect on Thermal Performance," ASHRAE Trans., Vol. 95, Pt. 1 (1989).

52. J. A. Hall, Radiant Barrier Testing to Assess Effects of Dust Accumulation, Attic Ventilation, and Other Key Variables, TVA/OP/ED&T-88/25, Tennessee Valley Authority (July 1988).

53. R. Akers, private communication (1989).

54. R. C. Bourne and M. A. Hoeschele, Simulated Performance of Attic Radiant Barriers in Sacramento, Davis Energy Group, Inc. (April 1988).

55. M. A. Hoeschele, private communication (1989).

56. K. Labs, J. Carmody, R. Sterling, L. Shen, Y. J. Huang, and D. Parker, Building Foundation Design Handbook, ORNL/Sub/86-72143/1, p. 12 (May 1988).

57. ASHRAE Handbook of Fundamentals, pg. 20.13, American Society of Heating, Refrigerating, and Air Conditioning Engineers, Atlanta, GA (1989).

58. Strategy of Experimentation, E. I. duPont de Nemours & Co. (1975).

APPENDIX A

LISTING OF COMPUTER PROGRAM FOR ATTIC/RADIANT BARRIER MODEL

```
C*********************************************************************
C**                                                                 **
C**                        PROGRAM RBSOR1BO (RB1)                   **
C**                                                                 **
C*********************************************************************
C  THIS PROGRAM CALCULATES THE HEAT TRANSFER THROUGH THE CEILING
C  BELOW A GABLED ATTIC HAVING A FIVE-SIDED CROSS SECTION
C  VERSION "B" IS USED WITH WEATHER DATA PROCESSED FROM WEATHER TAPES
C  BY THE DOE-2 PREPROCESSOR
C  THIS VERSION LIMITS THE MOISTURE CONTENT OF WOOD TO 30 PERCENT
C  ASSUMES THE AIR WITHIN THE ATTIC IS NOT WELL-MIXED
C  INCLUDES APPROXIMATE CALCULATIONS FOR LATENT HEAT EFFECTS
C  DUE TO MOISTURE ADSORPTION AND DESORPTION
C  THIS VERSION INCLUDES CONDENSATION OF MOISTURE ON A
C    HORIZONTAL RADIANT BARRIER
C  INCLUDES DIFFUSION OF WATER VAPOR AND CONVECTIVE FLOW
C    OF MOISTURE THROUGH THE CEILING
C  SURFACE TEMPERATURES ON INSIDE OR OUTSIDE, OR VENTILATION RATE
C  MAY BE SPECIFIED THROUGH KFLAG(I) = 1
C  NOMENCLATURE:
C   N(I) = NUMBER OF CONDUCTION TRANSER FUNCTIONS FOR SURFACE I
C   U(I) = SURFACE-TO-SURFACE U-VALUE FOR SURFACE I
C   CR(I) = COMMON RATIO OF RESPONSE FACTORS FOR SURFACE I
C   BETA(I) = TEMPERATURE DEPENDENT COEFFICIENT FOR CONDUCTION
C             TRANSFER FUNCTIONS FOR SURFACE I
C   X(I,J), Y(I,J), Z(I,J) = CONDUCTION TRANSFER FUNCTIONS FOR
C             SURFACE I
C   SURFACES ARE NUMBERED AS (FOR NORTH-SOUTH RIDGE):
C     1 = CEILING
C     2 = EAST ROOF
C     3 = WEST ROOF
C     4 = SOUTH GABLE
C     5 = NORTH GABLE
C     6 = EAST EAVE WALL
C     7 = WEST EAVE WALL
C   ALF(I) = SOLAR ABSORPTANCE FOR SURFACE I
C   EO(I) = INFRARED EMITTANCE FOR OUTSIDE OF SURFACE I
C   EI(I) = INFRARED EMITTANCE FOR INSIDE OF SURFACE I
C   TIS(I,J) = INSIDE SURFACE TEMPERATURE FOR SURFACE I
C   TOS(I,J) = OUTSIDE SURFACE TEMPERATURE FOR SURFACE I
C   TA = AVERAGE TEMPERATURE OF AIR IN ATTIC
C   QI(I,J) = INSIDE HEAT FLUX FOR SURFACE I
C   QO(I,J) = OUTSIDE HEAT FLUX FOR SURFACE I
C   HCI(I) = CONVECTION COEFFICIENT FOR INSIDE OF SURFACE I
C   HR(I,K) = RADIATION INTERCHANGE COEFFICIENT FROM SURFACE I
C             TO SURFACE K
C   AA(I,J) = MATRIX OF COEFFICIENTS FOR SIMULTANEOUS EQUATIONS
C   BB(I) = KNOWN VECTOR FOR SIMULTANEOUS EQUATIONS
C   XXX(I) = SOLUTION VECTOR FOR SIMULTANEOUS EQUATIONS
C   QSOL(I) = SOLAR RADIATION INCIDENT ON SURFACE I
C   A(I) = AREA OF SURFACE I
```

```
C   G(I,K) = OVERALL RADIATION VIEW FACTOR FROM SURFACE I TO
C            SURFACE K
C   HCO(I) = CONVECTION COEFFICIENT ON OUTSIDE OF SURFACE I
C   HRO(I) = RADIATION COEFFICIENT ON OUTSIDE OF SURFACE I
C   R(I) = SURFACE-TO-SURFACE RESISTANCE FOR SURFACE I
C   AMC(I) = MOISTURE CONTENT (WEIGHT FRACTION) FOR SURFACE I
C   PERM(I) = MOISTURE PERMEANCE OF SURFACE I
C   AWRAT(I) = RATIO OF EXPOSED SURFACE AREA TO PROJECTED SURFACE
C              AREA FOR SURFACE I
C   AMASS(I) = MASS PER UNIT AREA OF SURFACE I THAT PARTICIPATES IS
C              MOISTURE EXCHANGE
C   AMW(I) = MOISTURE FLUX TOWARD SURFACE I
C   BMW(I) = TERM IN TAYLOR SERIES EXPANSION FOR MOISTURE FLUX
C   TS(I) = TEMPERATURE OF INSIDE OF SURFACE I
C   KFLAG = FLAG FOR SPECIFIED SURFACE TEMPERATURES
C       0 = PARAMETER NOT SPECIFIED
C       1 = PARAMETER SPECIFIED
C       I = 1,7 FOR TIS(I,1)
C       I = 8,14 FOR TOS(I-7,1)
C       I = 15 FOR VENTILATION RATE
C   AL = LENGTH OF ATTIC, FEET
C   W  = WIDTH OF ATTIC, FEET
C   PITCH1 = PITCH OF EAST ROOF, DEGREES
C   PITCH2 = PITCH OF WEST ROOF, DEGREES
C   ORIENT = ORIENTATION OF HOUSE
C   H1 = HEIGHT OF VERTICAL WALLS AT EAVES, FEET
C   AI = AREA OF INLET VENT, SQUARE FEET
C   AO = AREA OF OUTLET VENT, SQUARE FEET
C   ITYPE = TYPE VENTS
C       1 = SOFFIT AND RIDGE VENTS
C       2 = SOFFIT AND GABLE VENTS
C       3 = SOFFIT VENTS ONLY
C   QLAT = HEAT OF VAPORIZATION OF WATER, BTU/LBM
C   EXFIL = RATE OF FLOW OF AIR FROM HOUSE TO ATTIC, LB/HR
C   AL1 ... AL7 = CHARACTERISTIC LENGTHS OF SURFACES 1 ... 7, FEET
C   TO = OUTDOOR TEMPERATURE, F
C   QSOLH = SOLAR RADIATION INCIDENT ON HORIZONTAL SURFACE
C           BTU/(HR.-SQ.FT.)
C   WS = WIND SPEED, MPH
C   DIR = WIND DIRECTION
C   HUM = OUTDOOR RELATIVE HUMIDITY, PERCENT
C   TI = INDOOR TEMPERATURE, F
C   HUMI = INDOOR RELATIVE HUMIDITY, PERCENT
C   VDOT = VENTILATION RATE, CUBIC FEET PER HOUR
C   IVFLAG = FLAG FOR CALCULATING FLOW VELOCITY
C        0 = FLOW THROUGH BOTH SIDE OF ATTIC
C        1 = FLOW THROUGH ONE SIDE OF ATTIC
C   FLUX = MEASURED CEILING HEAT FLUX, BTU/(HR.-SQ.FT.)
C   TAIR = MEASURED ATTIC AIR TEMPERATURE, F
C   TEXIT = MEASURED EXIT AIR TEMPERATURE, F
C   H = HEIGHT, FEET
C   AMDOT = VENTILATION RATE, POUNDS PER HOUR
```

```
C   AMCDOT = VENTILATION RATE TIMES SPECIFIC HEAT
C   V = CRUDE ESTIMATE OF AIR SPEED THROUGH ATTIC, FEET PER HOUR
C   ACH = AIR CHANGE RATE FOR ATTIC, AIR CHANGES PER HOUR
C NEXT LINE ADDED FOR VERSION 1A
      COMMON /CLOUD/CLDAMT,ICLDTY,CC
C NEXT LINE ADDED FOR VERSION 1B
      COMMON /HUMID/WO,PATM
      DIMENSION N(7),U(7),CR(7),BETA(7),X(7,100),Y(7,100),Z(7,100)
      DIMENSION ALF(7),EO(7),EI(7),TIS(7,100),TOS(7,100),TA(2)
      DIMENSION QI(7,2),QO(7,2),HCI(7),HR(7,7),AA(15,15),BB(15)
      DIMENSION XXX(15),QSOL(7),A(7),G(7,7),HCO(7),HRO(7),R(7)
      DIMENSION AMC(7),PERM(7),AWRAT(7),AMASS(7),AMW(7),TS(7)
      DIMENSION BMW(7),KFLAG(15)
      DATA TIS/700*75.0/,TOS/700*75.0/,AA/225*0.0/,TR/75.0/
      DATA TA/2*75.0/,QI/14*0.0/,QO/14*0.0/,BMW/7*0.0/
C  READ IN KFLAG
      READ (5,*) (KFLAG(I),I=1,7)
      READ (5,*) (KFLAG(I),I=8,14)
      READ (5,*) KFLAG(15)
C  READ IN CONDUCTION TRANSFER FUNCTIONS
      DO 100 I = 1,7
      READ (5,*)  N(I),U(I),CR(I),BETA(I)
      M = N(I)
      DO 100 J = 1,M
      READ (5,*) X(I,J),Y(I,J),Z(I,J)
  100 CONTINUE
      DO 101 I = 1,7
  101 R(I) = 1./U(I)
C  CONVENTION FOR CTF'S IS SAME AS USED IN TARP
C  CONVENTION FOR ATTIC MODEL IS THAT INSIDE SURFACES
C  FACE THE ATTIC SPACE
C  CTF'S FOR THE CEILING ARE CALCULATED FOR USE IN A
C  WHOLE HOUSE MODEL, WHERE THE OUTSIDE SURFACE FACES
C  THE ATTIC;  THEREFORE, FOR USE INTERNAL TO THE ATTIC
C  MODEL, INTERCHANGE THE X'S AND THE Z'S
      M = N(1)
      DO 110 J = 1,M
      XX = X(1,J)
      X(1,J) = Z(1,J)
      Z(1,J) = XX
  110 CONTINUE
C  READ IN SOLAR ABSORPTANCES OF OUTSIDE SURFACES AND
C  EMITTANCES OF BOTH OUTSIDE AND INSIDE SURFACES
      READ(5,*)  (ALF(I), I = 1,7)
      READ(5,*)  (EO(I), I = 1,7)
      READ(5,*)  (EI(I), I = 1,7)
C  READ IN ATTIC GEOMETRY:  LENGTH, WIDTH, PITCHES OF ROOF
C  SURFACES(DEGREES), ORIENTATION ANGLE OF HOUSE
C  AND HEIGHT OF SIDE WALLS
      READ (5,*)  AL,W,PITCH1,PITCH2,ORIENT,H1
C  READ VENT INLET AND OUTLET AREAS, AND VENT TYPE
C  TYPE 1 = SOFFIT AND RIDGE VENTS
```

```
C  TYPE 2 = SOFFIT AND GABLE VENTS
C  TYPE 3 = SOFFIT VENTS ONLY
      READ(5,*) AI,AO,ITYPE
C  READ WATER VAPOR PERMEANCES OF ATTIC SURFACES
C  PERM = GRAINS PER (HR-FT2-INCH HG)
      READ (5,*) (PERM(I),I=1,7),PERMRB
C CONVERT PERM VALUES TO POUNDS PER (HR-FT2-PSIA)
      DO 120 I = 1,7
  120 PERM(I) = PERM(I)*(29.921/14.696)/7000.
      PERMRB = PERMRB*(29.921/14.696)/7000.
C  READ RATIO OF TOTAL AREA OF EXPOSED WOOD TO GEOMETRICAL
C  PROJECTION OF SURFACE AREAS
      READ (5,*) (AWRAT(I),I=1,7)
C  READ WEIGHT OF WOOD PER UNIT PROJECTED AREA FOR EACH SURFACE
      READ (5,*) (AMASS(I),I=1,7)
C  READ INITIAL MOISTURE CONTENTS OF WOOD, WEIGHT FRACTION
      READ (5,*) (AMC(I),I=1,7)
C  READ LATENT HEAT OF VAPORIZATION, BTU/LB
      READ (5,*) QLAT
C  READ RATE OF FLOW OF HOUSE AIR INTO ATTIC, POUNDS PER HOUR
      READ (5,*) EXFIL
C  INITIALIZE WATER ON RADIANT BARRIER
      WRB = 0.0
      WRBTOT = 0.0
      CALL VIEW2(AL,W,PITCH1,PITCH2,H1,EI,G,7)
C  CALCULATE CHARACTERISTIC LENGTHS AND AREAS OF SURFACES
C  CHAR. LENGTHS ARE TAKEN TO BE:
C  CEILING - AVERAGE OF LENGTH AND WIDTH
C  ROOF - DISTANCE FROM EAVE TO RIDGE
C  GABLE - AVERAGE HEIGHT
C  SIDE WALLS - HEIGHT
      AL1 = (AL+W)/2.
      P1 = PITCH1*3.14159265/180.
      P2 = PITCH2*3.14159265/180.
      P3 = 3.14159265 - P1 - P2
      IP1 = PITCH1
      IP2 = PITCH2
      IP3 = 180.0 - PITCH1 - PITCH2
      IF(IP3.EQ.180) GO TO 5
      AL2 = W*SIN(P2)/SIN(P3)
      AL3 = W*SIN(P1)/SIN(P3)
      AL4 = 0.5*(AL2*SIN(P1)) + H1
      GO TO 6
    5 AL2 = W/2.0
      AL3 = W/2.0
      AL4 = H1
    6 AL5 = AL4
      AL6 = H1
      AL7 = H1
      A(1) = AL*W
      A(2) = AL*AL2
      A(3) = AL*AL3
```

```
      A(4) = W*AL4
      A(5) = A(4)
      A(6) = AL*H1
      A(7) = AL*H1
C*********************************************************************
C  THIS BLOCK ADDED FOR VERSION 1A
C  READ LATITUDE, LONGITUDE, TIME ZONE, CLEARNESS NUMBER,
C  GROUND REFLECTANCE, AND FLAG FOR AMOUNT OF SOLAR DATA
C  TIME ZONE = 5 FOR EASTERN, = 6 FOR CENTRAL, ETC.
C  ISUN = 1, MEASURED TOTAL HORIZONTAL AND DIRECT AVAILABLE
C  ISUN = 2, MEASURED TOTAL HORIZONTAL ONLY AVAILABLE
C  ISUN = 3, NO MEASURED SOLAR, BUT MEASURED CLOUD COVER
C  NOTE, VERSION 1B EXPECTS ISUN = 1
C  IN VERSION 1B CLRNES WILL BE READ IN EACH HOUR
      READ(5,*) STALAT,STALON,ITIMZ,CLRNES,RHOG,ISUN
      STALAT = STALAT*3.14159265/180.
      SSTALA = SIN(STALAT)
      CSTALA = COS(STALAT)
      STALON = STALON*3.14159265/180.
C     ORIENT = ORIENT*3.14159265/180.
      BAZIM = ORIENT*3.14159265/180.
      SBAZIM = SIN(BAZIM)
      CBAZIM = COS(BAZIM)
C  READ BEGINNING DAY OF YEAR AND HOUR OF DAY
C  DISABLED FOR VERSION 1B
C     READ(5,*) IDOY,IHR
C     IHR = IHR - 1
C     CALL SUN1(STALAT,IDOY)
C*********************************************************************
C  READ LINE OF WEATHER DATA
C*********************************************************************
C  NEXT 6 LINES DELETED FOR VERSION 1B
C  10 READ(5,*,END = 999) TO,QSOLH,WS,DIR,HUM,TI,HUMI,(TIS(I,1),I=1,7),
C    & (TOS(I,1),I=1,7),VDOT,IVFLAG,FLUX,TAIR,TEXIT,CLDAMT,ICLDTY
C  RESTORE ESTIMATES FOR TEMPERATURES NOT SPECIFIED
C     DO 15 I = 1,7
C     IF(KFLAG(I).EQ.0) TIS(I,1) = TIS(I,2)
C  15 IF(KFLAG(I+7).EQ.0) TOS(I,1) = TOS(I,2)
C  NEXT LINES ADDED FOR VERSION 1B, FIRST LINE OF DATA ARE FIXED
C  SECOND LINE IS HOURLY VALUES
      READ(5,*) TI,HUMI,IVFLAG,VDOT
   10 READ(10,*,END=999)  IDOY,IHR,TO,PATM,CLDAMT,DIR,WO,QSOLH,DIRSOL,
     &                    ICLDTY,WS,CLRNES
C NEXT LINE ADDED 10-11-89
      IF(WO.LT.0.0001) WO = 0.00005
C CONVERT WIND DIRECTION TO BUILDING FRAME OF REFERENCE
      DIR = ORIENT - DIR
C SET UP DUMMY OUTDOOR RELATIVE HUMIDITY, NOT USED IN PROGRAM
      HUM = 50.0
C*********************************************************************
C*********************************************************************
C THIS BLOCK ADDED FOR VERSION 1A
```

```
C MODIFIED FOR VERSION 1B
C     IHR = IHR + 1
C     IF(IHR.GT.24) THEN
C        IHR = IHR - 24
C        IDOY = IDOY + 1
      IF(IHR.EQ.1)  CALL SUN1(STALAT,IDOY)
C     END IF
C  NEXT LINE CHANGED FOR ALTERATION OF SUBROUTINE SKY IN VERSION 1B
C     CALL SKY(TO,HUM,IHR,CLDAMT,ICLDTY,TSKY)
      CALL SKY(TO,IHR,CLDAMT,ICLDTY,TSKY)
      TS2 = (((1.0 - COS(P1))/2.0*(TO+459.67)**4)
     &    +  ((1.0 + COS(P1))/2.0*(TSKY+459.67)**4))**0.25 - 459.67
      TS3 = (((1.0 - COS(P2))/2.0*(TO+459.67)**4)
     &    +  ((1.0 + COS(P2))/2.0*(TSKY+459.67)**4))**0.25 - 459.67
      TSV = (0.5*(TO+459.67)**4 + 0.5*(TSKY+459.67)**4)**0.25 - 459.67
      IF(ISUN.NE.1) DIRSOL = 0.0
      CALL WDTSUN(IHR,ITIMZ,STALON,STALAT,SSTALA,CSTALA,SBAZIM,CBAZIM,
     &            CLRNES,QSOLH,DIRSOL,ISUN)
C  CALCULATE SOLAR LOAD ON EACH SURFACE
      QSOL(1) = 0.0
      QSOL(2) = SUN3OR(90.,PITCH1,RHOG)
      QSOL(3) = SUN3OR(270.,PITCH2,RHOG)
      QSOL(4) = SUN3OR(180.,90.,RHOG)
      QSOL(5) = SUN3OR(0.,90.,RHOG)
      QSOL(6) = SUN3OR(90.,90.,RHOG)
      QSOL(7) = SUN3OR(270.,90.,RHOG)
C*********************************************************************
      NIT = 1
C*********************************************************************
C  CALCULATE ATTIC VENTILATION RATE AND FLOW VELOCITY
      H = AL4 + AL2*SIN(P1)/2.0
   20 CONTINUE
      IF(KFLAG(15).EQ.0) THEN
        CALL VENT(TO,TA(1),WS,DIR,H,AI,AO,ITYPE,AMCDOT,AMDOT,VDOT)

      ELSE
C  ASSUME VENTILATION RATES ARE BASED ON OUTSIDE AIR TEMPERATURE
        AMDOT = VDOT*22.0493/((TO+459.67)/1.8)
        AMCDOT = AMDOT*(3.4763 + 1.066E-4*((TO+459.67)/1.8))*0.068559
      END IF
C  ESTIMATE CRUDE FLOW VELOCITY
      IF(IVFLAG.EQ.0) V = VDOT/(AL4*AL)
      IF(IVFLAG.EQ.1) V = VDOT*2.0/(AL4*AL)
C     AMCDOT = AMCDOT/100.
C     AMDOT = AMDOT/100.
C     VDOT = VDOT/100.
C     V = V/100.
      ACH = VDOT/A(4)/AL
C*********************************************************************
C  CALCULATE CONVECTION COEFFICIENTS AT INSIDE SURFACES
      CALL HCON(TIS(1,1),TA(1),0.0,AL1,1,V,HCI(1))
      CALL HCON(TIS(2,1),TA(1),PITCH1,AL2,2,V,HCI(2))
```

```
      CALL HCON(TIS(3,1),TA(1),PITCH2,AL3,2,V,HCI(3))
      CALL HCON(TIS(4,1),TA(1),90.0,AL4,1,V,HCI(4))
      CALL HCON(TIS(5,1),TA(1),90.0,AL5,1,V,HCI(5))
      CALL HCON(TIS(6,1),TA(1),90.0,AL6,1,V,HCI(6))
      CALL HCON(TIS(7,1),TA(1),90.0,AL7,1,V,HCI(7))
C  CALCULATE CONVECTION COEFFICIENTS AT OUTSIDE SURFACES
      WS1 = WS*5280.
      CALL HCON(TOS(1,1),TI,0.0,AL1,2,0.0,HCO(1))
      CALL HCON(TOS(2,1),TO,PITCH1,AL2,1,WS1,HCO(2))
      CALL HCON(TOS(3,1),TO,PITCH2,AL3,1,WS1,HCO(3))
      CALL HCON(TOS(4,1),TO,90.0,AL4,1,WS1,HCO(4))
      CALL HCON(TOS(5,1),TO,90.0,AL5,1,WS1,HCO(5))
      CALL HCON(TOS(6,1),TO,90.0,AL6,1,WS1,HCO(6))
      CALL HCON(TOS(7,1),TO,90.0,AL7,1,WS1,HCO(7))
C  CALCULATE RADIATION COEFFICIENTS AT INSIDE SURFACES
      DO 200 I = 1,7
      DO 200 J = 1,7
      HR(I,J) = HRAD(G(I,J),TIS(I,1),TIS(J,1))
  200 CONTINUE
C  CALCULATE RADIATION COEFFICIENTS AT OUTSIDE SURFACES
      HRO(1) = HRAD(EO(1),TOS(1,1),TI)
      HRO(2) = HRAD(EO(2),TOS(2,1),TS2)
      HRO(3) = HRAD(EO(3),TOS(3,1),TS3)
      DO 250 I = 4,7
      HRO(I) = HRAD(EO(I),TOS(I,1),TSV)
  250 CONTINUE
C  CALCULATE MOISTURE BALANCES, LATENT HEATS
      IF(QLAT.LE.1.) THEN
         DO 259 I = 1,7
         AMW(I) = 0.0
         BMW(I) = 0.0
  259    CONTINUE
      ELSE
      DO 260 I = 1,7
  260 TS(I) = TIS(I,1)
      CALL MOISTM(TS,TO,TI,TA(1),HCI,A,AWRAT,AMC,AMASS,HUM,HUMI,PERM,
     &   AMDOT,EXFIL,AMW,BMW,7,PERMRB,WRB,AMWRB,BMWRB,RHATC)
      DO 270 I = 1,7
      IF(AMC(I).LE.1.E-6.AND.AMW(I).LT.0.0) THEN
         AMW(I) = 0.0
         BMW(I) = 0.0
      ELSE IF(AMW(I).LT.0.0.AND.ABS(AMW(I)).GT.(AMC(I)*AMASS(I))) THEN
         FACT = ABS(AMC(I)*AMASS(I)/AMW(I))
         AMW(I) = AMW(I)*FACT
         BMW(I) = BMW(I)*FACT
      ELSE
         CONTINUE
      END IF
  270 CONTINUE
C  NEXT 12 LINES ADDED FOR MOISTURE ON RB
      IF(WRB.LT.1.E-6.AND.AMWRB.LT.0.0)  THEN
        AMWRB = 0.0
```

```
        BMWRB = 0.0
      ELSE IF(AMWRB.LT.0.0.AND.ABS(AMWRB).GT.WRB)  THEN
        FACT = ABS(WRB/AMWRB)
        AMWRB = AMWRB*FACT
        BMWRB = BMWRB*FACT
      ELSE
        CONTINUE
      END IF
      AMW(1) = AMW(1) + AMWRB
      BMW(1) = BMW(1) + BMWRB
      END IF
C*********************************************************************
C  SET UP MATRIX OF COEFFICIENTS IN HEAT BALANCE EQUATIONS
      DO 300 I = 1,7
      DO 300 J = 1,7
      AA(I,J) = -HR(I,J)
  300 CONTINUE
      DO 310 I = 1,7
      DO 305 J = 1,7
  305 AA(I,I) = AA(I,I) + HR(I,J)
  310 AA(I,I) = AA(I,I) + Z(I,1) + HCI(I)
C  ADD IN LATENT HEAT TERMS
      DO 315 I = 1,7
  315 AA(I,I) = AA(I,I) + BMW(I)*QLAT
C*********************************************************************
      DO 320 I = 1,7
      AA(I,I+7) = - Y(I,1)
      AA(I,15) = -HCI(I)
      AA(I+7,I) = -Y(I,1)
      AA(I+7,I+7) = X(I,1) + HCO(I) + HRO(I)
  320 AA(15,I) = A(I)*HCI(I)
C*********************************************************************
      C1 = 0.0
      DO 330 I = 1,7
  330 C1 = C1 + A(I)*HCI(I)
      C2I = (AMCDOT + EXFIL*0.24)/C1
      IF(C2I.GT.0.02)  C3 = EXP(-1./C2I) - 1.0
      IF(C2I.LE.0.02)  C3 = -1.0
      AA(15,15) = -C1/(1. + C2I*C3)
C*********************************************************************
C  SET UP VECTOR FOR RIGHT HAND SIDE OF HEAT BALANCE EQUATIONS
      DO 400 I = 1,7
      BB(I) = TR*(Z(I,1)-Y(I,1)) - CR(I)*QI(I,2)
      BB(I) = BB(I) -BETA(I)/2.*(Z(I,1)*(TIS(I,1)-TR)**2
     &   -Y(I,1)*(TOS(I,1)-TR)**2)
      DO 400 J = 2,N(I)
  400 BB(I)=BB(I)-Z(I,J)*(TIS(I,J)-TR)+Y(I,J)*(TOS(I,J)-TR)
     &  -BETA(I)/2.*(Z(I,J)*(TIS(I,J)-TR)**2
     &  -Y(I,J)*(TOS(I,J)-TR)**2)
C  ADD IN LATENT HEAT EFFECTS
      DO 405 I = 1,7
  405 BB(I) = BB(I) + AMW(I)*QLAT + BMW(I)*QLAT*TIS(I,1)
```

```
      DO 410 I = 1,7
      BB(I+7) = TR*(X(I,1)-Y(I,1)) + CR(I)*QO(I,2)
      BB(I+7) = BB(I+7) -BETA(I)/2.*(X(I,1)*(TOS(I,1)-TR)**2
     &    -Y(I,1)*(TIS(I,1)-TR)**2)
      DO 410 J = 2,N(I)
  410 BB(I+7) = BB(I+7)-X(I,J)*(TOS(I,J)-TR)+Y(I,J)*(TIS(I,J)-TR)
     &  -BETA(I)/2.*(X(I,J)*(TOS(I,J)-TR)**2
     &  -Y(I,J)*(TIS(I,J)-TR)**2)
      BB(8) = BB(8) + HCO(1)*TI + HRO(1)*TI
      BB(9) = BB(9) + HCO(2)*TO + HRO(2)*TS2 + ALF(2)*QSOL(2)
      BB(10) = BB(10) + HCO(3)*TO + HRO(3)*TS3 + ALF(3)*QSOL(3)
      DO 420 I = 4,7
  420 BB(I+7) = BB(I+7) + HCO(I)*TO + HRO(I)*TSV + ALF(I)*QSOL(I)
      BB(15) = (AMCDOT*TO + EXFIL*0.24*TI)*C3/(1.0 + C2I*C3)
C*********************************************************************
C  THIS SECTION DISABLED FOR VERSION 1B
C     SKBIG = 1.E20
C     DO 450 I = 1,7
C     IF(KFLAG(I).EQ.0)  GO TO 460
C     AA(I,I) = AA(I,I)*SKBIG
C     BB(I) = TIS(I,1)*AA(I,I)
C 460 IF(KFLAG(I+7).EQ.0) GO TO 450
C     AA(I+7,I+7) = AA(I+7,I+7)*SKBIG
C     BB(I+7) = TOS(I,1)*AA(I+7,I+7)
C 450 CONTINUE
C*********************************************************************
C  SOLVE SYSTEM OF EQUATIONS
      CALL SOLVP(15,AA,BB,XXX)
C*********************************************************************
C  TEST FOR CONVERGENCE OF SOLUTION
      EPS = 1.E-3
      IFLAG = 0
      DO 500 I = 1,7
  500 IF(ABS(XXX(I)-TIS(I,1)).GT.EPS)  GO TO 600
      DO 510 I = 1,7
  510 IF(ABS(XXX(I+7)-TOS(I,1)).GT.EPS)  GO TO 600
      IF(ABS(XXX(15)-TA(1)).GT.EPS)  GO TO 600
C*********************************************************************
      GO TO 700
  600 IFLAG = 1
  700 CONTINUE
C*********************************************************************
      DO 800  I = 1,7
      TIS(I,1) = XXX(I)
  800 TOS(I,1) = XXX(I+7)
      TA(1) = XXX(15)
C*********************************************************************
      S1 = 0.0
      DO 850 I = 1,7
  850 S1 = S1 + A(I)*HCI(I)*TIS(I,1)
      TE = AMCDOT*TO + EXFIL*0.24 + (S1 - C1*TA(1))
      TE = TE/(AMCDOT + EXFIL)
```

```
      NIT = NIT + 1
      IF(IFLAG.EQ.1.AND.NIT.LE.15)  GO TO 20
C  CALCULATE HEAT FLUXES
      DO 900 I = 1,7
      QI(I,1) = CR(I)*QI(I,2)
  900 QO(I,1) = CR(I)*QO(I,2)
      DO 950 I = 1,7
      DO 950 J = 1,N(I)
      QI(I,1) = QI(I,1) + Z(I,J)*(TIS(I,J)-TR)-Y(I,J)*(TOS(I,J)-TR)
     & +BETA(I)/2.*(Z(I,J)*(TIS(I,J)-TR)**2-Y(I,J)*(TOS(I,J)-TR)**2)
  950 QO(I,1) = QO(I,1) + Y(I,J)*(TIS(I,J)-TR)-X(I,J)*(TOS(I,J)-TR)
     &  +BETA(I)/2.*(Y(I,J)*(TIS(I,J)-TR)**2-X(I,J)*(TOS(I,J)-TR)**2)
C  CALCULATE TOTAL CEILING HEAT FLOW
      QCEIL = QO(1,1)*A(1)
C  CALCULATE NEW MOISTURE CONTENTS
      DO 960 I = 1,7
      AMC(I) = AMC(I) + AMW(I)/AMASS(I)
C  NEXT LINE ADDED 10-1-89
      IF(AMC(I).GT.0.30) AMC(I) = 0.3
  960 IF(AMC(I).LE.0.0) AMC(I) = 0.0
C  NEXT TWO LINES ADDED FOR MOISTURE ON RB
      WRB = WRB + AMWRB
      IF(WRB.LE.0.0)  WRB = 0.0
      IF(AMWRB.GT.0.0) WRBTOT = WRBTOT + AMWRB
C  WRITE OUT RESULTS
C  MODIFIED FOR VERSION 1B
C     WRITE(6,1001) TO,TOS(2,1),TOS(3,1),QO(1,1),FLUX,TA(1),TAIR,
C    &              TE,TEXIT,ACH,AMC(2),NIT,HCO(1),HRO(1),WRB,RHATC
C1000 FORMAT(2X,2F15.4,I10)
C1001 FORMAT(1X,3F7.2,2F10.4,4F7.2,F15.4,F6.3,I5,2F6.3,F10.6,F10.2)
C     WRITE(6,1005) QO(1,1)
C1005 FORMAT(1X,F10.4)
      WRITE(6,1006) QO(1,1)
 1006 FORMAT(1X,F10.4)
C  NEXT TWO LINES ADDED FOR MOISTURE ON RB
      WRITE(7,1007) WRB,TIS(1,1)
 1007 FORMAT(1X,F10.6,F7.2)
C  UPDATE TEMPERATURES AND HEAT FLUXES FOR NEXT HOUR
      DO 1100 I = 1,7
      QI(I,2) = QI(I,1)
      QO(I,2) = QI(I,1)
      DO 1100 J = 1,N(I)-1
      TIS(I,N(I)-J+1) = TIS(I,N(I)-J)
 1100 TOS(I,N(I)-J+1) = TOS(I,N(I)-J)
      TA(2) = TA(1)
      GO TO 10
  999 STOP
      END
C*********************************************************************
C**                                                                 **
C**                          FUNCTION FMN                           **
C**                                                                 **
```

```
C*********************************************************************
      FUNCTION FMN(A,B,C,PHI)
C  THIS FUNCTION CALCULATES THE VIEW FACTOR BETWEEN TWO FINITE
C  RECTANGULAR PLATES SHARING AN EDGE
C  SEE APPENDIX A OF SPARROW AND CESS, CONFIGURATION 2
C  SEE ALSO A. FEINGOLD, PROC. ROY. SOC., A, VOL. 292, PP. 51-60 (1965)
C  VIEW FACTOR FROM PLATE 1 TO PLATE 2
C  A = WIDTH OF PLATE 2, C = WIDTH OF PLATE 1
C  B = LENGTH OF BOTH PLATES
C  PHI = ANGLE BETWEEN PLATES (RADIANS)
C  NUMERICAL INTEGRATION PERFORMED BY SIMPSON'S RULE
      DIMENSION Q(65)
      X = A/B
      Y = C/B
      SP = SIN(PHI)
      S2P = SIN(2.*PHI)
      CP = COS(PHI)
      C2P = COS(2.*PHI)
      Z = X*X + Y*Y - 2.*X*Y*CP
      DXI = Y/64.
      DO 1 N = 1,65
      ANM1 = N - 1
      XI = DXI*ANM1
      E = SQRT(1. + XI*XI*SP*SP)
      F = ATAN((X-XI*CP)/E) + ATAN(XI*CP/E)
    1 Q(N) = E*F
      AINT = Q(1) + 4.*Q(64) + Q(65)
      DO 2  N = 1,31
      K = 2*N
    2 AINT = AINT + 4.*Q(K) + 2.*Q(K+1)
      FMN = CP*AINT*DXI/3.
      E = SQRT(1.+X*X*SP*SP)
      F = ATAN(X*CP/E) + ATAN((Y-X*CP)/E)
      FMN = FMN + SP*S2P/2.*X*E*F
      FMN = FMN + X*ATAN(1./X) + Y*ATAN(1./Y)
     &      - SQRT(Z)*ATAN(1./SQRT(Z))
      E = 1. + X*X
      F = 1. + Y*Y
      FMN = FMN + (0.5 - SP*SP/4.)*ALOG(E*F/(1.+Z))
      FMN = FMN + SP*SP/4.*(Y*Y*ALOG(Y*Y*(1.+Z)/F/Z)
     &      + X*X*(ALOG(X*X/Z) + C2P*ALOG(E/(1.+Z))))
      E = Y*Y*ATAN((X-Y*CP)/Y/SP) + X*X*ATAN((Y-X*CP)/X/SP)
      FMN = FMN - S2P/4.*(X*Y*SP + (3.14159265/2. - PHI)
     &      * (X*X + Y*Y) + E)
      FMN = FMN/3.14159265/Y
      RETURN
      END
C*********************************************************************
C**                                                                 **
C**                          FUNCTION FP                            **
C**                                                                 **
C*********************************************************************
```

```
      FUNCTION FP(A,B,C)
C  THIS FUNCTION CALCULATES THE VIEW FACTOR BETWEEN TWO FINITE EQUAL
C  PARALLEL PLATES
C  SEE APPENDIX A OF SPARROW AND CESS, CONFIGURATION 1
C  A AND B = DIMENSIONS OF PLATES, C = SEPARATION OF PLATES
      X = A/C
      Y = B/C
      D = SQRT(1.+X*X)
      E = SQRT(1.+Y*Y)
      F = SQRT(1.+X*X+Y*Y)
      FP = ALOG(D*E/F) + Y*D*ATAN(Y/D) + X*E*ATAN(X/E)
     &     - Y*ATAN(Y) - X*ATAN(X)
      FP = FP*2./(3.14159265*X*Y)
      RETURN
      END
C*********************************************************************
C**                                                                 **
C**                          SUBROUTINE HCON                        **
C**                                                                 **
C*********************************************************************
      SUBROUTINE HCON(TS,TA,PHI,AL,IFLAG,V,HC)
C  THIS SUBROUTINE CALCULATES NATURAL CONVECTION HEAT TRANSFER
C  COEFFICIENTS BASED ON ISOLATED ISOTHERMAL FLAT PLATES
C  CALCULATES FORCED CONVECTION COEFFICIENTS AND TOTAL
C  CONVECTION HEAT TRANSFER COEFFICIENTS
C  SEE HOLMAN, 5TH EDITION, PP. 272-286
C  TS = SURFACE TEMPERATURE, F
C  TA = AIR TEMPERATURE, F
C  PHI = TILT ANGLE, DEGREES, 0 FOR HORIZONTAL, 90 FOR VERTICAL
C  AL = CHARACTERISTIC LENGTH OF SURFACE
C  IFLAG = 1 FOR SURFACE FACING UPWARD
C  IFLAG = 2 FOR SURFACE FACING DOWNWARD
C  V = AIR SPEED, FEET PER HOUR
C  HCF = FORCED CONVECTION COEFFICIENT
C  HCN = NATURAL CONVECTION COEFFICIENT
C  HC = TOTAL CONVECTION COEFFICIENT
C
      REAL NUS,K,MU,NU
      DT = TS - TA
      IF (IFLAG.EQ.2)  DT = -DT
C  CALCULATE FILM TEMPERATURE
      TF = (TS+TA)/2.0
      TF1 = TF
      IF(ABS(PHI).GT.1.E-3.AND.ABS(PHI-90.).GT.1.E-3)
     &    TF = TS - 0.25*(TS-TA)
      IF(ABS(PHI).GT.1.E-3.AND.ABS(PHI-90.).GT.1.E-3)
     &    TF1 = TA + 0.25*(TS-TA)
      TK = (TF+459.67)/1.8
C  THERMAL CONDUCTIVITY OF AIR FROM EQUATION IN NBS CIRC. 564
C  THERMAL COND. IN BTU/(HR-FT-F)
      K = 0.6325E-5*SQRT(TK)/(1.+(245.4*10.**(-12./TK))/TK)*241.77
C  DYNAMIC VISCOSITY OF AIR FROM EQUATION IN NBS CIRC. 564
```

```
C  LB/(HR-FT)
      MU = (145.8*TK*SQRT(TK)/(TK+110.4))*241.90E-7
C  PRANDTL NUMBER, LINEAR REGRESSION FROM 220 K TO 360 K
C  FROM NBS CIRC. 564
      PR = 0.7880 - 2.631E-4*TK
C  VOLUME EXPANSION COEFFICIENT OF AIR, 1/TABS, PERFECT GAS
      BETA = 1./(TF1+459.67)
C  DENSITY OF AIR, PERFECT GAS, NBS CIRC. 564, LB/CF
      RHO = 22.0493/TK
C  KINEMATIC VISCOSITY, FT2/HR
      NU = MU/RHO
C  SPECIFIC HEAT OF AIR, LINEAR REGRESSION FROM 220 K TO 360 K
C  FROM NBS CIRC. 564, BTU/(LB-F)
      CP = (3.4763 + 1.066E-4*TK)*0.068559
C  RAYLEIGH NUMBER, LEADING COEFFICIENT IS
C  32.174*3600*3600, FT/HR2
      RA = (4.16975E8)*BETA*RHO*CP*ABS(DT)*(AL**3)/NU/K
C  BRANCH TO DIFFERENT CORRELATIONS DEPENDING UPON
C  SURFACE ORIENTATION
      IF(ABS(PHI).LE.1.E-3)  GO TO 100
      IF(ABS(PHI-90.).LE.1.E-3)  GO TO 200
      IF(ABS(PHI).GT.1.E-3.AND.ABS(PHI).LT.2.)  GO TO 300
      IF(ABS(PHI).GT.2.0.AND.ABS(PHI-90.).GT.1.E-3)  GO TO 400
C  FOR HORIZONTAL SURFACES
  100 IF(DT.LT.0.0)  GO TO 150
      NUS = 0.15*RA**(1./3.)
      IF(RA.LT.8.E6)  NUS = 0.54*RA**0.25
      GO TO 1000
  150 NUS = 0.58*RA**0.2
      GO TO 1000
C  FOR VERTICAL SURFACES
  200 NUS = 0.10*RA**(1./3.)
      IF(RA.LT.1.E9)  NUS = 0.59*RA**0.25
      GO TO 1000
C  FOR NEARLY HORIZONTAL(UP TO 2 DEGREES TILT) SURFACES
  300 IF(DT.GT.0.0)  GO TO 450
      NUS = 0.58*RA**0.2
      GO TO 1000
C  FOR TILTED SURFACES
  400 IF(DT.GT.0.0)  GO TO 450
      NUS = 0.56*(RA*COS((90.-PHI)*3.14159265/180.))**0.25
      GO TO 1000
  450 GRC = 10.0**(PHI/(1.1870+0.0870*PHI))
      IF(ABS(PHI).LT.15.)  GRC = 1.E6
      IF(ABS(PHI).GT.75.)  GRC = 5.E9
      GR = RA/PR
      IF(GR.LE.GRC)  NUS=0.56*(RA*COS((90.-PHI)*3.14159265/180.))**0.25
      IF(GR.GT.GRC)  NUS = 0.14*(RA**(1./3.) - (GRC*PR)**(1./3.))
     &   +0.56*(GRC*PR*COS((90.-PHI)*3.14159265/180.))**0.25
      GO TO 1000
 1000 HCN = NUS*K/AL
C  CALCULATE FORCED CONVECTION COEFFICIENT
```

```
C  SEE HOLMAN, 5TH EDITION, PG. 191, EQN. 5-44, 5-46
C  AND PG. 202, EQN. 5-85
      RE = V*AL/NU
      IF(RE.LT.5.E5)  NUS = 0.664*(PR**(1./3.))*SQRT(RE)
      IF(RE.GT.5.E5)  NUS = (PR**(1./3.))*(0.037*(RE**0.8)-850.)
      HCF = NUS*K/AL
C  COMBINE NATURAL AND FORCED CONVECTION COEFFICIENTS
C  USING CHURCHILL'S CORRELATION
C  SEE J. HEAT TRANS., VOL. 108, PP. 835-840 (1986)
C  ASSUME ASSISTING FLOW IN ALL CASES
      HC = (HCF**3 + HCN**3)**(1./3.)
      RETURN
      END
C*********************************************************************
C**                                                                 **
C**                        SUBROUTINE HMASS                         **
C**                                                                 **
C*********************************************************************
      SUBROUTINE HMASS(TS,TA,HC,HM)
C  THIS SUBROUTINE CALCULATES THE MASS TRANSFER COEFFICIENT FOR
C  MOISTURE TRANSFER BETWEEN A SURFACE AND MOIST AIR
C  USING THE LEWIS RELATIONSHIP, AND EVALUATING ALL THERMOPHYSICAL
C  PROPERTIES AS THOSE OF DRY AIR
C  SEE HOLMAN, 5TH EDITION, PP. 494
C  TS = SURFACE TEMPERATURE, F
C  TA = AIR TEMPERATURE, F
C  HC = CONVECTION HEAT TRANSFER COEFFICIENT
C  HM = MASS TRANSFER COEFFICIENT, LB/(HR-FT2)
C
      REAL K
C  CALCULATE FILM TEMPERATURE
      TF = (TS+TA)/2.0
      TK = (TF+459.67)/1.8
C  THERMAL CONDUCTIVITY OF AIR FROM EQUATION IN NBS CIRC. 564
C  THERMAL COND. IN BTU/(HR-FT-F)
      K = 0.6325E-5*SQRT(TK)/(1.+(245.4*10.**(-12./TK))/TK)*241.77
C  DENSITY OF AIR, PERFECT GAS, NBS CIRC. 564, LB/CF
      RHO = 22.0493/TK
C  SPECIFIC HEAT OF AIR, LINEAR REGRESSION FROM 220 K TO 360 K
C  FROM NBS CIRC. 564, BTU/(LB-F)
      CP = (3.4763 + 1.066E-4*TK)*0.068559
C  CALCULATE THERMAL DIFFUSIVITY, FT2/HR
      ALF = K/CP/RHO
C  CALCULATE DIFFUSION COEFFICIENT FOR WATER VAPOR THROUGH AIR
C  D = FT2/HR, SEE 1985 ASHRAE HANDBOOK, PG. 5.2
      D = 0.035883/101.32*(TK**2.5)/(TK+245.0)
      HM = HC/CP/((ALF/D)**(2.0/3.0))
      RETURN
      END
C*********************************************************************
C**                                                                 **
C**                        FUNCTION HRAD                            **
```

```
C**                                                                   **
C*********************************************************************
      FUNCTION HRAD(G,T1,T2)
C  THIS FUNCTION CALCULATES RADIATIVE COEFFICIENTS FOR HEAT BALANCE
C  EQUATIONS
      T1R = (T1 + 459.67)/100.
      T2R = (T2 + 459.67)/100.
      HRAD = 1.714E-3*(T1R*T1R+T2R*T2R)*(T1R+T2R)*G
      RETURN
      END
C*********************************************************************
C**                                                                   **
C**                          SUBROUTINE MOISTM                        **
C**                                                                   **
C*********************************************************************
      SUBROUTINE MOISTM(TS,TO,TI,TA,HCI,A,AWRAT,AMC,AMASS,HUM,HUMI,PERM,
     1   AMDOT,EXFIL,AMW,BMW,K,PERMRB,WRB,AMWRB,BMWRB,RHATC)
C  NEXT LINE ADDED FOR VERSION 1B
      COMMON /HUMID/WO,PATM
C  THIS SUBROUTINE PERFORMS A MOISTURE BALANCE ON THE ATTIC SPACE
C  TS = SURFACE TEMPERATURE, DEGREES F
C  TO = OUTSIDE AIR TEMPERATURE
C  TI = INSIDE AIR TEMPERATURE
C  TA = ATTIC AIR TEMPERATURE
C  HCI = CONVECTION HEAT TRANSFER COEFFICIENTS
C  A = PROJECTED SURFACE AREAS
C  AWRAT = RATIO OF EXPOSED WOOD SURFACE AREAS TO PROJECTED AREAS
C  AMC = WOOD MOISTURE CONTENTS, FRACTION OF DRY WEIGHT
C  HUM = RELATIVE HUMIDITY OF OUTSIDE AIR
C  HUMI = RELATIVE HUMIDITY OF INSIDE AIR
C  PERM = WATER VAPOR PERMEANCES
C  AMDOT = MASS FLOW OF VENTILATION AIR
C  EXFIL = MASS FLOW OF AIR FROM HOUSE INTO ATTIC
C  AMW = MOISTURE ADSORBED PER UNIT PROJECTED AREA
C  BMW = COEFFICIENT OF LINEAR TERM IN TAYLOR SERIES
C        EXPANSION OF WS(I)
C  K = NUMBER OF SURFACES
C  PERMRB = WATER VAPOR PERMEANCE OF HORIZONTAL RADIANT BARRIER
C  WRB = AMOUNT OF WATER ACCUMULATED ON BOTTOM OF HORIZONTAL RADIANT
C        BARRIER, POUNDS PER SQUARE FOOT
C  AMWRB = AMOUNT OF WATER CONDENSED ON BOTTOM OF HORIZONTAL RADIANT
C          BARRIER, POUNDS PER SQUARE FOOT, DURING CURRENT HOUR
C  RHATC = RELATIVE HUMIDITY IN ATTIC SPACE
      DIMENSION TS(K),HCI(K),A(K),AWRAT(K),AMC(K),PERM(K),AMW(K)
      DIMENSION WS(10),P(10),HM(10),AMASS(K),BMW(K)
      EPS = 1.E-3
C  CALCULATE HUMIDITY RATIOS AT WOOD SURFACES
      DO 10 I = 1,K
   10 WS(I) = WDHUM(AMC(I),TS(I))
C  CALCULATE HUMIDITY RATIOS OF INSIDE AND  OUTSIDE AIR
      CALL PSY(TI,HUMI,PI,WI)
C  NEXT LINE DISABLED FOR VERSION 1B
```

```
C       CALL PSY(TO,HUM,PO,WO)
C   NEXT 2 LINES ADDED FOR VERSION 1B
        XX = WO/0.62198
        PO = PATM*XX/(1.0 + XX)
C   NEXT 2 LINES ADDED FOR MOISTURE ON RB
C   CALCULATE SATURATION VAPOR PRESSURE AT HORIZONTAL RADIANT BARRIER
        CALL PSY1(TS(1),100.,PRBSAT,WRBSAT,DWSDT)
C   CALCULATE MASS TRANSFER COEFFICIENTS
        DO 20 I = 1,K
   20   CALL HMASS(TS(I),TA,HCI(I),HM(I))
C   SET UP WATER VAPOR PARTIAL PRESSURES
        P(1) = PI
        DO 30 I = 2,K
   30   P(I) = PO
C CALCULATE HUMIDITY RATIO OF ATTIC AIR FROM MOISTURE BALANCE
        PA = PO
C   NEXT 6 LINES ADDED FOR MOISTURE ON RB
        PRB = PA + (PI-PA)*PERM(1)/PERMRB
        IF(WRB.GT.0.0)  PRB = PRBSAT
        IF(PRB.GT.PRBSAT)  PRB = PRBSAT
        NIT = 0
  100   X = 0.0
        X = X + A(1)*(PERMRB*PRB + AWRAT(1)*HM(1)*WS(1))
        DO 40 I = 2,K
        X = X + A(I)*PERM(I)*P(I)
   40   X = X + A(I)*AWRAT(I)*HM(I)*WS(I)
C   NEXT LINE DELETED AND FOLLOWING 8 LINES ADDED FOR MOIST. ON RB
C       X = X + AMDOT*WO + EXFIL*WI
        X = X + AMDOT*WO
        IF(WRB.GT.0.0)  THEN
          X = X + EXFIL*WRBSAT
        ELSE IF(WI.GE.WRBSAT) THEN
          X = X + EXFIL*WRBSAT
        ELSE
          X = X + EXFIL*WI
        END IF
C   NEXT 2 LINES DELETED AND FOLLOWING LINE ADDED FOR MOIST. ON RB
C       NIT = 0
C 100   Y = 0.0
        Y = 0.0
        DO 50 I = 1,K
   50   Y = Y + A(I)*AWRAT(I)*HM(I)
        Y = Y + AMDOT + EXFIL
C   NEXT LINE ADDED FOR MOIST. ON RB
        Y = Y + A(1)*PERMRB*(PATM - PA)/0.62198
C   IN FOLLOWING, PATM HAS BEEN SUBSTITUTED FOR 14.696 IN VERSION 1B
        DO 60 I = 2,K
C   60  Y = Y + A(I)*PERM(I)*(14.696 - PA)/0.62198
   60   Y = Y + A(I)*PERM(I)*(PATM - PA)/0.62198
        WA = X/Y
        XX = WA/0.62198
C       PANEW = 14.696*XX/(1.0 + XX)
```

```
      PANEW = PATM*XX/(1.0 + XX)
C  NEXT 3 LINES ADDED FOR MOIST. ON RB
      PRBNEW = PANEW + (PI - PANEW)*PERM(1)/PERMRB
      IF(WRB.GT.0.0) PRBNEW = PRBSAT
      IF(PRBNEW.GT.PRBSAT) PRBNEW = PRBSAT
      NIT = NIT + 1
      IF (NIT.GT.10)  GO TO 200
C  NEXT LINE CHANGED FOR MOIST. ON RB
      IF(ABS(1.-PANEW/PA).LT.EPS.AND.ABS(1.-PRBNEW/PRB).LT.EPS)
     &   GO TO 200
      PA = PANEW
C  NEXT LINE ADDED FOR MOIST. ON RB
      PRB = PRBNEW
      GO TO 100
  200 CONTINUE
C  CALCULATE WATER ADSORBED BY EACH SURFACE
      DO 300 I = 1,K
  300 AMW(I) = HM(I)*AWRAT(I)*(WA-WS(I))
C  NEXT 4 LINES ADDED FOR MOIST. ON RB
      AMWRB = 1./(1./PERM(1) - 1./PERMRB)*(PI - PRB)
     &        + PERMRB*(PA - PRB)
      IF(WRB.GT.0.0.OR.WI.GE.WRBSAT)
     &    AMWRB = AMWRB + EXFIL/A(1)*(WI - WRBSAT)
C  CALCULATE CORRECTION TERM FOR TAYLOR SERIES EXPANSION OF
C  ADSORBED WATER
      DO 310 I = 1,K
  310 BMW(I) = HM(I)*AWRAT(I)*WS(I)/28.6
C  NEXT 3 LINES ADDED FOR MOIST. ON RB
      BMWRB = EXFIL/A(1)*DWSDT
      CALL PSY(TA,100.0,PASAT,WASAT)
      RHATC = PA/PASAT*100.0
      RETURN
      END
C***********************************************************************
C**                                                                   **
C**                          SUBROUTINE PSY                           **
C**                                                                   **
C***********************************************************************
      SUBROUTINE PSY(T,HUM,P,W)
C  NEXT LINE ADDED FOR VERSION 1B
      COMMON /HUMID/WO,PATM
C  THIS SUBROUTINE CALCULATES THE WATER VAPOR PARTIAL PRESSURE AND
C  THE HUMIDITY RATIO, GIVEN THE TEMPERATURE AND RELATIVE HUMIDITY
C  USING EQUATION FROM 1989 ASHRAE FUNDAMENTALS P.6.6
C  T = DRYBULB TEMPERATURE, DEGREES F
C  HUM = RELATIVE HUMIDITY, PERCENT
C  P = WATER VAPOR PARTIAL PRESSURE, PSIA
C  W = HUMIDITY RATIO, POUNDS OF WATER PER POUNDS OF DRY AIR
      C1 = -10214.16462
      C2 = -4.89350301
      C3 = -0.537657944E-2
      C4 = 0.192023769E-6
```

```
      C5 = 0.355758316E-9
      C6 = -0.0903446883E-12
      C7 = 4.1635019
      C8 = -10440.39708
      C9 = -11.2946496
      C10 = -0.027022355
      C11 = 0.12890360E-4
      C12 = -0.2478068E-8
      C13 = 6.5459673
      TR = T + 459.67
      IF(T.GE.32.0)  GO TO 10
      X = C1/TR + C2 + C3*TR + C4*TR*TR +C5*TR**3+C6*TR**4+C7*ALOG(TR)
      GO TO 20
   10 X = C8/TR + C9 + C10*TR + C11*TR*TR + C12*TR**3 + C13*ALOG(TR)
   20 PSAT = EXP(X)
      DPSDT = PSAT*DXDT
      P = (HUM/100.0)*PSAT
C     W = 0.62198*P/(14.696-P)
      W = 0.62198*P/(PATM-P)
      RETURN
      END
C*********************************************************************
C**                                                                 **
C**                        SUBROUTINE SOLVP                         **
C**                                                                 **
C*********************************************************************
      SUBROUTINE SOLVP (I,C,D,X)
C  SUBROUTINE TAKEN FROM NBSLD
C  THIS SUBROUTINE SOLVES A SET OF SIMULTANEOUS LINEAR EQUATIONS
C  USING GAUSSIAN ELIMINATION
C  I = NUMBER OF EQUATIONS TO BE SOLVED
C  C = MATRIX OF COEFFICIENTS OF SET OF EQUATIONS
C  D = VECTOR ON RIGHT HAND SIDE OF EQUATIONS
C  X = SOLUTION VECTOR, CX = D
      DIMENSION A(100,101),C(I,I),D(I),X(I)
      M = I
      N = M + 1
      DO 10 IX = 1,M
      DO 10 IY = 1,M
   10 A(IX,IY) = C(IX,IY)
      DO 20 IZ = 1,M
   20 A(IZ,N) = D(IZ)
      L = 1
   30 AA = A(L,L)
      DO 40 K = L,N
   40 A(L,K) = A(L,K)/AA
      DO 60 K = 1,M
      IF (K.EQ.L)  GO TO 60
      AA = -A(K,L)
      DO 50 IA = L,N
   50 A(K,IA) = A(K,IA) + AA*A(L,IA)
   60 CONTINUE
```

```
      L = L + 1
      IF (L.LE.M)  GO TO 30
      DO 70 IP = 1,M
   70 X(IP) = A(IP,N)
      RETURN
      END
C*********************************************************************
C**                                                                 **
C**                        SUBROUTINE VENT                          **
C**                                                                 **
C*********************************************************************
      SUBROUTINE VENT(TO,TA,WS,DIR,H,AI,AO,ITYPE,AMCDOT,AMDOT,V)
C  THIS SUBROUTINE CALCULATES THE VENTILATION RATE FOR A GABLED ATTIC
C  TO = OUTDOOR AIR TEMPERATURE, F
C  TA = AVERAGE ATTIC AIR TEMPERATURE, F
C  WS = WIND SPEED, MPH
C  DIR = WIND DIRECTION
C  H = HEIGHT OF ATTIC
C  AI = AREA OF VENT INLET, SQUARE FEET
C  AO = AREA OF VENT OUTLET, SQUARE FEET
C  ITYPE = 1, SOFFIT AND RIDGE VENTS
C  ITYPE = 2, SOFFIT AND GABLE VENTS
C  ITYPE = 3, SOFFIT VENTS
C  AMCDOT = AIR MASS FLOW RATE TIMES SPECIFIC HEAT, BTU/HR-F
C  V = VOLUME FLOW RATE, CUBIC FEET PER HOUR
C  CALCULATE ABSOLUTE TEMPERATURES, R
      TOR = TO + 459.67
      TAR = TA + 459.67
C CALCULATE DENSITIES AND SPECIFIC HEATS OF AIR
      RHOO = 22.0493/(TOR/1.8)
      RHOA = 22.0493/(TAR/1.8)
      CP = (3.4763 + 1.066E-4*(TAR/1.8))*0.068559
C  DETERMINE MINIMUM VENT AREA AND MAXIMUM VENT AREAS
      AMIN = AMIN1(AI,AO)
      AMAX = AMAX1(AI,AO)
C  CALCULATE HEIGHT OF NEUTRAL PRESSURE LEVEL FROM LOWER OPENING
C  SEE PG. 22.3 OF 1985 ASHRAE HANDBOOK OF FUNDAMENTALS
      HNPL = H/(1.+AI*AI/AO/AO*TAR/TOR)
      IF(TAR.LT.TOR)  HNPL = H/(1.+AI*AI/AO/AO*TOR/TAR)
C  CALCULATE FLOW DUE TO STACK EFFECT, SEE ASHRAE PG. 22.7
      IF(TAR.GE.TOR)  QSTACK = 0.65*AMIN*SQRT(2.0*32.174*3600.*3600.
     &                         *HNPL*(TAR-TOR)/TAR)
      IF(TAR.GE.TOR)  AMSTACK = QSTACK*RHOO
      IF(TAR.LT.TOR)  QSTACK = 0.65*AMIN*SQRT(2.0*32.174*3600.*3600.
     &                         *HNPL*(TOR-TAR)/TOR)
      IF(TAR.LT.TOR)  AMSTACK = QSTACK*RHOA
      IF(ITYPE.EQ.3)  QSTACK = 0.0
      IF(ITYPE.EQ.3)  AMSTACK = 0.0
C  CALCULATE FLOW DUE TO WIND PRESSURE, SEE ASHRAE PG. 22.6
      QWIND = 5280.0*0.6*AMIN*WS
C  MULTIPLY BY EFFECTIVENESS COEFFICIENT DERIVED FROM
C  BURCH AND TREADO'S DATA FOR ATTIC VENTILATION
```

```
C  TYPE 1 = SOFFIT AND RIDGE VENTS
C  TYPE 2 = SOFFIT AND ROOF VENTS, ASSUMED TO BE SAME AS SOFFIT AND
C           GABLE VENTS
C  TYPE 3 = SOFFIT VENTS ONLY
      IF(ITYPE.EQ.1) CF = 0.38
      IF(ITYPE.EQ.2) CF = 0.54
      IF(ITYPE.EQ.3) THEN
         IF(DIR.EQ.0.OR.DIR.EQ.180.) CF = 0.089
         IF(DIR.NE.0.0.AND.DIR.NE.180.0)
     &   CF = 0.089 + 0.132*(ABS(SIN(DIR*3.14159265/180.)))**2.5
      END IF
      QWIND = QWIND/0.6*CF
      AMWIND = QWIND*RHOO
C  COMBINE STACK AND WIND FLOWS, SEE ASHRAE PG. 22.5
      AMDOT = SQRT(AMSTACK*AMSTACK + AMWIND*AMWIND)
C  CORRECT FOR UNEQUAL INLET AND OUTLET AREAS (ASHRAE PG. 22.7)
      ARAT = AMIN/AMAX
      AMDOT = AMDOT * (1.0 + 0.4077*(1.0-ARAT**1.5))
      AMCDOT = CP*AMDOT
C  CALCULATE VOLUME FLOW RATE, CUBIC FEET PER HOUR
      V = AMDOT/RHOA
      RETURN
      END
C*********************************************************************
C**                                                                 **
C**                        SUBROUTINE VIEW2                         **
C**                                                                 **
C*********************************************************************
      SUBROUTINE VIEW2(AL,W,PITCH1,PITCH2,H1,EI,G,K)
C  THIS SUBROUTINE CALCULATES THE VIEW FACTORS AMONG THE SURFACES
C  IN A GABLED ATTIC, HAVING A FIVE-SIDED CROSS-SECTION, AND
C  HAVING ARBITRARILY PITCHED ROOF SURFACES
C  AL = LENGTH OF ATTIC
C  W = WIDTH OF ATTIC
C  PITCH1 = PITCH OF SOUTH ROOF, DEGREES
C  PITCH2 = PITCH OF NORTH ROOF, DEGREES
C  H1 = HEIGHT OF SIDE WALL
C  SURFACE 1 = CEILING
C  SURFACE 2 = SOUTH ROOF (FOR E-W RIDGE)
C  SURFACE 3 = NORTH ROOF
C  SURFACE 4 = EAST GABLE
C  SURFACE 5 = WEST GABLE
C  SURFACE 6 = SOUTH SIDE WALL
C  SURFACE 7 = NORTH SIDE WALL
C  EI = EMITTANCE OF SURFACE FACING ATTIC SPACE
C  F(I,J) = RADIATION VIEW FACTOR FROM SURFACE I TO
C           SURFACE J
C  G(I,J) = RADIATION FACTOR
      DIMENSION F(7,7),CHI(7,7),PSI(7,7),E(7),B(7),EI(K),G(7,7)
      PI = 3.14159265
      PIO2 = PI/2.0
      P1 = PITCH1*PI/180.
```

```
      P2 = PITCH2*PI/180.
      F(1,1) = 0.0
      F(2,2) = 0.0
      F(3,3) = 0.0
      F(4,4) = 0.0
      F(5,5) = 0.0
      F(6,6) = 0.0
      F(7,7) = 0.0
      P3 = (180.-PITCH1-PITCH2)*PI/180.
      IP1 = PITCH1
      IP2 = PITCH2
      IP3 = 180.0 - PITCH1 - PITCH2
      IF(IP1.EQ.90.AND.IP2.EQ.90) STOP
      IF(IP1.EQ.0.AND.IP2.NE.0)  STOP
      IF(IP1.NE.0.AND.IP2.EQ.0)  STOP
      IF(IP1.EQ.0)  GO TO 20
      A2 = W*SIN(P2)/SIN(P3)
      A3 = W*SIN(P1)/SIN(P3)
      A2EXT = H1/SIN(P1)
      A3EXT = H1/SIN(P2)
      IF(IP1.NE.90)  W2EXT = H1/TAN(P1)
      IF(IP1.EQ.90)  W2EXT = 0.0
      IF(IP2.NE.90)  W3EXT = H1/TAN(P2)
      IF(IP2.EQ.90)  W3EXT = 0.0
      A2P = A2 + A2EXT
      A3P = A3 + A3EXT
      W2P = W + W2EXT
      W3P = W + W3EXT
      IF(IP1.NE.90)  F(1,2) = (W2P*FMN(A2P,AL,W2P,P1)
     &        +W2EXT*FMN(A2EXT,AL,W2EXT,P1)
     &        -W2P*FMN(A2EXT,AL,W2P,P1)-W2EXT*FMN(A2P,AL,W2EXT,P1))/W
      IF(IP1.EQ.90)  F(1,2) = FMN(A2P,AL,W,P1)-FMN(H1,AL,W,P1)
      IF(IP2.NE.90)  F(1,3) = (W3P*FMN(A3P,AL,W3P,P2)
     &        +W3EXT*FMN(A3EXT,AL,W3EXT,P2)
     &        -W3P*FMN(A3EXT,AL,W3P,P2)-W3EXT*FMN(A3P,AL,W3EXT,P2))/W
      IF(IP2.EQ.90)  F(1,3) = FMN(A3P,AL,W,P2)-FMN(H1,AL,W,P2)
      F(1,6) = FMN(H1,AL,W,PIO2)
      F(1,7) = FMN(H1,AL,W,PIO2)
      F(1,4) = (1.0 - F(1,2) - F(1,3) - F(1,6) - F(1,7))/2.0
      F(1,5) = F(1,4)
      F(2,1) = W*AL*F(1,2)/A2/AL
      F(2,3) = FMN(A3,AL,A2,P3)
      ANG = P1 + PIO2
      IF(IP1.NE.90)  F(2,6) = FMN(H1,AL,A2,ANG)
      IF(IP1.EQ.90)  F(2,6) = 0.0
      ANG = PIO2 - P1
      IF(IP1.EQ.90) GO TO 5
      A2P = W/SIN(ANG)
      A2EXT = A2P - A2
      H1EXT = W/TAN(ANG)
      H1P = H1 + H1EXT
C NEXT LINE ADDED 4-6-88
```

```
      IF(IP2.NE.90) THEN
      F(2,7) = (A2P*FMN(H1P,AL,A2P,ANG)+A2EXT*FMN(H1EXT,AL,A2EXT,ANG)
     &         -A2P*FMN(H1EXT,AL,A2P,ANG)-A2EXT*FMN(H1P,AL,A2EXT,ANG))/A2
C NEXT 3 LINES ADDED 4-6-88
      ELSE
      F(2,7) = FMN(H1P,AL,A2,ANG) - FMN(H1EXT,AL,A2,ANG)
      END IF
      GO TO 6
    5 F(2,7) = ((A2+H1)*FP((A2+H1),AL,W)-H1*FP(H1,AL,W)-A2*FP(A2,AL,W))/
     &           2.0/A2
    6 F(2,4) = (1.0 - F(2,1) - F(2,3) - F(2,6) - F(2,7))/2.0
      F(2,5) = F(2,4)
      F(3,1) = W*AL*F(1,3)/A3/AL
      F(3,2) = A2*AL*F(2,3)/A3/AL
      ANG = P2 + PIO2
      IF(IP2.NE.90)  F(3,7) = FMN(H1,AL,A3,ANG)
      IF(IP2.EQ.90)  F(3,7) = 0.0
      ANG = PIO2 - P2
      IF(IP2.EQ.90) GO TO 7
      A3P = W/SIN(ANG)
      A3EXT = A3P - A3
      H1EXT = W/TAN(ANG)
      H1P = H1 + H1EXT
C NEXT LINE ADDED 4-6-88
      IF(IP1.NE.90) THEN
      F(3,6) = (A3P*FMN(H1P,AL,A3P,ANG)+A3EXT*FMN(H1EXT,AL,A3EXT,ANG)
     &         -A3P*FMN(H1EXT,AL,A3P,ANG)-A3EXT*FMN(H1P,AL,A3EXT,ANG))/A3
C NEXT 3 LINES ADDED 4-6-88
      ELSE
      F(3,6) = FMN(H1P,AL,A3,ANG) - FMN(H1EXT,AL,A3,ANG)
      END IF
      GO TO 8
    7 F(3,6) = ((A3+H1)*FP((A3+H1),AL,W)-H1*FP(H1,AL,W)-A3*FP(A3,AL,W))/
     &           2.0/A3
    8 F(3,4) = (1.0 - F(3,1) - F(3,2) - F(3,6) - F(3,7))/2.0
      F(3,5) = F(3,4)
      F(6,1) = W*AL*F(1,6)/H1/AL
      F(6,2) = A2*AL*F(2,6)/H1/AL
      F(6,3) = A3*AL*F(3,6)/H1/AL
      F(6,7) = FP(H1,AL,W)
      F(6,4) = ( 1.0 - F(6,1) - F(6,2) - F(6,3) - F(6,7))/2.0
      F(6,5) = F(6,4)
      F(7,1) = W*AL*F(1,7)/H1/AL
      F(7,2) = A2*AL*F(2,7)/H1/AL
      F(7,3) = A3*AL*F(3,7)/H1/AL
      F(7,6) = F(6,7)
      F(7,4) = F(6,4)
      F(7,5) = F(7,4)
      F(4,1) = W*AL*F(1,4)/(0.5*A2*SIN(P1)*W + W*H1)
      F(4,2) = A2*AL*F(2,4)/(0.5*A2*SIN(P1)*W + W*H1)
      F(4,3) = A3*AL*F(3,4)/(0.5*A2*SIN(P1)*W + W*H1)
      F(4,6) = H1*AL*F(6,4)/(0.5*A2*SIN(P1)*W + W*H1)
```

```
      F(4,7) = H1*AL*F(7,4)/(0.5*A2*SIN(P1)*W + W*H1)
      F(4,5) = 1.0 - F(4,1) - F(4,2) - F(4,3) - F(4,6) - F(4,7)
      F(5,1) = F(4,1)
      F(5,2) = F(4,2)
      F(5,3) = F(4,3)
      F(5,4) = F(4,5)
      F(5,6) = F(4,6)
      F(5,7) = F(4,7)
      GO TO 50
   20 F(1,2) = 0.5*FP(W,AL,H1)
      F(1,3) = F(1,2)
      F(1,4) = FMN(H1,W,AL,PIO2)
      F(1,5) = F(1,4)
      F(1,6) = FMN(H1,AL,W,PIO2)
      F(1,7) = F(1,6)
      F(2,1) = 2.0*F(1,2)
      F(2,3) = 0.0
      X = W/2.0
      F(2,6) = FMN(H1,AL,X,PIO2)
      X = W/2.0
      F(2,7) = H1*(FMN(W,AL,H1,PIO2)-FMN(X,AL,H1,PIO2))/X
      F(2,4) = (1.0 - F(2,1) - F(2,3) - F(2,6) - F(2,7))/2.0
      F(2,5) = F(2,4)
      F(3,1) = F(2,1)
      F(3,2) = 0.0
      F(3,4) = F(2,4)
      F(3,5) = F(2,5)
      F(3,6) = F(2,7)
      F(3,7) = F(2,6)
      F(4,1) = AL*F(1,4)/H1
      F(4,2) = (AL*W/2.0)*F(2,4)/(H1*W)
      F(4,3) = F(4,2)
      F(4,5) = FP(H1,W,AL)
      F(4,6) = FMN(AL,H1,W,PIO2)
      F(4,7) = F(4,6)
      F(5,1) = F(4,1)
      F(5,2) = F(4,2)
      F(5,3) = F(4,3)
      F(5,4) = F(4,5)
      F(5,6) = F(4,6)
      F(5,7) = F(4,7)
      F(6,1) = W*F(1,6)/H1
      F(6,2) = (AL*W/2.0)*F(2,6)/(AL*H1)
      F(6,3) = (AL*W/2.0)*F(3,6)/(AL*H1)
      F(6,4) = W*F(4,6)/AL
      F(6,5) = F(6,4)
      F(6,7) = FP(H1,AL,W)
      F(7,1) = F(6,1)
      F(7,2) = F(6,3)
      F(7,3) = F(6,2)
      F(7,4) = F(6,4)
      F(7,5) = F(6,5)
```

```
      F(7,6) = F(6,7)
C
   50 CONTINUE
      DO 100 I = 1,7
      DO 100 J = 1,7
  100 CHI(I,J) = -(1. - EI(I))*F(I,J)/EI(I)
      DO 200 I = 1,7
  200 CHI(I,I) = CHI(I,I) + 1./EI(I)
C  INVERT CHI MATRIX TO OBTAIN PSI MATRIX
      DO 500  L = 1,7
      DO 300 I = 1,7
      E(I) = 0.0
  300 IF(I.EQ.L)  E(I) = 1.0
      CALL SOLVP(7,CHI,E,B)
      DO 400 I = 1,7
  400 PSI(I,L) = B(I)
  500 CONTINUE
      DO 600  I = 1,7
      DO 600  J = 1,7
  600 G(I,J) = PSI(I,J)*EI(I)/(1. - EI(I))
C     DO 1000 I = 1,7
C1000 WRITE(6,2000) (F(I,J),J=1,7)
C     WRITE(6,2000)
C     DO 1001 I = 1,7
C1001 WRITE(6,2000) (CHI(I,J),J=1,7)
C     WRITE(6,2000)
C     DO 1002 I = 1,7
C1002 WRITE(6,2000) (PSI(I,J),J=1,7)
C     WRITE(6,2000)
C     DO 1003 I = 1,7
C1003 WRITE(6,2000) (G(I,J),J=1,7)
C     WRITE(6,2000)
C2000 FORMAT(1X,7F10.4)
      RETURN
      END
C*********************************************************************
C**                                                                 **
C**                        FUNCTION WDHUM                           **
C**                                                                 **
C*********************************************************************
      FUNCTION WDHUM(AMC,T)
C  THIS FUNCTION CALCULATES THE HUMIDITY RATIO OF A WOOD SURFACE
C  USING THE EQUATION FROM P. G. CLEARY (1985).
C  WDHUM = HUMIDITY RATIO, POUNDS OF WATER PER POUND OF DRY AIR
C  AMC = WOOD MOISTURE CONTENT, FRACTION OF DRY WEIGHT OF WOOD
C  T = WOOD SURFACE TEMPERATURE, DEGREES F
      A = 28.6
      B = -0.00049
      C = 0.0172
      D = -0.060
      E = 0.076
      WDHUM = B + C*AMC + D*AMC*AMC + E*AMC**3
```

```
C NEXT LINE ADDED 11-2-88
      IF(WDHUM.LT.0.0) WDHUM = 0.0
      WDHUM = WDHUM * EXP(T/A)
      RETURN
      END
C*********************************************************************
C**                                                                 **
C**                          SUBROUTINE SUN1                        **
C**                                                                 **
C*********************************************************************
      SUBROUTINE SUN1(STALAT,IDOY)
C KW  SUBROUTINE SUN1
C  CALCULATES DAILY DATA ON SOLAR RADIATION
CKW SUBROUTINE BORROWED FROM DOE 2.1C WITH MODIFICATIONS
C
CKW   COMMON /LOCALD/STALAT,STALON,ITIMZ,BAZIM,BALTIT,
CKW  1               SSTALA,CSTALA,TSTALA,SBAZIM,CBAZIM,
CKW  2               BXORG,BYORG,SHCOEF,TP1,TP2,WSTP1,WSTP2,
CKW  3               WSHGT
CKW   DIMENSION LOCALD(18)
CKW   EQUIVALENCE (LOCALD(1), STALAT)
      COMMON /SUND/ISUNUP,GUNDOG,HORANG,TDECLN,EQTIME,SOLCON,
     1             ATMEXT,SKYDFF,RAYCOS(3),RDN,
     2             BSUN,DECLN,CD,SD,FSUNUP
CKW   COMMON /TIME/IDOY,IDOW,IDSTF,ISCHR,ISCDAY,
CKW  1             IMO,IDAY,IYR,IHR,CLOCK(10),IHLFLG,IDSFLG,
CKW  2             MONDSC(12),MONLEN(12),MONSDA(12),IEODMR
C  GET SIN, COS OF DAY OF YEAR/365
      C1 = COS(0.01721*FLOAT(IDOY))
      S1 = SIN(0.01721*FLOAT(IDOY))
      S2 = 2.*S1*C1
      C2 = C1*C1 - S1*S1
      C3 = C1*C2 - S1*S2
      S3 = C1*S2 + S1*C2
C  CALC TANGENT OF DECLINATION ANGLE
      TDECLN = 0.00527 - 0.4001*C1 - 0.003996*C2 - 0.004240*C3
     &         + 0.0672*S1
C  CALC EQUATION OF TIME
      EQTIME = 0.696E-4 + 0.706E-2*C1 - 0.0533*C2 - 0.157E-2*C3-0.122*S1
     &         -0.156*S2 - 0.556E-2*S3
C  CALCULATE SOLAR CONSTANT
      SOLCON = 368.44 + 24.52*C1 - 1.14*C2 - 1.09*C3 + 0.58*S1 - 0.18*S2
     &         +0.28*S3
C  IF SOUTHERN HEMISPHERE, SHIFT AIRMASS AND ATMOSPHERIC
C  EXTINCTION CURVES BY 6 MONTHS
      IF(STALAT.GE.0.) GO TO 10
      C1 = -C1
      S1 = -S1
      C3 = -C3
      S3 = -S3
   10 CONTINUE
C  CALCULATE ATMOSPHERIC EXTINCTION COEFFICIENT
```

```
      ATMEXT = 0.1717 - 0.0344*C1 + 0.0032*C2 + 0.0024*C3 - 0.0043*S1
     &         -0.0008*S3
C  CALCULATE SKY DIFFUSIVITY
      SKYDFF = 0.0905 - 0.0410*C1 + 0.0073*C2 + 0.0015*C3 - 0.0034*S1
     &         +0.0004*S2 - 0.0006*S3
C  CALCULATE HOUR ANGLE OF SUNRISE
C NEXT LINE ADDED BY K. WILKES
      TSTALA = TAN(STALAT)
      GUNDOG = ACOS(-TSTALA*TDECLN)
      DECLN = ATAN(TDECLN)
      CD = COS(DECLN)
      SD = SIN(DECLN)
      RETURN
      END
C*********************************************************************
C**                                                                 **
C**                        SUBROUTINE WDTSUN                        **
C**                                                                 **
C*********************************************************************
      SUBROUTINE WDTSUN(IHR,ITIMZ,STALON,STALAT,SSTALA,CSTALA,SBAZIM,
     &                  CBAZIM,CLRNES,SOLRAD,DIRSOL,ISUN)
CKW   SUBROUTINE WDTSUN
CKW CALCULATE WEATHER DATA AND SUN HOURLY DATA
CKW SUBROUTINE BORROWED FROM DOE 2.1C, WITH MODIFICATIONS
CKW IHR = HOUR OF DAY
CKW ITIMZ = TIME ZONE INDICATOR, = 5 FOR EASTERN, = 6 FOR CENTRAL,ETC.
CKW STALON = LONGITUDE
CKW STALAT = LATITUDE
CKW SSTALA = SIN OF LATITUDE
CKW CSTALA = COSINE OF LATITUDE
CKW SBAZIM = SIN OF BUILDING AZIMUTH
CKW CBAZIM = COSINE OF BUILDING AZIMUTH
CKW CLRNES = ATMOSPHERIC CLEARNESS NUMBER
CKW QSOLH = SOLAR RADIATION ON HORIZONTAL SURFACE
CKW CLDAMT = CLOUD AMOUNT
CKW ICLDTY = CLOUD TYPE
CKW ISUN = FLAG FOR TYPE OF SOLAR DATA AVAILABLE
CKW ISUN = 1, MEASURED TOTAL HORIZONTAL AND DIRECT AVAILABLE
CKW ISUN = 2, MEASURED TOTAL HORIZONTAL ONLY AVAILABLE
CKW ISUN = 3, NO MEASURED SOLAR, BUT MEASURED CLOUD AMOUNT
CKW RDNCC = DIRECT NORMAL SOLAR, WITH CLOUD COVER
CKW BSCC = DIFFUSE WITH CLOUD COVER
CKW   COMMON /CLCFLG/IFSTHR,IPRDFL,IGOLGE,NDD,IDDFLG,LDSTYP
CKW   COMMON /INFPAR/PTWV,DUMG(8),PSE
CKW   COMMON /LOCALD/STALAT,STALON,ITIMZ,BAZIM,BALTIT,
CKW  1               SSTALA,CSTALA,TSTALA,SBAZIM,CBAZIM,
CKW  2               BXORG,BYORG,SHCOEF,TP1,TP2,WSTP1,WSTP2,
CKW  3               WSHGT
CKW   DIMENSION LOCALD(18)
CKW   EQUIVALENCE (LOCALD(1), STALAT)
      COMMON /SUND/ISUNUP,GUNDOG,HORANG,TDECLN,EQTIME,SOLCON,
     1             ATMEXT,SKYDFF,RAYCOS(3),RDN,
```

```
     2              BSUN,DECLN,CD,SD,FSUNUP
CKW   COMMON /TIME/IDOY,IDOW,IDSTF,ISCHR,ISCDAY,
CKW  1              IMO,IDAY,IYR,IHR,CLOCK(10),IHLFLG,IDSFLG,
CKW  2              MONDSC(12),MONLEN(12),MONSDA(12),IEODMR
CKW   COMMON /WEATH/IWDID(5),LRECX,WLAT,WLONG,LTIMZ,IFX,IWSIZ,
CKW  1               CLRNES,TGNDR,WBT,DBT,PATM,CLDAMT,ISNOW,IRAIN,
CKW  2        IWNDDR,HUMRAT,DENSTY,ENTHAL,DIFSOL,DIRSOL,SOLRAD,ICLDTY,
CKW  3               WNDSPD,IDUMMY,DPT,WNDDRR,CLDCOV,RDNCC,BSCC,SKYA,
CKW  4               DBTR,GTEMP(12),CLR(12)
CKW NEXT TWO COMMONS ADDED BY K. WILKES
      COMMON /SUN2/RDNCC,BSCC
      COMMON /CLOUD/CLDAMT,ICLDTY,CC
CKW   IF(NDD.GT.0) GO TO 50
C  IF NOT DESIGN DAY, GET WEATHER DATA FROM THE HOURLY WEATHER FILE
CKW   CALL WEATHI
CKW   GO TO 60
C  OTHERWISE, GET DESIGN DAY WEATHER
CKW50 CALL DESWTH
CKW60 CONTINUE
C  CONVERT WIND DIRECTION FROM 16THS OF CIRCLE TO RADIANS
CKW   WNDDRR = FLOAT(IWNDDR)*0.39269908
C   CALCULATE PRESSURE DUE TO WIND VELOCITY
CKW   PTWV = 0.000638*WNDSPD*WNDSPD
C  SET RADIATION LOSS TO SKY FOR TILT = 0
CKW   SKYA = (10. - CLDAMT)*2.
C  CALCULATE HOUR ANGLE
      HORANG = 0.2618*(FLOAT(IHR-12+ITIMZ) + EQTIME - 0.5) - STALON
C  SET TEST TO BE THE HOUR ANGLE OF THE BIN EDGE NEAREST NOON
      TEST = HORANG + 0.1309
      IF(IHR.GE.12) TEST = HORANG - 0.1309
C  IF SUN IS DOWN, SKIP
      IF(ABS(TEST).GT.ABS(GUNDOG)) GO TO 1800
C  SUN IS UP. SET FLAG
      ISUNUP = 1
C  TEST TO SEE IF THIS HOUR BIN CONTAINS SUNRISE OR SUNSET
      FSUNUP = 1
      DIFF = ABS(GUNDOG) - ABS(TEST)
      IF((DIFF.LT.0.) .OR. (DIFF.GE.0.2618)) GO TO 200
C  RESET THE HOUR ANGLE HALF WAY BETWEEN SUNRISE OR
C  SUNSET AND THE BIN EDGE NEAREST NOON
      IF(IHR.LT.12)  HORANG = HORANG + 0.5*(0.2618 - DIFF)
      IF(IHR.GE.12)  HORANG = HORANG - 0.5*(0.2618 - DIFF)
C  SET FSUNUP TO BE THE FRACTION OF THE HOUR THE SUN WAS UP
      FSUNUP = 3.8197*DIFF
  200 CONTINUE
      CHCD = COS(HORANG)*CD
      SHCD = SIN(HORANG)*CD
      CLSD = SD*CSTALA
      CHCDSC = CHCD*SSTALA - CLSD
C  CALCULATE SOLAR DIRECTION COSINES
      RAYCOS(1) = CHCDSC*SBAZIM - SHCD*CBAZIM
      RAYCOS(2) = -CHCDSC*CBAZIM - SHCD*SBAZIM
```

```
      RAYCOS(3) = SSTALA*SD + CSTALA*CHCD
      IF(RAYCOS(3).LT.0.001)  GO TO 1800
CKW   IF((IFX.GE.5) .AND. (NDD.LE.0)) GO TO 2000
CKW NEXT LINE ADDED BY K. WILKES
      IF(ISUN.EQ.1) GO TO 2000
C  CALCULATE DIRECT NORMAL AND DIFFUSE RADIATION FOR SKY WITH
C  NO CLOUDS
C  IBM MACHINE PROBLEM WITH EXPONENT UNDERFLOW FOR EXP( ).
C  PROBABLE CAUSE < RAYCOS(3) VERY SMALL --> ARGUMENT VERY LARGE.
C  FIX < CHECK ARGUMENT FOR LARGE NEGATIVE NUMBER. RDN = 0 IF SO.
      ARGUE = -ATMEXT/RAYCOS(3)
      IF(ARGUE.LT.-50.0) GO TO 1
      RDN = SOLCON*CLRNES*EXP(ARGUE)
      GO TO 2
C1    WRITE(6,3)
C2    FORMAT('>>>>NOTE<WILL HAVE EXPONENT UNDERFLOW. RESULT 0')
C  LET'S NOT PRINT OUT ANY MESSAGE (JUST A NUISANCE<)
    1 CONTINUE
      RDN = 0.0
    2 CONTINUE
      BSUN = RDN*SKYDFF/(CLRNES*CLRNES)
CKW NEXT LINE ADDED BY K. WILKES
      IF(ISUN.EQ.2) GO TO 4000
C  GET CLDCOV, THE CLOUD COVER MODIFIER
      CALL CCM
      CLDCOV = CC
      IF(CLDAMT.LE.0.001) CLDCOV = 1.0
C  GET DIRECT NORMAL AND DIFFUSE FOR A CLOUDY DAY
      SOLRAD = (RDN*RAYCOS(3) + BSUN)*CLDCOV*FSUNUP
      RDNCC = FSUNUP*RDN*(1.0-0.1*CLDAMT)
      BSCC = SOLRAD - RDNCC*RAYCOS(3)
      BSCC = AMAX1(BSCC,0.)
      GO TO 3000
CKW NEXT 9 LINES ADDED BY K. WILKES
 4000 IF((RDN*RAYCOS(3) + BSUN).LE.SOLRAD) THEN
          CLDCOV = 1.0
          ELSE
          CLDCOV = SOLRAD/((RDN*RAYCOS(3) + BSUN)*FSUNUP)
      END IF
      CC = CLDCOV
      AL = RAYCOS(3)
      CALL CCMINV(CLDCOV,AL,CLDAMT)
      RDNCC = FSUNUP*RDN*(1.0 - CLDAMT/10.0)
      BSCC = SOLRAD - RDNCC*RAYCOS(3)
      BSCC = AMAX1(BSCC,0.)
      GO TO 3000
C  SUN DOWN
 1800 ISUNUP = 0
      RDN = 0.
      BSUN = 0.
      CLDCOV = 0.
      RDNCC = 0.
```

```
      BSCC = 0.
      SOLRAD = 0.
      DIRSOL = 0.
      DIFSOL = 0.
      RAYCOS(3) = 0.
      GO TO 3000
 2000 CONTINUE
C  USE MEASURED SOLAR DATA
      RDN = 0.
      BSUN = 0.
      RDNCC = DIRSOL
      BSCC = SOLRAD - DIRSOL*RAYCOS(3)
C     IF(IFX.GE.7) BSCC = DIFSOL
      IF(BSCC.LT.0.) BSCC = 0.
 3000 CONTINUE
      RETURN
      END
C*********************************************************************
C**                                                                 **
C**                          SUBROUTINE CCM                         **
C**                                                                 **
C*********************************************************************
      SUBROUTINE CCM
CKW SUBROUTINE BORROWED FROM DOE 2.1C, WITH MODIFICATIONS
CKW  CALCULATE CLOUD COVER MODIFIER AS A FUNCTION OF CLOUD
CKW  TYPE, CLOUD AMOUNT, AND SOLAR ALTITUDE
      COMMON /SUND/ISUNUP,GUNDOG,HORANG,TDECLN,EQTIME,SOLCON,
     1             ATMEXT,SKYDFF,RAYCOS(3),RDN,
     2             BSUN,DECLN,CD,SD,FSUNUP
CKW   COMMON /WEATH/IWDID(5),LRECX,WLAT,WLONG,LTIMZ,IFX,IWSIZ,
CKW  1               CLRNES,TGNDR,WBT,DBT,PATM,CLDAMT,ISNOW,IRAIN,
CKW  2        IWNDDR,HUMRAT,DENSTY,ENTHAL,DIFSOL,DIRSOL,SOLRAD,ICLDTY,
CKW  3               WNDSPD,IDUMMY,DPT,WNDDRR,CLDCOV,RDNCC,BSCC,SKYA,
CKW  4               DBTR,GTEMP(12),CLR(12)
      REAL ICLD
CKW   EQUIVALENCE (ICLD,CLDAMT),(ICLTP,ICLDTY)
CKW  1            ,(CLDCOV,CC  ),(AL,RAYCOS(3))
CKW  NEXT FOUR LINES ADDED BY K. WILKES
      COMMON /CLOUD/CLDAMT,ICLDTY,CC
      ICLD = CLDAMT
      ICLTP = ICLDTY
      AL = RAYCOS(3)
C
      SQ = ICLD*ICLD
      J = ICLTP + 1
      IF(J-2) 130,100,160
C CLOUD TYPE 1
  100 IF(AL.GT.0.707) GO TO 120
C LOW SUN
      CC = 0.598+0.00026*ICLD+0.00021*SQ-0.00035*ICLD*SQ
      RETURN
C HIGH SUN
```

```
  120 CC = 0.908-0.03214*ICLD+0.0102*SQ-0.00114*ICLD*SQ
      RETURN
C CLOUD TYPE 0
  130 IF(AL.GT.0.707) GO TO 150
C LOW SUN
      CC = 0.849-0.01277*ICLD+0.00360*SQ-0.00059*ICLD*SQ
      RETURN
C HIGH SUN
  150 CC = 1.010-0.01394*ICLD+0.00553*SQ-0.00068*ICLD*SQ
      RETURN
C CLOUD TYPE TWO
  160 IF(AL.GT.0.707) GO TO 180
C  LOW SUN
      CC = 0.724-0.00625*ICLD+0.00191*SQ-0.00047*ICLD*SQ
      RETURN
C HIGH SUN
  180 CC = 0.959-0.02304*ICLD+0.00787*SQ-0.00091*ICLD*SQ
      RETURN
      END
C*********************************************************************
C**                                                                 **
C**                          FUNCTION SUN3OR                        **
C**                                                                 **
C*********************************************************************
      FUNCTION SUN3OR(WA,WT,RHOG)
C  THIS FUNCTION CALCULATES THE SOLAR RADIATION INCIDENT ON A TILTED
C  SURFACE
C  ADAPTED FROM SUBROUTINE SUN3 IN DOE 2.1C
      COMMON /SUND/ISUNUP,GUNDOG,HORANG,TDECLN,EQTIME,SOLCON,
     1             ATMEXT,SKYDFF,RAYCOS(3),RDN,
     2             BSUN,DECLN,CD,SD,FSUNUP
      COMMON /SUN2/RDNCC,BSCC
      PI = 3.14159265
      BG = RHOG*(BSCC + RDNCC*RAYCOS(3))
      IF(ABS(WT).GT.0.1) GO TO 110
C TILT = 0
      GAMMA = 1.0
      SWT = 0.
      ETA = RAYCOS(3)
      GO TO 240
  110 IF(ABS(WT - 90.).GT.0.1) GO TO 130
C TILT = 90 DEG.
      GAMMA = 0.0
      SWT = 1.0
      GO TO 140
C  OTHERWISE
  130 GAMMA = COS(WT*PI/180.)
      SWT = SIN(WT*PI/180.)
  140 CONTINUE
      IF(ABS(WA).GT.0.1) GO TO 150
C AZIMUTH = 0
      SWA = 0.
```

```
      CWA = 1.0
      GO TO 230
  150 IF(ABS(WA-90.).GT.0.1) GO TO 160
C AZIMUTH = 90 DEG.
      SWA = 1.0
      CWA = 0.
      GO TO 230
  160 IF(ABS(WA-180.).GT.0.1) GO TO 170
C AZIMUTH = 180 DEG
      SWA = 0.0
      CWA = -1.0
      GO TO 230
  170 IF(ABS(WA-270.).GT.0.1) GO TO 180
C  AZIMUTH = 270 DEG.
      SWA = -1.0
      CWA = 0.0
      GO TO 230
C OTHERWISE
  180 SWA = SIN(WA*PI/180.)
      CWA = COS(WA*PI/180.)
C  CALCULATE ETA IN GENERAL CASE
  230 ETA = (RAYCOS(1)*SWA + RAYCOS(2)*CWA)*SWT
     &       + RAYCOS(3)*GAMMA
C  ETA > 0 MEANS NO DIRECT SOLAR
  240 IF(ETA.GT.0.) GO TO 260
      RDIR = 0.
      GO TO 270
C  CALCULATE DIRECT RADIATION ON WALL
  260 RDIR = RDNCC*ETA
  270 FFG = (1.0 - GAMMA)*0.5
      FFS = 1.0 - FFG
      RDIF = FFS*BSCC + FFG*BG
      SUN3OR = RDIF + RDIR
      RETURN
      END
C*********************************************************************
C**                                                                 **
C**                        SUBROUTINE CCMINV                        **
C**                                                                 **
C*********************************************************************
      SUBROUTINE CCMINV(CLDCOV,AL,CLDAMT)
C  THIS SUBROUTINE CALCULATES THE CLOUD AMOUNT FROM THE CLOUD COVER,
C  ASSUMING TYPE 2 CLOUDS
      IF(AL.GT.0.707) GO TO 100
C  LOW SUN
      IF(CLDCOV.GE.1.0) THEN
         CLDAMT = 0.0
      ELSE IF(CLDCOV.GE.0.71919) THEN
         CLDAMT = (1.0 - CLDCOV)/(1.0 - 0.71919)
      ELSE IF(CLDCOV.LE.0.3825) THEN
         CLDAMT = 10.0
      ELSE
```

```
         Y0 = CLDCOV
         K = 1
         XK = 9.995
   10    XKP1 = XK - (0.724-0.00625*XK+0.00191*XK*XK-0.00047*XK*XK*XK
     &         -Y0)/(-0.00625+2.*0.00191*XK-3.*0.00047*XK*XK)
         IF(ABS(XKP1-XK).GE.0.01) THEN
            XK = XKP1
            K = K + 1
            IF(K.GT.25) STOP 'ERROR IN CCMINV'
            GO TO 10
         ELSE
            CLDAMT = XKP1
         END IF
      END IF
      GO TO 200
C  HIGH SUN
  100 IF(CLDCOV.GE.1.0) THEN
         CLDAMT = 0.0
      ELSE IF(CLDCOV.GE.0.94292) THEN
         CLDAMT = (1.0 - CLDCOV)/(1.0 - 0.94292)
      ELSE IF(CLDCOV.LE.0.6056) THEN
         CLDAMT = 10.0
      ELSE
         Y0 = CLDCOV
         K = 1
         XK = 9.995
   20    XKP1 = XK - (0.959-0.02304*XK+0.00787*XK*XK-0.00091*XK*XK*XK
     &         -Y0)/(-0.02304+2.*0.00787*XK-3.*0.00091*XK*XK)
         IF(ABS(XKP1-XK).GE.0.01) THEN
            XK = XKP1
            K = K + 1
            IF(K.GT.25) STOP 'ERROR IN CCMINV'
            GO TO 20
         ELSE
            CLDAMT = XKP1
         END IF
      END IF
  200 CONTINUE
      RETURN
      END
C*********************************************************************
C**                                                                 **
C**                          SUBROUTINE SKY                         **
C**                                                                 **
C*********************************************************************
C  SUBROUTINE MODIFIED FOR VERSION 1B
C     SUBROUTINE SKY(TO,HUM,IHR,CLDAMT,ICLDTY,TS)
      SUBROUTINE SKY(TO,IHR,CLDAMT,ICLDTY,TS)
      COMMON /HUMID/WO,PATM
C     CALL PSY(TO,HUM,P,W)
C     ALF = ALOG(P*29.921/14.696)
      XX = WO/0.62198
```

```
      P = PATM*XX/(1. + XX)
      ALF = ALOG(P*29.921/14.696)
      IF(P.GT.0.08865) TDP = 79.047 + 30.5790*ALF + 1.8893*ALF*ALF
      IF(P.LE.0.08865) TDP = 71.98 + 24.873*ALF + 0.8927*ALF*ALF
      TD = (TDP+459.67)/1.8 - 273.15
      EPS = 0.711 + 0.56*TD/100. + 0.73*(TD/100.)*(TD/100.) + 0.013*
     &  COS(2.0*3.14159265/24.*FLOAT(IHR))
      EPS = EPS + (1.0 - EPS)*CLDAMT/10.*0.784
      TS = (TO+459.67)*SQRT(SQRT(EPS)) - 459.67
      RETURN
      END
C*********************************************************************
C**                                                                 **
C**                          SUBROUTINE PSY1                        **
C**                                                                 **
C*********************************************************************
      SUBROUTINE PSY1(T,HUM,P,W,DWSDT)
C  NEXT LINE ADDED FOR VERSION 1B
      COMMON /HUMID/WO,PATM
C  THIS SUBROUTINE CALCULATES THE WATER VAPOR PARTIAL PRESSURE AND
C  THE HUMIDITY RATIO, GIVEN THE TEMPERATURE AND RELATIVE HUMIDITY
C  USING EQUATION FROM 1989 ASHRAE FUNDAMENTALS P.6.6
C  T = DRYBULB TEMPERATURE, DEGREES F
C  HUM = RELATIVE HUMIDITY, PERCENT
C  P = WATER VAPOR PARTIAL PRESSURE, PSIA
C  W = HUMIDITY RATIO, POUNDS OF WATER PER POUNDS OF DRY AIR
      C1 = -10214.16462
      C2 = -4.89350301
      C3 = -0.537657944E-2
      C4 = 0.192023769E-6
      C5 = 0.355758316E-9
      C6 = -0.0903446883E-12
      C7 = 4.1635019
      C8 = -10440.39708
      C9 = -11.2946496
      C10 = -0.027022355
      C11 = 0.12890360E-4
      C12 = -0.2478068E-8
      C13 = 6.5459673
      TR = T + 459.67
      IF(T.GE.32.0)  GO TO 10
      X = C1/TR + C2 + C3*TR + C4*TR*TR +C5*TR**3+C6*TR**4+C7*ALOG(TR)
      DXDT = -C1/TR/TR + C3 + 2.0*C4*TR + 3.0*C5*TR*TR + 4.0*C6*TR**3
     &       + C7/TR
      GO TO 20
   10 X = C8/TR + C9 + C10*TR + C11*TR*TR + C12*TR**3 + C13*ALOG(TR)
      DXDT = -C8/TR/TR + C10 + 2.0*C11*TR + 3.0*C12*TR*TR + C13/TR
   20 PSAT = EXP(X)
      DPSDT = PSAT*DXDT
      P = (HUM/100.0)*PSAT
C     W = 0.62198*P/(14.696-P)
      W = 0.62198*P/(PATM-P)
```

```
C       DWSDT = 14.696*0.62198/(14.696-PSAT)/(14.696-PSAT)*DPSDT
        DWSDT = PATM*0.62198/(PATM-PSAT)/(PATM-PSAT)*DPSDT
        RETURN
        END
```

INTERNAL DISTRIBUTION

1-40. K. E. Wilkes
41. P. S. Gillis
42. V. D. Baxter
43. M. A. Brown
44. R. S. Carlsmith
45. F. C. Chen
46. J. E. Christian
47. G. E. Courville
48. F. A. Creswick
49. M. B. Gettings
50. E. A. Hirst
51. R. B. Honea
52. M. A. Karnitz
53. J. O. Kolb
54. M. A. Kuliasha
55. W. P. Levins
56. H. A. McLain
57. W. R. Mixon
58-68. R. R. Parks
69. D. E. Reichle
70. R. B. Shelton
71. J. N. Stone
72. M. P. Ternes
73. R. L. Wendt
74. T. J. Wilbanks
75. ORNL Patent Office
76. Central Research Library
77. Document Reference Section
78-80. Laboratory Records
81. Laboratory Records - RC

EXTERNAL DISTRIBUTION

82. A. Adams, Solar Energy Applications Laboratory, Colorado State University, Fort Collins, CO 80523
83. R. Akers, 661 East Monterey Avenue, Pomona, CA 91767
84. F. Arumi-Noi, University of Texas, Austin, TX 78756
85. Sam Ashley, Public Service Company of Oklahoma, P.O. Box 867, Owasso, OK 74055
86. G. L. Askew, Tennessee Valley Authority, SP 2S 51D-C, Chattanooga, TN 37402-2801
87. L. Aulisio, Celotex Corp., 1500 North Dale Mabry Highway, Tampa, FL 33607
88. E. L. Bales, New Jersey Institute of Technology, School of Architecture, 323 High Street, Newark, NJ 07102
89. K. R. Barnes, Oklahoma Gas and Electric Company, P.O. Box 321, Oklahoma City, OK 73101
90. T. Becker, Alumax Company, P.O. Box 4515, Lancaster, PA 17604
91. F. E. Bitting, Director, Research and Development, Lamtec Corporation, P.O. Box 37, Flanders, NJ 07836-0037
92. J. J. Boulin, U.S. Department of Energy, Conservation and Renewable Energy, CE-131, FORSTL, 1000 Independence Avenue S.W., Washington, D.C. 20585
93. T. W. Bradley, P.E., Atlanta Gas Light Company, P.O. Box 4569, Atlanta, GA 30302
94. Glenn Brower, Marketing Manager, Knauf Fiberglass, 240 Elizabeth St., Shelbyville, IN 46176-1496
95. B. G. Buchanan, Computer Science Dept., University of Pittsburgh, 206 Mineral Industries Bldg., Pittsburgh, PA 15260

96. J. Buddin, Manager, Residential Conservation Program, Florida Power Corp., (C-2-D), 3201 34th Street, S., St. Petersburg, FL 33733
97. T. Bullock, 3321 Pines Road, Shreveport, LA 71119
98. A. Carter, Boston Edison Company, 900 Boylston St., Boston, MA 02199
99. J. R. Carter, Horry County Council of Architects, P.O. Box 172, Myrtle Beach, SC 29577
100. G. Douglas Carver, Tennessee Valley Authority, SP 3N 61A-C, Chattanooga, TN 37402-2801
101. S. Chandra, Florida Solar Energy Center, 300 State Road 401, Cape Canaveral, FL 32920
102. Liz Chase, Tennessee Valley Authority, W4 C1 43C-K, Chattanooga, TN 37402-2801
103. W. Chinn, Manager, Marketing Programs, Florida Power and Light Co., P.O. Box 029100, Miami, FL 33102
104. A. B. Coleman, Tennessee Valley Authority, W4 C1 43C-K, Chattanooga, TN 37402-2801
105. C. Cromer, Florida Solar Energy Center, 300 State Road 401, Cape Canaveral, FL 32920
106. L. Crum, Reflectix, Inc., P. O. Box 108, Markleville, IN 46056
107. J. J. Cuttica, Vice President of Research and Development, Gas Research Institute, 8600 W. Bryn Mawr Avenue, Chicago, IL 60631
108. Andre Desjarlais, Dynatech R/D Company, 99 Erie Street, Cambridge, MA 02139
109. R. C. Diamond, Lawrence Berkeley Laboratory, Building 90-3074, Berkeley, CA 94720
110. R. D. Doering, University of Central Florida, Department of Industrial Engineering and Management Systems, Orlando, FL 32816
111. Judy Driggans, Tennessee Valley Authority, SP 2S 55D-C, Chattanooga, TN 37402-2801
112. G. S. Dutt, Center for Energy and Environmental Studies, Engineering Quad, Princeton University, Princeton, NJ 08544
113. G. H. East, Jr., Mississippi Power Corporation, 2992 W. Beach, Gulfport, MS 39501
114. W. M. Edmunds, Owens-Corning Fiberglas, P.O. Box 415, Building 7201 Granville, OH 43023
115. W. P. Ellis, Standards Consultant, 754 Bob-Bea Lane, Harleysville, PA 19438
116. P. Fairey, Florida Solar Energy Center, 300 State Road 401, Cape Canaveral, FL 32920
117. D. Farmer, Weatherization Program Specialist, Tennessee Department of Human Services, 400 Deaderick, 14th Floor, Nashville, TN 37219
118. A. P. Fickett, Director, Electric Power Research Institute, 3412 Hillview Avenue, Palo Alto, CA 94303
119. C. Fowlkes, Fowlkes Engineering, 31 Gardner Park Drive, Bozeman, MT 59715-9296
120. E. Frankel, House Committee on Science and Technology, Rayburn Bldg., Room 2320, Washington, D.C. 20515
121. E. C. Freeman, Department of Energy, CE-133, FORSTL, 1000 Independence Avenue, S.W., Washington, D.C. 20585
122. J. Gardner, Jr., Division of Weatherization, U.S. Department of Energy, CE-232, FORSTL, 1000 Independence Avenue, S.W., Washington, D.C. 20585

123. P. S. Gee, North Carolina Alternative Energy Corp., P. O. Box 12699, Research Triangle Park, NC 27709
124. C. F. Gilbo, Editor-in-Chief, J. of Thermal Insulation, 201 E. Ross Street, Lancaster, PA 17602
125. D. Goldenberg, P.E., Technical Consultant, EnerServ, P.O. Box 3393, Oak Ridge, TN 37830
126. M. Gorelick, U.S. Department of Energy, CE-131, FORSTL, 1000 Independence Avenue, S.W., Washington, D.C. 20585
127. J. Gregory, Carolina Power and Light Co., P.O. Box 1551, Raleigh, NC 27602
128. T. Grether, Owens-Corning Fiberglas, Fiberglas Tower, 23rd Floor, Toledo, OH 43659
129. R. Griffin, Edison Electric Institute, 1111 19th Street, N.W., Washington, D.C. 20036
130. E. I. Griggs, Tennessee Technological University, P.O. Box 5014, Cookeville, TN 38505
131. R. Groberg, U.S. Department of Housing and Urban Development, 451 7th Street, S.W., Washington, D.C. 20410
132. J. R. Hagan, Jim Walter Research Corp., 10301 Ninth Street, N., St. Petersburg, FL 33702
133. James Hall, Tennessee Valley Authority, 2N38A Missionary Ridge Place, Chattanooga, TN 37402-2801
134. B. J. Harris, Central and Southwest Corp., 2121 San Jacinto Street, Dallas, TX 75266-0164
135. L. Harris, Assistant Commissioner for Administration, Tennessee Dept. of Human Services, 400 Deaderick, 14th Floor, Nashville, TN 37219
136. D. T. Harrje, Princeton University, CEES, Engineering Quad, Princeton, NJ 08544
137. Jack Haslam, Department of Community Affairs, Division of Housing and Community Development, 2571 Executive Center Circle East, Tallahassee, FL 32301
138. R. Hauser, Hauser Laboratories, 5680 Central Avenue, P.O. Box G, Boulder, CO 80306
139. J. P. Hawke, State Office of Community Services, Capitol Complex, Carson City, NV 89710
140. M. High, Tennessee Valley Authority, 3N 78A-C, Chattanooga, TN 37402-2801
141. G. Himmeger, Insulation Specialist, P.O. Box 82, Troy, IL 62294
142. Dr. A. Hirsch, Vice President, Environmental Sciences and Director Washington Operations, 5109 Leesburg Pike, Suite 414, Falls Church, VA 22041
143. V. Hodge, Science Applications International Corp., 1710 Goodrich Drive, McLean, VA 22102
144. G. Hollern, Alumax, Home Products Division, P.O. Box 4515, Lancaster, PA 17604-4515
145. S. Hooks, Manager, Energy Utilization Technology, Edison Electric Institute, 1111 19th Street, N.W., Washington, D.C. 20036
146. M. Hopkins, Alliance to Save Energy, 1925 K Street, N.W., Suite 206, Washington, D.C. 20006
147. Bion Howard, Alliance to Save Energy, 1925 K Street, N.W., Suite 206, Washington, D. C. 20006

148. K. C. Howerton, Federal Trade Commission, 6th and Pennsylvania Avenue, N.W., Washington, D.C. 20508
149. J. G. Hust, National Bureau of Standards, National Engineering Laboratory, 3215 Broadway, Boulder, CO 80303
150. B. Hyma, General Manager, Energy Saver Imports (E.S.I.) Company, 8611 West 71st Circle, Arvada, CO 80004
151. Leif Isaaksen, ACES, Inc., 4029 S. Via Marina, Suite F205, Marina del Rey, CA 90292
152. S. Jaeger, Resource Management Dept., City of Austin, 3000 S.I.H. 35, Austin, TX 78704
153. R. Jarnagan, Battelle Pacific Northwest Laboratories, P.O. Box C5395, Seattle, WA 98105
154. C. Jernigan, North Carolina Dept. of Commerce, Energy Division, Dobbs Building, Raleigh, NC 27611
155. P. F. Juneau, Alfol, Inc., 9839-T York Road, Charlotte, NC 28210
156. J. P. Kalt, Professor of Economics, Kennedy School of Government, Harvard University, 79 John F. Kennedy Street, Cambridge, MA 02138
157. John Kesselring, Electric Power Research Institute, 3412 Hillview Avenue, P.O. Box 10412, Palo Alto, CA 94303
158. M. K. Khattar, Senior Systems Engineer, Research and Development Division, Florida Solar Energy Center, 300 State Road 401, Cape Canaveral, FL 32920
159. R. H. Klein, Tennessee Valley Authority, SP 1S 57A-C, Chattanooga, TN 37402-2801
160. D. K. Knight, U.S. Department of Energy, EH-2Y/7E-088, 1000 Independence Avenue, S.W., Washington, D.C. 20585
161. J. Kragh, CEM, Jim Kragh and Associates, 218 Jackson Street, Maitland, FL 32751
162. P. Kunjeer, U.S. Department of Energy, CE-133, FORSTL, 1000 Independence Avenue, S.W., Washington, D.C. 20585
163. Myron B. Lacher, CertainTeed Corporation, P.O. Box 860, Valley Forge, PA 19482
164. A. Lanus, Electric Power Research Institute, 3412 Hillview Avenue, Palo Alto, CA 94303
165. R. H. Larson, Manville Engineering and Technical Services, P. O. Box 5108, Denver, CO 80217
166. B. M. Levine, Alabama Solar Energy Center, The University of Alabama at Huntsville, P.O. Box 1247, Huntsville, AL 35999
167. M. Levine, Building 90, Room 3074, Lawrence Berkeley Laboratory, Berkeley, CA 94720
168. D. D. Lovich, Owens-Corning Fiberglas, 6650 Power Ferry Road, Suite 200, Atlanta, GA 30334
169. G. Maples, Joint Legislative Committee on Energy, 104 Blatt Bldg., Columbia, SC 29201
170. T. D. Marron, Edison Electric Institute, 1111 19th Street, N.W., Washington, D.C. 20036
171. G. Mascari, Aluma-Foil Insulation, 12908 S. Main Street, Los Angeles, CA 90061
172. D. McCaa, CertainTeed Corporation, 1400 Union Meeting Road, Blue Bell, PA 19422
173. F. C. McQuiston, Oklahoma State University, Mechanical Engineering Department, Stillwater OK 74078

174. D. E. Meiners, Mississippi Power and Light Company, Electric Building, Box 1640 Jackson, MS 39215-1640
175. K. D. Mentzer, Mineral Insulation Manufacturers Assoc., 1420 King Street, Alexandria, VA 22314
176. R. Meyer, Office of Energy Resources, 270 Washington Street, S.W., Suite 615, Atlanta, GA 30334
177. G. Miller, Jim Walter Research Corp., 10301 9th Street, North, St. Petersburg, FL 33702
178. William J. Miller, Tennessee Valley Authority, 1 SO 46A Signal Place, Chattanooga, TN 37402-2801
179. J. P. Millhone, Deputy Assistant Secretary, U.S. Department of Energy, CE-13, 5E-080 FORSTL, 1000 Independence Avenue, S.W., Washington, D.C. 20585
180. M. Millspaugh, Reflectix, Inc., P.O. Box 108, Markleville, IN 46056
181. M. A. Milne, UCLA, Graduate School of Architecture and Urban Planning, Los Angeles, CA 90024
182. H. Misuriello, W. S. Fleming and Associates, Inc., 536 Seventh St., S.E., Washington, D.C. 20003
183. M. Modera, Lawrence Berkeley Laboratory, Building 90, Room 3074, Berkeley, CA 94720
184. T. L. Moody, Associate Professor of Physics, Department of Chemistry and Physics, Middle Tennessee State University, P.O. Box 273, Murfreesboro, TN 37132
185. D. E. Morrison, Professor of Sociology, Michigan State University, 201 Berkey Hall, East Lansing, MI 48824-1111
186. J. R. Mumaw, Owens-Corning Fiberglas, G/20-3, P.O. Box 415, Granville, OH 43023
187. Ralph Nader, Post Office Box 19367, Washington, D.C. 20036
188. N. Naumovich, Jr., President, Parsec, Inc., P.O. Box 38534, Dallas, TX 75238
189. D. G. Ober, Research Associate, Manville Service Corp., P.O. Box 5108, Denver, CO 80217
190. D. L. O'Neal, Dept. of Mechanical Engineering, Texas A/M University, College Station, TX 77643
191. Bruce Nelson, Minnesota Energy Office, American Center Building, Room 900, St. Paul, Minnesota 55101
192. T. Paison, Thermal Envelope Group Building, Physics Division, Center for Building Technology, National Bureau of Standards, Gaithersburg, MD 20899
193. D. Parker, Florida Solar Energy Center, 300 State Road 401, Cape Canaveral, FL 32920
194. R. L. Perrine, Professor of Engineering and Applied Science, Civil Engineering Department, Engineering I, Room 2066, University of California, Los Angeles, CA 90024
195. L. Peterson, Thermoguard Insulation Company, 1040 Andover Park West, Seattle, WA 98188
196. S. Peterson, National Bureau of Standards, Bldg. 224, Room B-120, Gaithersburg, MD 20899
197. G. D. Pine, Gas Research Institute, 8600 West Bryn Mawr Avenue, Chicago, IL 60631
198. Jon Polcha, Public Service Company of Oklahoma, P.O. Box 867, Owasso, OK 74055

199. T. Potter, Solar Energy Research Institute, 1617 Cole Blvd., Golden, CO 80401
200. F. J. Powell, 12218 Cattail Lane, Jacksonville, FL 32223
201. F. Powell, National Bureau of Standards, 3215 Broadway, Boulder, CO 80303
202. J. S. Prince, Ethyl Corporation, P.O. Box 2448, Richmond, VA 23218
203. Frank Raphbun, The Aluminum Association, 818 Connecticut Avenue, N.W., Washington, D.C. 20036
204. R. J. Ray, Manville Corporation, P.O. Box 5108, Denver CO 80217
205. R. Ray, Aluminum Company of America, 1501 Alcoa Building, Pittsburgh, PA 15219
206. F. R. Robertson, Tennessee Valley Authority, Chattanooga, TN 37402-2801
207. T. R. Rohweber, Manville Corporation, P.O. Box 5108, Denver, CO 80217
208. A. H. Rosenfeld, Lawrence Berkeley Laboratory, Building 90-3058, Berkeley, CA 94720
209. J. A. Roux, Department of Mechanical Engineering, University of Mississippi, University, MS 38677
210. S. Rubin, Solar Energy Research Institute, 1617 Cole Blvd., Golden, CO 80401
211. C. R. Sanders, Alabama Power Company, P.O. Box 2641, Birmingham, AL 35291
212. P. Scofield, Department of Energy, CE-421, FORSTL, 1000 Independence Avenue, S.W., Washington, D.C. 20585
213. Tom J. Secrest, Pacific Northwest Laboratories, Sigma IV Bldg., Box 999, Richland, WA 99352
214. C. W. Shabica, Northeastern Illinois University, 5500 N. St. Louis Avenue, Chicago, IL 60625
215. M. Shaw, Energy Management, 218-220 Jackson Street, Maitland, FL 32751
216. E. Shepherd, New York State Energy Research and Development Authority, Two Rockefeller Plaza, Albany, NY 12223
217. D. Smith, National Center for Appropriate Technology, P.O. Box 3838, Butte, MT 59702-3838
218. J. A. Smith, Director, Building Systems Division, U.S. Department of Energy, CE-111, FORSTL, 1000 Independence Avenue, S.W., Washington, D.C. 20585
219. M. J. Smith, Lamotite, Inc., 2905 East 79th Street, Cleveland, OH 44104
220. R. Smith, Program Manager, Florida Department of Community Affairs, Bureau of Local Government Assistance, 2571 Executive Center Circle East, Tallahassee, FL 32301
221. R. C. Sonderegger, Morgan Systems Corporation, 1654 Solano Avenue, Berkeley, CA 94707
222. J. Sparrell, Sparrell Engineering, Box 130, Damariscotta, ME 04543
223. J. G. Spoor, Administrative Manager, Denny Sales Corporation, 3121 S.W. 15th Street, Pompano Beach, FL 33069-4806
224. R. Squitieri, Electric Power Research Institute, 3412 Hillview Avenue, Palo Alto, CA 94303
225. J. Stone, U.S. Department of Energy, CE-44, FORSTL, 1000 Independence Avenue, S.W., Washington, D.C. 20585
226. E. Storey, Insul-Tray, Inc., 4985 N. Cascade Place, Oak Harbor, WA 98277
227. W. Strzepek, P.O. Box 515, Granville, OH 43023

228. G. E. Stubbins, Duke Power Company, 422 South Church Street, Charlotte, NC 28242
229. T. W. Swanson, Tennessee Valley Authority, SP 1S 35A-C, Chattanooga, TN 37402-2801
230. J. Talley, Georgia Power Company, P.O. Box 4545, Atlanta, GA 30302
231. W. D. Turner, Texas A/M University, Mechanical Engineering Dept., College Station, TX 77643
232. J. Turrell, The Electric Letter, Route 2, Box 238, Mt. Vernon, IL 62864
233. R. P. Tye, 292 Jerusalem Road, Cohasset, MA 02025
234. J. Viegel, North Carolina Alternative Energy Corporation, P.O. Box 12699, Research Triangle Park, NC 27709
235. B. Wadsworth, Innovative Energy Division, 1119 W. 145th Avenue, Crown Point, IN 46307
236. J. Warner, American Consulting Engineering Council, Research Management Foundation, 1015 15th Street, Suite 802, Washington, D. C. 20005
237. C. Wentowski, Program Manager, Alabama Department of Economic and Community Affairs, 3465 Norman Bridge Road, Montgomery, AL 36105-0930
238. B. Wilkinson, Orlando Housing Authority, 200 Victor Avenue, Orlando, FL 32801
239. Dr. M. Williams, Dept. of Economics, Northern Illinois University, DeKalb, IL 60115
240. Larry M. Windingland, U.S. Army Corps of Engineers, P.O. Box 4005, Champaign, IL 61820
241. E. Woods, Savannah Electric and Power Company, P.O. Box 968, Savannah, GA 31402
242. D. W. Yarbrough, Professor of Chemical Engineering, Tennessee Technological University, Box 5013, Cookeville, TN 38501
243. Albert W. Young, Guardian Fiberglass, Inc., 1810 Williamsburg Pike, Richmond, IN 47374
244. O. Zimmerman, Electric Power Research Institute, 3412 Hillview Avenue, Palo Alto, CA 94303
245. Office of the Assistant Manager for Energy Research and Development, DOE-ORO, P.O. Box 2001, Oak Ridge, TN 37831-8600

246-256. OSTI, U.S. Department of Energy, P.O. Box 62, Oak Ridge, TN 37831